



**GE Nuclear Energy**

C.J. Deacon  
Manager, Advanced Reactor Programs

General Electric Company  
175 Curtner Avenue, M/C 365 San Jose, CA 95125-1014  
408 925-2469 (phone) 408 925-5474 (facsimile)

MFN 03-010

Project 717

February 27, 2003

U.S. Nuclear Regulatory Commission  
ATTN: Document Control Desk  
One White Flint North  
11555 Rockville Pike  
Rockville, MD 20852-2738

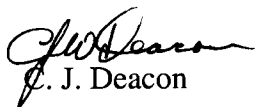
Reference: Letter S. Hucik, GE to S. Collins, NRC, Pre-application Review of ESBWR, dated April 18, 2002

Subject: **TRACG Qualification for SBWR, Vol. 1 and 2, NEDO-32725, Revision 1 - Document Transmittal for Pre-Application Review of ESBWR – Non-Proprietary Report**

The CD accompanying this letter contains the GE non-proprietary report NEDO-32725, Revision 1, TRACG Qualification for SBWR, Vol. 1 and 2.

If you have any questions about the information provided here, please contact Atam Rao at (408) 925-1885, or myself.

Sincerely,

  
C. J. Deacon

cc: A. Cubbage USNRC (with CD)  
J. Lyons USNRC (w/o CD)  
G.B. Stramback GE (with CD)




NEDO-32725  
Revision 1  
Class I  
DRF 0000-0006-8900  
August 2002

# TRACG Qualification for SBWR

## Volume 1

Authors:

J. R. Fitch  
D. Abdollahian  
Md. Alamgir  
T. Bandurski (PSI)  
Y.K. Cheung  
J.M. Healzer  
A. Hunsbedt  
A.J. Illich  
L.A. Klebanov  
U. C. Saxena  
B. S. Shiralkar  
S. Sitaraman  
M. Stempniewicz (KEMA)  
A. I. Yang  
J. Wouters (KEMA)

Approved:   
C.J. Deacon, Manager  
Advanced Reactor Projects

**IMPORTANT NOTICE REGARDING  
CONTENTS OF THIS REPORT  
PLEASE READ CAREFULLY**

*Neither the General Electric Company nor any of the contributors to this document:*

*a. Makes any warranty or representation, express or implied, with respect to the accuracy, completeness, or usefulness of the information contained in this document, or that the use of any information, apparatus, method, or process disclosed in this document may not infringe privately owned rights;*

*or*

*b. Assumes any liabilities, including but not limited to nuclear liability, with respect to the use of, or for damages resulting from the use of any information, apparatus, method, or process disclosed in this document.*

*This work was performed partially as part of a contract between various utilities and GE for "ESBWR Development".*

## **ACKNOWLEDGMENT**

The contributions of the following individuals to analyses which form the basis of this report are gratefully acknowledged:

G. Bianchini (ENEA)  
P.F. Billig  
P.K. Dill  
R. E. Gamble  
K. Kobayashi (JAPC)  
P. Masoni (ENEA)  
J. Morales (IIE)

In addition, the support of C. Heck and J. G. M. Andersen in the development of the models needed in TRACG is gratefully acknowledged. K. Miyata and T. Narazaki of JAPC, and A. Petry of GRS made contributions to several sections and also provided technical review of the document. Special recognition and acknowledgment are given to Trish Bautista, Yolanda Espino and Malin Swope for their assistance in the typing, compilation, editing and final preparation of this report. The work reported in this document was performed under an EPRI contract. The contributions of T. J. Mulford and R. T. Fernandez of EPRI are greatly appreciated.

## Table of Contents

### — VOLUME 1 —

	<u>Page</u>
<b>EXECUTIVE SUMMARY</b>	<b>S-1</b>
<b>1. INTRODUCTION</b>	<b>1.1-1</b>
<b>1.1 Relationship to Generic TRACG Qualification Report</b>	<b>1.1-1</b>
<b>1.2 Relationship to Other Documents Needed for TRACG Application</b>	<b>1.2-1</b>
<b>1.3 Report Road Map</b>	<b>1.3-1</b>
<b>1.4 References</b>	<b>1.4-1</b>
<b>2. QUALIFICATION STRATEGY</b>	<b>2-1</b>
<b>2.1 Assessment Matrix and Coverage of PIRT Phenomena</b>	<b>2.1-1</b>
2.1.1 Separate Effects Tests	2.1-2
2.1.2 Component Tests	2.1-3
2.1.3 Integral System Response Tests	2.1-3
2.1.4 Plant Operating Data	2.1-5
2.1.5 Summary of Test Coverage	2.1-5
<b>2.2 References</b>	<b>2.2-1</b>
<b>3. SEPARATE EFFECTS TESTS</b>	<b>3.1-1</b>
<b>3.1 Toshiba Low Pressure Void Fraction Tests</b>	<b>3.1-1</b>
3.1.1 Introduction	3.1-1
3.1.2 Test Facility and Test Matrix	3.1-1
3.1.3 Applicability of Data to SBWR	3.1-2
3.1.4 TRACG Model	3.1-3
3.1.5 Test Simulation	3.1-3
3.1.6 Results of Calculations	3.1-4
3.1.7 Summary and Conclusions	3.1-4
3.1.8 References	3.1-5
<b>3.2 Ontario Hydro Void Fraction Tests</b>	<b>3.2-1</b>
3.2.1 Introduction	3.2-1
3.2.2 Description of Ontario Hydro Void Fraction Tests	3.2-1
3.2.3 Applicability of Data to SBWR	3.2-5
3.2.4 TRACG Model	3.2-6
3.2.5 TRACG Simulation	3.2-6

**Table of Contents**

(continued)

	<b><u>Page</u></b>
3.2.6 Results of Calculations	3.2-7
3.2.6.1 Accuracy of TRACG Calculations	3.2-7
3.2.7 Summary and Conclusions	3.2-8
3.2.8 References	3.2-8
<b>3.3 Summary of Separate Effects Comparisons</b>	<b>3.3-1</b>
3.3.1 Void Fraction Data	3.3-1
3.3.2 PSTF Level Swell Tests	3.3-3
3.3.3 Condensation in the Presence of Noncondensibles - University Tests	3.3-4
3.3.4 Critical Flow	3.3-5
3.3.5 Frictional Pressure Drop	3.3-5
3.3.6 Critical Power	3.3-6
3.3.6.1 ATLAS Critical Power Data	3.3-6
3.3.6.2 Applicability of GEXL Correlation for Bundles with 2.8m Length	3.3-7
3.3.7 SPERT Reactivity Insertion Test	3.3-7
3.3.8 Thermal Hydraulic Stability	3.3-8
3.3.9 Flow Oscillations at Low Pressure	3.3-9
3.3.10 Humboldt Bay and Bodega Bay Pressure Suppression Test Programs	3.3-9
3.3.11 References	3.3-10
<b>4. COMPONENT PERFORMANCE TESTS</b>	<b>4.1-1</b>
<b>4.1 Panthers PCC Performance</b>	<b>4.1-1</b>
4.1.1 Introduction	4.1-1
4.1.2 Test Facility/Test Matrix	4.1-2
4.1.2.1 Test Facility	4.1-2
4.1.2.2 Test Matrix and Data Analysis	4.1-3
4.1.3 Applicability of Data To SBWR	4.1-5
4.1.3.1 Scope	4.1-5
4.1.3.2 SBWR	4.1-5
4.1.3.3 PANTHERS	4.1-8
4.1.3.4 PIRT Phenomena and Coverage	4.1-12
4.1.3.5 Scaling	4.1-13
4.1.3.6 Conclusion	4.1-14
4.1.4 TRACG Models and Nodalization	4.1-14
4.1.4.1 One-Tube Model	4.1-14
4.1.4.2 Eight-Tube Model	4.1-18
4.1.4.3 Six-Tube Model	4.1-19
4.1.4.4 Determination of Hydraulic Loss Factors	4.1-19
4.1.4.5 TRACG Heat Transfer Correlations	4.1-21

**Table of Contents**

(continued)

	<b><u>Page</u></b>
4.1.5 Test Simulation	4.1-21
4.1.5.1 Steady-State Tests	4.1-21
4.1.5.2 Transient Tests	4.1-22
4.1.5.3 Atmospheric Pressure Boundary Condition	4.1-23
4.1.6 Results and Discussion	4.1-23
4.1.6.1 Steady-State Pure-Steam Tests	4.1-24
4.1.6.2 Steady-State Steam-Air Tests	4.1-24
4.1.6.3 Transient Tests	4.1-26
4.1.6.4 Evaluation of Tube Wall Temperature Data	4.1-28
4.1.6.5 Accuracy of TRACG Calculations	4.1-34
4.1.7 Summary and Conclusions	4.1-34
4.1.7.1 Condenser Performance Under Prototypical Conditions	4.1-35
4.1.7.2 Condenser Performance under Non-Prototypical Conditions	4.1-35
4.1.7.3 Evaluation of TRACG Qualification Needs	4.1-36
4.1.8 References	4.1-38
<b>4.2 PANTHERS IC Performance</b>	<b>4.2-1</b>
4.2.1 Introduction	4.2-1
4.2.2 Test Facility and Test Matrix	4.2-1
4.2.2.1 Test Facility	4.2-1
4.2.2.2 Test Matrix and Data Analysis	4.2-2
4.2.3 Applicability of Data to SBWR	4.2-3
4.2.3.1 Steady-State Tests	4.2-3
4.2.3.2 Transient Tests	4.2-4
4.2.3.3 PIRT Phenomena and Coverage	4.2-4
4.2.3.4 Scaling	4.2-5
4.2.4 TRACG Model and Nodalization	4.2-5
4.2.4.1 Model Description	4.2-6
4.2.4.2 TRACG Heat Transfer Correlations	4.2-8
4.2.5 Test Simulation	4.2-8
4.2.5.1 Steady-State Tests	4.2-8
4.2.5.2 Transient Tests	4.2-9
4.2.6 Results and Discussion	4.2-9
4.2.6.1 Steady-State Tests	4.2-10
4.2.6.2 Transient Tests	4.2-10
4.2.6.3 Accuracy of TRACG Calculations	4.2-12
4.2.7 Summary and Conclusions	4.2-12
4.2.7.1 Pure Steam Condensation Performance	4.2-12
4.2.7.2 Noncondensable Accumulation and Venting	4.2-13
4.2.7.3 IC Pool Level Effects	4.2-13
4.2.7.4 Evaluation of TRACG Qualification Needs	4.2-13

**Table of Contents**  
(continued)

	<u>Page</u>	
4.2.8	References	4.2-15
<b>4.3</b>	<b>PANDA PCC Performance</b>	<b>4.3-1</b>
4.3.1	Introduction	4.3-1
4.3.2	Test Facility and Test Matrix	4.3-1
4.3.2.1	Test Facility	4.3-1
4.3.2.2	Test Matrix	4.3-2
4.3.3	Applicability of Data to SBWR	4.3-2
4.3.3.1	Overview of Data Applicability and Test Facility Scaling	4.3-2
4.3.3.2	PIRT Phenomena and Coverage	4.3-3
4.3.4	TRACG Model	4.3-4
4.3.5	Test Simulation	4.3-6
4.3.6	Results of Post-Test Calculations	4.3-7
4.3.6.1	Comparison of Experimental and Calculated Results	4.3-7
4.3.6.2	Effect of Reduced Pool Water Level	4.3-8
4.3.6.3	Accuracy of TRACG Calculations	4.3-8
4.3.7	Summary and Conclusions	4.3-8
4.3.7.1	Condenser Performance	4.3-8
4.3.7.2	Evaluation of TRACG Qualification Needs	4.3-9
4.3.8	References	4.3-11
<b>4.4</b>	<b>Suppression Pool Stratification Tests</b>	<b>4.4-1</b>
4.4.1	Introduction	4.4-1
4.4.2	Test Facility/Test Matrix	4.4-1
4.4.3	Applicability of Data to SBWR	4.4-2
4.4.3.1	General Data Applicability and Test Facility Scaling	4.4-2
4.4.3.2	PIRT Phenomena and Coverage	4.4-2
4.4.3.3	Scaling Parameters Range	4.4-3
4.4.4	TRACG Model	4.4-3
4.4.5	Test Simulation	4.4-4
4.4.6	Results of Post-Test Calculations	4.4-5
4.4.6.1	Test 5707-01	4.4-5
4.4.6.2	Test 5807-29	4.4-6
4.4.6.3	Condensation of Blowdown Steam	4.4-6
4.4.6.4	Accuracy of TRACG Calculations	4.4-6
4.4.7	Summary and Conclusions	4.4-7
4.4.8	References	4.4-7

— VOLUME 2 —

<b>5.</b>	<b>INTEGRAL SYSTEMS TESTS</b>	<b>5.1-1</b>
<b>5.1</b>	<b>GIST</b>	<b>5.1-4</b>
5.1.1	Introduction	5.1-4



**Table of Contents**

(continued)

	<b><u>Page</u></b>
5.1.2 Description of GIST Facility and Tests	5.1-4
5.1.3 Applicability of Data to SBWR	5.1-5
5.1.3.1 General Test Facility Scaling	5.1-5
5.1.3.2 PIRT Phenomena and Coverage	5.1-6
5.1.3.3 Conclusions on Data Applicability	5.1-9
5.1.4 TRACG Model	5.1-10
5.1.5 TRACG Simulation of GIST Tests	5.1-11
5.1.5.1 Initial Conditions	5.1-11
5.1.5.2 Test Control	5.1-11
5.1.5.3 Tests Analyzed with TRACG	5.1-12
5.1.6 Results of Post-Test Calculations	5.1-13
5.1.6.1 TRACG/GIST Comparisons for Bottom Drain Break LOCA (Test A07)	5.1-13
5.1.6.2 TRACG/GIST Comparisons for Other LOCA Types	5.1-14
5.1.6.3 RPV Dome Pressure (Figures 5.1-17 through 5.1-20)	5.1-15
5.1.6.4 GDCS Flow (Figures 5.1-21 through 5.1-24)	5.1-15
5.1.6.5 Annulus Pressure Drop (Figures 5.1-25 through 5.1-28)	5.1-15
5.1.6.6 Core Pressure Drop (Figures 5.1-29 through 5.1-32)	5.1-16
5.1.6.7 Margin to Boiling Transition	5.1-16
5.1.7 Conclusions	5.1-16
5.1.8 References	5.1-16
<b>5.2 GIRAFFE Helium Tests</b>	<b>5.2-1</b>
5.2.1 Introduction	5.2-1
5.2.1.1 Purpose of Tests	5.2-1
5.2.1.2 Tests Selected for Post-Test Analysis	5.2-2
5.2.1.3 Purpose of Post-Test Analysis	5.2-3
5.2.2 Test Facility/Test Matrix	5.2-3
5.2.2.1 GIRAFFE Test Facility	5.2-3
5.2.2.2 Test Matrix	5.2-5
5.2.3 Applicability of Data to SBWR	5.2-5
5.2.3.1 General Data Applicability and Test Facility Scaling	5.2-6
5.2.3.2 PIRT Phenomena and Coverage	5.2-6
5.2.3.3 Conclusions on Data Applicability	5.2-10
5.2.4 TRACG Model	5.2-10
5.2.4.1 Nodalization of Test Facility	5.2-10
5.2.4.2 3-D Vessel Component	5.2-11
5.2.4.3 RPV and Associated Piping	5.2-11
5.2.4.4 PCC	5.2-11
5.2.4.5 Main Vent and Vacuum Breaker	5.2-12
5.2.4.6 Comparison to the SBWR Model	5.2-12
5.2.5 Test Simulation	5.2-13
5.2.5.1 Introduction	5.2-13

## Table of Contents

(continued)

	<u>Page</u>
5.2.5.2 Component Heat Loss and Decay Heat	5.2-13
5.2.5.3 Initial Conditions	5.2-14
5.2.6 Results and Discussion	5.2-15
5.2.6.1 Test Results	5.2-15
5.2.6.2 General Discussion	5.2-16
5.2.6.3 Test H1	5.2-16
5.2.6.4 Test H2	5.2-18
5.2.6.5 Test H3	5.2-21
5.2.6.6 Test H4	5.2-22
5.2.6.7 Test T2	5.2-24
5.2.6.8 Accuracy of TRACG Calculations	5.2-25
5.2.7 Conclusions	5.2-25
5.2.7.1 General Conclusions	5.2-25
5.2.7.2 PIRT Conclusions	5.2-27
5.2.8 References	5.2-27
<b>5.3 GIRAFFE Systems Interactions Tests</b>	<b>5.3-1</b>
5.3.1 Introduction	5.3-1
5.3.2 Test Facility	5.3-2
5.3.2.1 The Reactor Pressure Vessel (RPV)	5.3-2
5.3.2.2 Drywell	5.3-2
5.3.2.3 Wetwell	5.3-3
5.3.2.4 GDCS Pool	5.3-3
5.3.2.5 Passive Containment Cooling System (PCCS)	5.3-3
5.3.2.6 Isolation Condenser System (ICS)	5.3-3
5.3.3 Applicability of Data to SBWR	5.3-3
5.3.3.1 General Data Applicability and Test Facility Scaling	5.3-4
5.3.3.2 PIRT Phenomena and Coverage	5.3-5
5.3.3.3 Conclusions on Data Applicability	5.3-10
5.3.4 TRACG Model	5.3-10
5.3.4.1 3-D Vessel Component	5.3-11
5.3.4.2 RPV Internals	5.3-11
5.3.4.3 RPV Piping	5.3-11
5.3.4.4 Drywell Piping	5.3-12
5.3.4.5 Wetwell Piping	5.3-12
5.3.4.6 GDCS Piping	5.3-12
5.3.4.7 IC and PCC systems	5.3-12
5.3.4.8 Comparison with SBWR Nodalization	5.3-13
5.3.5 Test Simulation	5.3-13
5.3.5.1 Introduction	5.3-13
5.3.5.2 Heat Losses in the System	5.3-13
5.3.5.3 Decay Heat	5.3-14
5.3.5.4 Initial Conditions	5.3-14

**Table of Contents**

(continued)

	<b><u>Page</u></b>
5.3.6 Test and TRACG Simulation Results	5.3-14
5.3.6.1 Introduction	5.3-14
5.3.6.2 Test GS1	5.3-16
5.3.6.3 Test GS2	5.3-18
5.3.6.4 Test GS3	5.3-19
5.3.6.5 Test GS4	5.3-20
5.3.6.6 Sensitivity Studies	5.3-21
5.3.7 Summary and Conclusions	5.3-22
5.3.7.1 General Conclusions	5.3-22
5.3.7.2 Conclusions Related to Key PIRT Phenomena	5.3-22
5.3.7.3 Final Observations	5.3-23
5.3.8 References	5.3-24
<b>5.4 One-Sixth Scale Boron Mixing Tests</b>	<b>5.4-1</b>
5.4.1 Introduction	5.4-1
5.4.2 Test Facility	5.4-1
5.4.3 Applicability to SBWR	5.4-2
5.4.4 TRACG Model	5.4-4
5.4.4.1 Model Description	5.4-4
5.4.4.2 Test Initial Conditions	5.4-5
5.4.5 Test Simulation	5.4-6
5.4.5.1 Model 1	5.4-7
5.4.5.2 Model 2	5.4-7
5.4.6 TRACG Results	5.4-7
5.4.6.1 Model 1	5.4-7
5.4.6.2 Model 2	5.4-8
5.4.7 Conclusions	5.4-8
5.4.7.1 General Conclusions	5.4-8
5.4.7.2 Conclusions Related to Key PIRT Phenomena	5.4-8
5.4.8 References	5.4-9
<b>5.5 PSTF Mark III Containment Response</b>	<b>5.5-1</b>
5.5.1 Introduction	5.5-1
5.5.2 Test Facility/Test Matrix	5.5-1
5.5.3 Applicability of Data to SBWR	5.5-2
5.5.3.1 General Data Applicability and Test Facility Scaling	5.5-2
5.5.3.2 PIRT Phenomena and Coverage	5.5-2
5.5.3.3 Scaling Parameters Range	5.5-3
5.5.4 TRACG Model and Nodalization	5.5-4
5.5.5 Test Simulation	5.5-4
5.5.6 Results of Post-Test Calculations	5.5-4
5.5.6.1 Results for Test 5703-01	5.5-5
5.5.6.2 Results for Test 5703-02	5.5-5
5.5.6.3 Results for Test 5703-03	5.5-5

## Table of Contents

(continued)

	<u>Page</u>
5.5.6.4 Accuracy of TRACG Calculations	5.5-5
5.5.7 Summary and Conclusions	5.5-6
5.5.8 References	5.5-6
<b>5.6 4T/Mark II Containment Response</b>	<b>5.6-1</b>
5.6.1 Introduction	5.6-1
5.6.2 Test Facility/Test Matrix	5.6-1
5.6.3 Applicability of Data to SBWR	5.6-2
5.6.3.1 General Data Applicability and Test Facility Scaling	5.6-2
5.6.3.2 PIRT Phenomena and Coverage	5.6-2
5.6.3.3 Scaling Parameters Range	5.6-3
5.6.4 TRACG Model	5.6-3
5.6.5 Test Simulation	5.6-4
5.6.6 Results of Post-Test Calculations	5.6-4
5.6.6.1 Heated Drywell Tests	5.6-5
5.6.6.2 Unheated Drywell Test	5.6-7
5.6.6.3 Accuracy of TRACG Predictions	5.6-8
5.6.7 Summary and Conclusions	5.6-9
5.6.8 References	5.6-9
<b>5.7 PANDA Transient Tests (M-Series)</b>	<b>5.7-1</b>
5.7.1 Introduction	5.7-1
5.7.2 Test Facility and Test Matrix	5.7-2
5.7.3 Applicability of Data to SBWR	5.7-3
5.7.3.1 Overview of Data Applicability and Test Facility Scaling	5.7-3
5.7.3.2 PIRT Phenomena and Coverage	5.7-8
5.7.3.3 Conclusions on Data Applicability	5.7-12
5.7.4 PANDA TRACG Input Model Description	5.7-12
5.7.4.1 Wetwell, Drywell and GDCS Pool	5.7-12
5.7.4.2 RPV and Associated Piping	5.7-13
5.7.4.3 PCC and IC Condensers and Their Pools	5.7-13
5.7.4.4 Main Vents and Vacuum Breakers	5.7-14
5.7.4.5 System Line Flow Resistance	5.7-14
5.7.4.6 Component Heat Loss and Heat Capacity	5.7-15
5.7.4.7 Decay Heat	5.7-15
5.7.4.8 Comparison with SBWR Containment Model	5.7-16
5.7.4.9 Model Changes for Post-Test Analyses	5.7-17
5.7.5 TRACG Simulation of PANDA Tests	5.7-20
5.7.5.1 Initial Conditions	5.7-20
5.7.5.2 Test Control	5.7-21
5.7.5.3 Tests M3, M3A, and M3B	5.7-21
5.7.5.4 Tests M2, M10A, and M10B	5.7-22
5.7.5.5 Tests M6/8, M7, and M9	5.7-23

**Table of Contents**  
(continued)

	<u>Page</u>
5.7.6 Results Of Post-Test Calculations	5.7-23
5.7.6.1 Tests M3, M3A and M3B	5.7-25
5.7.6.2 Tests M2, M10A and M10B	5.7-30
5.7.6.3 Other Tests	5.7-37
5.7.6.4 Accuracy of TRACG Predictions	5.7-44
5.7.7 Summary and Conclusions	5.7-44
5.7.7.1 Purpose and Scope of Post-Test Evaluation	5.7-44
5.7.7.2 Evaluation of TRACG Qualification Needs	5.7-45
5.7.7.3 Summary of Conclusions	5.7-51
5.7.8 References	5.7-52
<b>6. NATURAL CIRCULATION AND FLOW OSCILLATION TESTS</b>	<b>6.1-1</b>
<b>6.1 Dodewaard Steady-State Operation</b>	<b>6.1-2</b>
6.1.1 Introduction	6.1-2
6.1.2 Description of Dodewaard	6.1-2
6.1.3 Applicability of Data to SBWR	6.1-3
6.1.4 TRACG Model	6.1-5
6.1.5 TRACG Simulation	6.1-6
6.1.6 Results of Calculations	6.1-7
6.1.7 Summary and Conclusions	6.1-8
6.1.8 References	6.1-8
<b>6.2 Analysis of February 1992 Startup of Dodewaard Natural Circulation BWR</b>	<b>6.2-1</b>
6.2.1 Introduction	6.2-1
6.2.2 Dodewaard Plant and Startup Procedure	6.2-1
6.2.2.1 Brief Description of Dodewaard	6.2-1
6.2.2.2 Normal Startup Procedure	6.2-2
6.2.2.3 Sequence of Steps During February 1992 Startup	6.2-2
6.2.2.4 General Discussion of First Phase of Startup	6.2-2
6.2.2.5 Discussion of the Measurements	6.2-3
6.2.3 Applicability of the Dodewaard Startup Data to the SBWR	6.2-5
6.2.4 TRACG Model of Dodewaard for Startup Simulation	6.2-7
6.2.4.1 Model Description	6.2-8
6.2.4.2 Vessel	6.2-8
6.2.5 Simulation of the February 1992 Startup	6.2-9
6.2.5.1 Initial Conditions	6.2-9
6.2.5.2 Boundary Conditions	6.2-10
6.2.6 Qualification Results	6.2-11
6.2.6.1 Comparison of TRACG Results with Measured Data	6.2-11
6.2.6.2 Analysis of Other TRACG Results	6.2-14
6.2.6.3 General Analysis of TRACG Results	6.2-15
6.2.6.4 Discussion of the Results	6.2-18

## Table of Contents

(continued)

	<u>Page</u>
6.2.6.5 Accuracy of TRACG Predictions	6.2-19
6.2.7 Conclusions/Results of the Assessment	6.2-19
6.2.7.1 General Conclusions	6.2-19
6.2.7.2 Adequacy of TRACG Models	6.2-20
6.2.8 References	6.2-20
<b>6.3 CRIEPI Low Pressure Oscillation Tests</b>	<b>6.3-1</b>
6.3.1 Introduction	6.3-1
6.3.2 Test Facility/Test Matrix	6.3-1
6.3.3 Applicability of Data to SBWR	6.3-2
6.3.4 TRACG Model	6.3-4
6.3.5 Test Simulation	6.3-4
6.3.6 Results of Post-Test Calculations	6.3-4
6.3.6.1 Accuracy of TRACG Calculations	6.3-7
6.3.7 Summary and Conclusion	6.3-7
6.3.8 References	6.3-7
<b>6.4 PANDA Exploratory Tests</b>	<b>6.4-1</b>
6.4.1 Introduction	6.4-1
6.4.2 Test Facility/Test Matrix	6.4-1
6.4.3 Applicability of Data to SBWR	6.4-3
6.4.4 TRACG Models	6.4-4
6.4.5 Test Simulation	6.4-5
6.4.6 Results of Post-Test Calculations	6.4-5
6.4.7 Summary and Conclusion	6.4-7
6.4.8 Reference	6.4-7
<b>6.5 Summary of Low-Power Stability Analyses</b>	<b>6.5-1</b>
6.5.1 Introduction	6.5-1
6.5.2 Review of Data from CRIEPI and PANDA Test Facilities	6.5-1
6.5.2.1 Sensitivity to Inlet Subcooling	6.5-2
6.5.2.2 Sensitivity to System Power	6.5-3
6.5.2.3 Sensitivity to System Pressure	6.5-3
6.5.2.4 Sensitivity to Static Head and Hydraulic Losses	6.5-3
6.5.3 Development of a Stability Map for Startup Oscillations	6.5-4
6.5.3.1 Criteria for the Upper Boundary	6.5-4
6.5.3.2 Criteria for the Lower Boundary	6.5-6
6.5.3.3 Effect of the Flashing Number	6.5-6
6.5.4 Implications for Dodewaard Startup	6.5-7
6.5.5 Implications for the SBWR Startup	6.5-8
6.5.6 Conclusions	6.5-9
6.5.7 References	6.5-10

**Table of Contents**

(continued)

	<u>Page</u>
<b>7. MODELING TECHNIQUES TO ADDRESS TRACG MODEL LIMITATIONS</b>	<b>7.1-1</b>
<b>7.1 Phenomena Requiring More Modeling Detail</b>	<b>7.1-1</b>
7.1.1 Passive Containment Condenser Modeling	7.1-1
7.1.2 Parallel PCC Operation	7.1-2
<b>7.2 Phenomena Treated with Bounding Models</b>	<b>7.2-1</b>
7.2.1 Operation of the Standby Liquid Control System (SLCS)	7.2-1
7.2.2 Suppression Pool Stratification	7.2-2
7.2.3 Stratification of Leakage Flow in the Wetwell Gas Space	7.2-3
7.2.4 Mixing of Drywell Noncondensable Gases	7.2-4
<b>7.3 Conclusions</b>	<b>7.3-1</b>
<b>7.4 References</b>	<b>7.4-1</b>
<b>8. SBWR PLANT NODALIZATION</b>	<b>8.1-1</b>
<b>8.1 SBWR Reactor Vessel</b>	<b>8.1-1</b>
8.1.1 Introduction	8.1-1
8.1.2 Evolution of SBWR Nodalization	8.1-1
8.1.3 Nodalization Rationale	8.1-2
8.1.4 Nodalization Feedback from Test Facility and BWR Plant Qualification	8.1-2
8.1.5 Nodalization for LOCA/ECCS	8.1-2
8.1.5.1 Reactor Vessel for LOCA/ECCS	8.1-3
8.1.5.2 Fuel Channels for LOCA/ECCS	8.1-4
8.1.5.3 Guide Tubes	8.1-5
8.1.5.4 Downcomer	8.1-5
8.1.5.5 GDCS Line	8.1-5
8.1.5.6 Chimney	8.1-6
8.1.5.7 Separators	8.1-6
8.1.5.8 Dryers	8.1-7
8.1.5.9 Main Steamlines for LOCA/ECCS	8.1-7
8.1.5.10 Feedwater System	8.1-8
8.1.5.11 Isolation Condensers	8.1-8
8.1.5.12 PCCS for LOCA/ECCS	8.1-8
8.1.5.13 Control System for LOCA/ECCS	8.1-9
8.1.5.14 Containment Model for LOCA/ECCS	8.1-9
8.1.6 Nodalization for Transients	8.1-9
8.1.6.1 Fuel Channels Grouping for Transients	8.1-10
8.1.6.2 Main Steamlines for Transients	8.1-10
8.1.6.3 Control System for Transients	8.1-11
8.1.7 References	8.1-11

**Table of Contents**

(continued)

	<b><u>Page</u></b>
<b>8.2 Containment</b>	<b>8.2-1</b>
8.2.1 RPV and Containment Volumes	8.2-1
8.2.2 One-Dimensional Components	8.2-2
8.2.2.1 Lower Drywell	8.2-3
8.2.2.2 Fuel Bundles	8.2-3
8.2.2.3 PCCS	8.2-3
8.2.2.4 ICS	8.2-4
8.2.2.5 GDCS One-Dimensional Components	8.2-4
8.2.2.6 Steamlines	8.2-4
8.2.2.7 SRVs	8.2-4
8.2.2.8 DPVs	8.2-5
8.2.2.9 LOCA Vents	8.2-5
8.2.2.10 Vacuum Breakers	8.2-5
8.2.2.11 Equalization Lines	8.2-5
8.2.2.12 RPV Pressure Taps	8.2-6
8.2.2.13 Gas Generation by Radiolysis and Metal/Water Reaction	8.2-6
8.2.2.14 DW-to-WW Bypass Leakage	8.2-6
8.2.2.15 Feedwater and Control Rod Drive Flow	8.2-6
8.2.2.16 Refill Pool	8.2-6
8.2.2.17 MSIVs	8.2-7
8.2.2.18 Components to Simulate Other Breaks	8.2-7
<b>9. ASSESSMENT OF TRACG QUALIFICATION</b>	<b>9.1-1</b>
<b>9.1 Adequacy of TRACG Models</b>	<b>9.1-1</b>
9.1.1 LOCA/ECCS	9.1-2
9.1.1.1 Key Safety Parameters	9.1-2
9.1.1.2 PIRT Phenomena	9.1-3
9.1.2 Transients	9.1-6
9.1.2.1 Key Safety Parameters	9.1-6
9.1.2.2 PIRT Phenomena	9.1-8
9.1.3 Stability	9.1-8
9.1.3.1 Key Safety Parameters	9.1-9
9.1.3.2 PIRT Phenomena	9.1-10
9.1.4 Containment	9.1-10
9.1.4.1 Key Safety Parameters	9.1-10
9.1.4.2 PIRT Phenomena	9.1-14
9.1.5 Plant Startup	9.1-16
9.1.5.1 Natural Circulation Flow (Startup Conditions)	9.1-17
9.1.5.2 Low Pressure Oscillations During Startup	9.1-17
9.1.6 References	9.1-18



**Table of Contents**  
(continued)

	<u><b>Page</b></u>
<b>9.2 Adequacy of Qualification Coverage</b>	<b>9.2-1</b>
9.2.1 Reactor Vessel and Core	9.2-1
9.2.1.1 Lower Plenum	9.2-1
9.2.1.2 Bypass	9.2-2
9.2.1.3 Core	9.2-3
9.2.1.4 Guide Tubes	9.2-8
9.2.1.5 Downcomer	9.2-8
9.2.1.6 Chimney	9.2-10
9.2.1.7 Separators	9.2-11
9.2.1.8 ATWS	9.2-12
9.2.1.9 Steamline	9.2-12
9.2.1.10 Isolation Condenser	9.2-13
9.2.1.11 Stability	9.2-13
9.2.1.12 RPV	9.2-14
9.2.1.13 Interactions	9.2-14
9.2.2 Containment	9.2-15
9.2.2.1 Break	9.2-15
9.2.2.2 Main Vent	9.2-15
9.2.2.3 SRV	9.2-16
9.2.2.4 Drywell	9.2-16
9.2.2.5 Wetwell	9.2-17
9.2.2.6 PCCS	9.2-18
9.2.2.7 Drywell/Wetwell Boundary	9.2-20
9.2.2.8 Vacuum Breaker	9.2-20
9.2.2.9 Equalizing Line	9.2-21
9.2.2.10 RPV	9.2-21
9.2.2.11 DPV	9.2-21
9.2.2.12 System Interactions	9.2-21
9.2.3 References	9.2-22
 <b>10. CONCLUSIONS</b>	 <b>10-1</b>
<b>10.1 References</b>	<b>10-2</b>
 <b>APPENDIX A Comparison Between TRACG02 and TRACG04</b>	 <b>A-1</b>

**List of Tables**

**— VOLUME 1 —**

	<b><u>Page</u></b>	
Table 1.2-1	Versions of TRACG used for Qualification Studies	1.2-5
Table 2.0-1	Database Used to Support TRACG Models and Qualification for SBWR	2-7
Table 2.1-1	PIRT Phenomena Added or Deleted for the LOCA/ECCS	2.1-7
Table 2.1-2	PIRT Parameters Added or Deleted for the LOCA/Containment	2.1-8
Table 2.1-3a	Separate Effects Tests for Highly Ranked Phenomena for TRACG Qualification for SBWR - Reactor and Core	2.1-9
Table 2.1-3b	Separate Effects Tests for Highly Ranked Phenomena for TRACG Qualification for SBWR - Containment	2.1-13
Table 2.1-4a	Component Tests for Highly Ranked Phenomena for TRACG Qualification for SBWR - Reactor and Core	2.1-15
Table 2.1-4b	Component Tests of Highly Ranked Phenomena for TRACG Qualification for SBWR - Containment	2.1-18
Table 2.1-5a	Integral System Tests for Highly Ranked Phenomena for TRACG Qualification for SBWR - Reactor Vessel and Core	2.1-20
Table 2.1-5b	Integral System Tests for Highly Ranked Phenomena for TRACG Qualification for SBWR - Containment	2.1-22
Table 2.1-6a	BWR Plant Data for Highly Ranked Phenomena for TRACG Qualification for SBWR - Reactor Vessel and Core	2.1-24
Table 2.1-7a	Overall TRACG Qualification Coverage of Highly Ranked Phenomena for SBWR - Reactor Vessel and Core	2.4-28
Table 2.1-7b	Overall TRACG Qualification Coverage of Highly Ranked Phenomena for SBWR - Containment	2.4-30
Table 3.1-1	Comparison of Range of Parameters for Toshiba Tests and SBWR	3.1-6
Table 3.1-2	Comparison of Toshiba Void Data with TRACG Calculations	3.1-7
Table 3.2-1	Comparison of Key Parameters in the OHT Test Facility and SBWR Chimney Partitions	3.2-9
Table 3.2-2	Comparison of TRACG/OHT Void Fraction During the Time Periods of Varying Mass Flow Rate (280°C/6.4 MPa)	3.2-9
Table 3.2-3	Assessment of TRACG Accuracy for Ontario Hydro Tests	3.2-9
Table 3.3-1	Range of Parameters for SBWR Regions	3.3-12
Table 3.3-2	Summary of Void Fraction Comparisons	3.3-13
Table 3.3-3	TRACG Calculation of Pressure Response and Level Change for PSTF Level Swell Tests	3.3-13
Table 3.3-4	TRACG Calculation of Critical Flow	3.3-14
Table 3.3-5	TRACG Calculation of Frictional Pressure Drop	3.3-14
Table 3.3-6	Calculation of Natural Circulation Flow and Power for Onset of Stability	3.3-14

**List of Tables**

(continued)

	<b><u>Page</u></b>	
Table 4.1-1	PANTHERS/PCC Steady-State Performance Matrix at 5 kg/s Steam Flowrate for TRACG Post-Test Analysis	4.1-40
Table 4.1-2	PANTHERS/PCC Steady-State Performance Matrix at Extreme and Intermediate Ranges for TRACG Post-Test Analysis	4.1-41
Table 4.1-3	PANTHERS/PCC Transient Performance Matrix for TRACG Post-Test Analysis	4.1-41
Table 4.1-4	PANTHERS/PCC TRACG One-Tube Model Components and Junction Elevations	4.1-42
Table 4.1-5	Heat Transfer Correspondence Between Condenser Tube Cells and PCC Pool Cells	4.1-43
Table 4.1-6	PANTHERS PCC TRACG Eight-Tube Model Components	4.1-43
Table 4.1-7	TRACG Calculated Pressure Losses for Test 15_1 Compared with PANTHERS DP Measurements	4.1-44
Table 4.1-8	Functions of TRACG Components for Specifying PANTHERS/PCC Test Boundary Conditions	4.1-45
Table 4.1-9	TRACG Input Flow Rates and Properties for Noncondensable Gas Accumulation Tests	4.1-45
Table 4.1-10	PANTHERS/PCC Tests Included in Post-Test Evaluation	4.1-46
Table 4.1-11	Test Conditions for Steady-State Pure-Steam Tests Included in Post-Test Evaluation	4.1-46
Table 4.1-12	Test Conditions for Steady-State Steam-Air Tests Included in Post-Test Evaluation	4.1-47
Table 4.1-13	Comparison of Results from 8-Tube and 1-Tube TRACG Input Models for Steady-State Steam-Air Tests	4.1-47
Table 4.1-14	Comparison of Inferred PANTHERS Film Coefficients with TRACG Calculations for Pure-Steam Tests	4.1-48
Table 4.1-15a	Test Conditions for Evaluation of Tube-to-Tube Variations	4.1-49
Table 4.1.15b	Axial Average Wall Temperature Difference for Four Instrumented Tubes	4.1-49
Table 4.1.15c	Axial Variation of External Tube Wall Temperature for Test 09_9	4.1-49
Table 4.1-16	Assessment of TRACG Accuracy for PANTHERS PCC SS Steam-Air Tests	4.1-50
Table 4.1-17	Assessment of TRACG Accuracy for PANTHERS PCC SS Pure-Steam Tests	4.1-51
Table 4.1-18	Maximum Measurement Uncertainties	4.1-51
Table 4.1-19	Maximum Measurement Uncertainty for Condenser Efficiency	4.1-52
Table 4.2-1	PANTHERS IC Test Maximum Measurement Uncertainties	4.2-16
Table 4.2-2	PANTHERS IC Steady-State Performance Matrix for TRACG Post-Test Analysis	4.2-16
Table 4.2-3	PANTHERS IC Transient Performance Matrix for TRACG Post-Test Analysis	4.2-16
Table 4.2-4	Components for Simulation of PANTHERS IC Test	4.2-17
Table 4.2-5	TRACG Input Flow Rate and Properties For Noncondensable Gas	4.2-18
Table 4.2-6	PANTHERS IC Tests Included in Post-Test Evaluation	4.2-18
Table 4.2-7	Test Conditions for Steady-State Post-Test Evaluation	4.2-18
Table 4.2-8	Comparison of PANTHERS and TRACG for Steady-State Evaluation	4.2-18
Table 4.2-9	Comparison of PANTHERS and TRACG Noncondensable Gas Inventory at 7.8 MPa for Test T12	4.2-19

**List of Tables**

(continued)

		<u>Page</u>
Table 4.2-10	Comparison of PANTHERS and TRACG Noncondensable Gas Inventory at 5.2 Mpa for Test T13	4.2-19
Table 4.2-11	TRACG Calculation of NC Gas Distribution at 5.23 MPa Inlet Pressure	4.2-19
Table 4.2-12	Assessment of TRACG Accuracy for PANTHERS IC Tests	4.2-20
Table 4.3-1	PANDA Steady-State PCC Performance Test Matrix	4.3-12
Table 4.3-2	Comparison of TRACG PCC Nodalizations for PANDA and SBWR. Containment Model	4.3-12
Table 4.3-3	Actual Conditions for PANDA Steady-State Performance Tests and TRACG Post-Test Calculations	4.3-13
Table 4.3-4	PCCS Inlet Velocities for TRACG Post-Test Calculations	4.3-13
Table 4.3-5	Void Fractions in Pool Cells with Liquid Levels	4.3-14
Table 4.3-6	Correspondence Between PANDA Measurements and TRACG Model Locations	4.3-14
Table 4.3-7	Maximum Measurement Uncertainties for PANDA Steady-State PCC Tests	4.3-15
Table 4.3-8	Condenser Efficiencies from PANDA Steady-State Steam-Air Tests Compared with TRACG Calculations	4.3-16
Table 4.3-9	Condenser Inlet Pressures from PANDA Steady-State Pure-Steam Tests Compared with TRACG Calculations	4.3-16
Table 4.3-10	Assessment of TRACG Accuracy for PANDA PCC Tests	4.3-17
Table 4.4-1	Comparison of PSTF and SBWR Parameters	4.4-8
Table 4.4-2	Comparison of Pool Total Thermal Energy - TRACG vs Data for Test 5807-29	4.4-9
Table 4.4-3	Assessment of TRACG Accuracy for PSTF Suppression Pool Stratification Tests	4.4-10

— VOLUME 2 —

Table 5.1-1	GIST Facility Tests Selected for TRACG Qualification	5.1-18
Table 5.1-2	GIST Nodalization vs SBWR Nodalization	5.1-19
Table 5.1-3	GIST Initial Conditions Used in TRACG Input	5.1-20
Table 5.1-4	GIST TRACG Comparison Results	5.1-20
Table 5.2-1	Test Matrix of Initial DW Conditions for GIRAFFE/Helium Tests	5.2-29
Table 5.2-2	Definition of TRACG Input Model Components	5.2-30
Table 5.2-3	Comparison of GIRAFFE/Helium and SBWR TRACG Containment Nodalization	5.2-31
Table 5.2-4	Initial Conditions for GIRAFFE/Helium Tests H1-H4	5.2-32
Table 5.2-5	Initial Conditions for GIRAFFE Test T2 <sup>2</sup>	5.2-32
Table 5.2-6	Assessment of TRACG Accuracy for GIRAFFE Helium Tests	5.2-33
Table 5.3-1	List of 1-D Components	5.3-25
Table 5.3-2	TRACG Nodalization vs. SBWR Nodalization	5.3-27
Table 5.3-3	Initial Conditions for Test GS1 GDC Line Break, DPV Failure, IC/PCC off	5.3-28
Table 5.3-4	Initial Conditions for GS2 GDC Line Break, DPV Failure, IC/PCC on	5.3-29
Table 5.3-5	Initial Conditions for GS3 BDL Break, DPV Failure, IC/PCC on	5.3-30

**List of Tables**

(continued)

	<b><u>Page</u></b>
Table 5.3-6	Initial Conditions for GS4 GDC Line Break, GDC Valve Failure, IC/PCC on 5.3-31
Table 5.3-7	Ratio of the Calculated Elevation Pressure Drop to the Total Pressure 5.3-32
	Drop Results from Test GS1
Table 5.3-8	Summary of Test and TRACG Comparisons 5.3-33
Table 5.4-1	Dimensions and Grouping of the Channels 5.4-10
Table 5.5-1	Test Initial Conditions 5.5-7
Table 5.5-2	Comparison of PSTF and SBWR Parameters 5.5-7
Table 5.5-3	Summary of TRACG Calculations vs Measured Data 5.5-8
Table 5.5-4	Assessment of TRACG Accuracy for PSTF Mark III Tests 5.5-9
Table 5.6-1	Test Series 5101 Tests for TRACG Simulation 5.6-10
Table 5.6-2	Comparison of 4T/Mark II PSTF and SBWR Parameters 5.6-10
Table 5.6-3	Summary of TRACG Results vs Test Data 5.6-11
Table 5.6-4	Drywell Wall Steam Condensation - TRACG vs Measured Data 5.6-11
Table 5.6-5	Assessment of TRACG Accuracy for 4T Mark II Tests 5.6-12
Table 5.7-1	PANDA/TRACG VSSL01 Component Breakdown 5.7-54
Table 5.7-2	PANDA/TRACG Components with Connections to VSSL01 Cells 5.7-55
Table 5.7-3	PANDA/TRACG RPV Components 5.7-55
Table 5.7-4	PANDA/TRACG PCCS Components 5.7-56
Table 5.7-5	PANDA/TRACG ICS Components 5.7-57
Table 5.7-6	Other PANDA/TRACG Components 5.7-57
Table 5.7-7	PANDA Heater Power vs. Time for All Tests Except M7 and M9 5.7-58
Table 5.7-8	PANDA Heater Power vs. Time for Test M9 5.7-59
Table 5.7-9	Comparison of PANDA and SBWR Component Nodalizations 5.7-60
Table 5.7-10	Initial Conditions for PANDA Test M3 5.7-61
Table 5.7-11	Initial Conditions for PANDA Test M3A 5.7-61
Table 5.7-12	Initial Conditions for PANDA Test M3B 5.7-61
Table 5.7-13	Initial Conditions for PANDA Test M2 5.7-62
Table 5.7-14	Initial Conditions for PANDA Test M10A 5.7-62
Table 5.7-15	Initial Conditions for PANDA Test M10B 5.7-62
Table 5.7-16	Initial Conditions for PANDA Test M6/8 5.7-63
Table 5.7-17	Initial Conditions for PANDA Test M7 5.7-63
Table 5.7-18	Initial Conditions for PANDA Test M9 5.7-63
Table 5.7-19	PCC Instrumentation for PANDA Post-Test Evaluation 5.7-65
Table 5.7-20	DW Instrumentation for PANDA Post-Test Evaluation 5.7-66
Table 5.7-21	WW Instrumentation for PANDA Post-Test Evaluation 5.7-67
Table 5.7-22	Oxygen Probe Instrumentation for PANDA Post-Test Evaluation 5.7-68
Table 5.7-23	IC Instrumentation for Post-Test Evaluation of PANDA Test M6/8 5.7-68
Table 5.7-24	Main Vent Instrumentation for Post-Test Evaluation of PANDA Tests 5.7-68
	M10A, M10B, and M7
Table 5.7-25	RPV and GDCS Level Instrumentation for Post-Test Evaluation of PANDA 5.7-69
	Tests M7 and M9
Table 5.7-26	PANDA Measurement Uncertainties 5.7-69
Table 5.7-27	Assessment of TRACG Accuracy for PANDA Transient (M-Series) Tests 5.7-70

**List of Tables**

(continued)

		<u>Page</u>
Table 6.1-1	Comparison of Dodewaard and SBWR Steady-State Parameters	6.1-10
Table 6.1-2	Dodewaard Nodalization vs. SBWR Nodalization	6.1-11
Table 6.1-3	Comparison of TRACG Steady-State Calculations to Plant Parameters	6.1-12
Table 6.2-1	Sequence of Steps of a Regular Startup	6.2-22
Table 6.2-2	Sequence of Steps During February 1992 Startup	6.2-23
Table 6.2-3	Overview of All Available Measurement Data	6.2-25
Table 6.2-4	Comparison of Key Features of Dodewaard and SBWR	6.2-26
Table 6.2-5	Vessel Axial and Radial Nodalization	6.2-27
Table 6.2-6	Channel Initial Conditions	6.2-28
Table 6.2-7	Measurement Data Used for Initial and Boundary Conditions	6.2-29
Table 6.2-8	Calculation of Subcooling Number and Phase Change Number	6.2-31
Table 6.2-9	Assessment of TRACG Accuracy for Dodewaard Startup Tests	6.2-32
Table 6.3-1	Forced Flow Data Points	6.3-9
Table 6.3-2	Test Matrix (System Pressure = 0.2 MPa , Channel Power = 2.5 kW/chan)	6.3-9
Table 6.3-3	Comparison of Nondimensional Parameters Between the Test Loop and SBWR	6.3-9
Table 6.3-4	Assessment of TRACG Accuracy for CRIEPI Low Pressure Oscillation Tests	6.3-10
Table 6.4-1	Test Matrix for PANDA E-series Tests	6.4-8
Table 6.4-2	Major Observations from PANDA E-series Tests ( Pressure)	6.4-9
Table 6.4-3	Major Observation from PANDA E-series Tests (Flow)	6.4-10
Table 6.4-4	Comparison of the Key Features of PANDA Facility and SBWR	6.4-11
Table 6.5-1	Dependence of the Period and Amplitude of CRIEPI Oscillations on Inlet Subcooling	6.5-11
Table 6.5-2	Dependence of the Upper and Lower CRIEPI Oscillatory Boundary on Channel Power (System Pressure = 0.2 MPa)	6.5-11
Table 6.5-3	Calculated Subcooling and Phase Change Numbers at Upper Boundary of Oscillatory Region	6.5-12
Table 6.5-4	Calculated Channel Inlet Subcooling at Lower Boundary of Oscillatory Region	6.5-12
Table 8.1-1a	Major Findings from Test Facility Nodalization Factored into the SBWR TRACG Model	8.1-12
Table 8.1-1b	SBWR Nodalization vs. TRACG Facility Nodalization for LOCA/ECCS and Transients	8.1-13
Table 8.1-1c	Justification of SBWR TRACG RPV Input Model Approach for LOCA/ECCS	8.1-16
Table 8.1-2	TRACG Components Used for LOCA/ECCS and Transient Decks	8.1-18
Table 8.1-3	SBWR TRACG Vessel Nodalization - Axial Levels (LOCA/ECCS)	8.1-19
Table 8.1-4	TRACG Description of the SBWR Vessel Regions (LOCA/ECCS)	8.1-20
Table 8.1-5	Grouping of Fuel Channels in Vessel Radial Rings (LOCA/ECCS)	8.1-21
Table 8.1-6	Grouping of Fuel Channels in Vessel Radial Rings (Transients)	8.1-21
Table 8.1-7	TRACG Description of the SBWR Containment (LOCA/ECCS)	8.1-22

**List of Tables**

(continued)

	<b><u>Page</u></b>	
Table 8.2-1	Radial Ring Boundaries of VSSL Component in SBWR TRACG Containment Model	8.2-8
Table 8.2-2	Axial Level Boundaries of VSSL Component in SBWR TRACG Containment Model	8.2-9
Table 8.2-3	SBWR TRACG Containment Model Components (* denotes connection is specific to main steamlines break simulation)	8.2-10
Table 8.2-4	SBWR TRACG Containment Model Approach vs. Test Facility Modeling Approach	8.2-14
Table 8.2-5	Justification of SBWR TRACG Containment Model Approach	8.2-18
Table 9.1-1	Accuracy of TRACG Calculations for RPV Level	9.1-19
Table 9.1-2	Accuracy of TRACG Calculations for Core Void Fraction	9.1-19
Table 9.1-3	Accuracy of TRACG Calculations for Chimney, Lower Plenum and Downcomer Void Fraction	9.1-20
Table 9.1-4	Accuracy of TRACG Calculations for RPV Break Flow	9.1-21
Table 9.1-5	Accuracy of TRACG Calculations for GDCS Flow	9.1-21
Table 9.1-6	Accuracy of TRACG Calculations for IC Heat Removal	9.1-21
Table 9.1-7	Accuracy of TRACG Calculations for Natural Circulation and Stability	9.1-22
Table 9.1-8	Accuracy of TRACG Calculations for Peak Neutron Flux	9.1-22
Table 9.1-9	Accuracy of TRACG Calculations for Short-Term Containment Pressure	9.1-23
Table 9.1-10	Accuracy of TRACG Calculations for Long-Term Containment Pressure	9.1-23
Table 9.1-11	Accuracy of TRACG Calculations for DW Temperature	9.1-24
Table 9.1-12	Accuracy of TRACG Calculations for WW Gas Temperature	9.1-24
Table 9.1-13	Accuracy of TRACG Calculations for Vent Clearing Time	9.1-25
Table 9.1-14	Accuracy of TRACG Calculations for WW Liquid Temperature	9.1-25
Table 9.1-15	Accuracy of TRACG Calculations for PCC Heat Removal	9.1-26
Table 9.1-16	Accuracy of TRACG Calculations for PCC Pressure Drop	9.1-26
Table 9.1-17	Accuracy of TRACG Calculations for Natural Circulation Flow (Startup Conditions)	9.1-27
Table 9.1-18	Accuracy of TRACG Calculations of Flow Oscillations During Startup	9.1-27

## List of Figures

### — VOLUME 1 —

	<u>Page</u>	
Figure 1.2-1	Road Map of SBWR TRACG Related Documentation	1.2-9
Figure 1.3-1	Qualification Report Roadmap	1.3-4
Figure 2.1-1	SBWR LOCA Phases and Major Test Coverage	2.1-32
Figure 3.1-1	Test Bundle Cross-Section [3.1-1]	3.1-8
Figure 3.1-2	External View of Test Section [3.1-1]	3.1-9
Figure 3.1-3	Void Measurement Section [3.1-1]	3.1-10
Figure 3.1-4	TRACG Model for Toshiba Test	3.1-11
Figure 3.1-5	TRACG Calculations of Toshiba CT Void Data (1.00 MPa and 1390 Kg/m <sup>2</sup> -s )	3.1-12
Figure 3.1-6	TRACG Calculation of Toshiba CT Void Data (1.00 MPa and 833 Kg/m <sup>2</sup> -s)	3.1-12
Figure 3.1-7	TRACG Calculation of Toshiba CT Void Data (0.50 MPa and 1390 Kg/m <sup>2</sup> -s )	3.1-13
Figure 3.2-1	Schematic Diagram of the Test Facility [3.2-2]	3.2-10
Figure 3.2-2	Schematic Diagram of the Test Section [3.2-2]	3.2-11
Figure 3.2-3	Radial Void Fraction Distribution at Nominal Temperature of 280°C	3.2-12
Figure 3.2-4	Average Void Fraction as Obtained from the Gamma Densitometer Measurements Versus those Obtained using the Axial Pressure Drop Measurements at Nominal Temperature of 280°C	3.2-13
Figure 3.2-5	TRACG Model Description of OHT Test	3.2-14
Figure 3.2-6	Local Void Fluctuations (around 2000 s) at Nominal Temperature of 280°C	3.2-15
Figure 3.2-7	Local Void Fluctuations (around 2500 s) at Nominal Temperature of 280°C	3.2-16
Figure 3.2-8	Comparison of TRACG and Time-averaged Data - Average Void Fraction at Nominal Temperature of 280°C	3.2-17
Figure 3.3-1	Critical Power vs. Length (Columbia Data) [3.3-17])	3.3-15
Figure 3.3-2	Critical Power Comparisons for 2.8m GE8 Fuel Bundle – GEXL02 Correlation vs. COBRAG	3.3-16
Figure 4.1-1	Passive Containment Condenser Test Article	4.1-53
Figure 4.1-2	PANTHERS/PCC Test Facility Schematic	4.1-54
Figure 4.1-3	PCC Operational Modes	4.1-55
Figure 4.1-4	PANTHERS Representation of PCC Operational Modes	4.1-56
Figure 4.1-5	TRACG PANTHERS/PCC Qualification Points	4.1-57
Figure 4.1-6	Schematic of TRACG PANTHERS/PCC One-Tube Input Model	4.1-58
Figure 4.1-7	Nodalization of Inlet Line (TEE22)	4.1-59
Figure 4.1-8	Nodalization of Upper (PIPE92) and Lower (TEE26) Headers	4.1-60
Figure 4.1-9	Nodalization of PCC Tubes (PIPE96)	4.1-61
Figure 4.1-10	Nodalization of Drain Line (PIPE46)	4.1-62



**List of Figures**  
(continued)

	<b><u>Page</u></b>
Figure 4.1-11 Nodalization of Vent Line (PIPE52)	4.1-63
Figure 4.1-12 Nodalization of Pools (VSSL01 and TEE40)	4.1-64
Figure 4.1-13 Nodalization of the PANTHERS/PCC Eight-Tube TRACG Model	4.1-65
Figure 4.1-14 Comparison of TRACG and PANTHERS Inlet Pressure for Pure-Steam Tests	4.1-66
Figure 4.1-15 Comparison of TRACG and Panthers Condensation Efficiency and Pressure Drop for Test 9	4.1-67
Figure 4.1-16 Comparison of TRACG and PANTHERS Condensation Efficiency and Pressure Drop for Test 15	4.1-68
Figure 4.1-17 Comparison of TRACG and PANTHERS Condensation Efficiency and Pressure Drop for Test 18	4.1-69
Figure 4.1-18 Comparison of TRACG and PANTHERS Condensation Efficiency and Pressure Drop for Test 23	4.1-70
Figure 4.1-19 Comparison of TRACG and PANTHERS Condensation Efficiency and Pressure Drop for Test 2	4.1-71
Figure 4.1-20 Comparison of TRACG and PANTHERS Condensation Efficiency and Pressure Drop for Test 17	4.1-72
Figure 4.1-21 Comparison of TRACG and PANTHERS Condensation Efficiency and Pressure Drop for Test 19	4.1-73
Figure 4.1-22 Comparison of TRACG and PANTHERS Condensation Efficiency and Pressure Drop for Test 22	4.1-74
Figure 4.1-23 Comparison of TRACG and PANTHERS Condensation Efficiency and Pressure Drop for Test 35	4.1-75
Figure 4.1-24 Comparison of TRACG and PANTHERS Condensation Efficiency and Pressure Drop for Test 2 with Heat Transfer Between Vent Line and Drain Line	4.1-76
Figure 4.1-25 Comparison of TRACG and PANTHERS Inlet Pressure for Test 51	4.1-77
Figure 4.1-26 Comparison of TRACG and PANTHERS Inlet Pressure for Test 76	4.1-78
Figure 4.1-27 Comparison of TRACG and PANTHERS Inlet Pressure for Test 78	4.1-79
Figure 4.1-28 Comparison of TRACG and PANTHERS Inlet Pressure for Test 54	4.1-80
Figure 4.1-29 Location of the PCC Instrumented Tubes and Thermocouples	4.1-81
Figure 4.1-30 Comparison of Average Tube Wall Temperature Measurements to TRACG Calculations - PANTHERS Test T15_1	4.1-82
Figure 4.1-31 Comparison of Average Tube Wall Temperature Measurements to TRACG Calculations - PANTHERS Test T43_2	4.1-83
Figure 4.2-1 Isolation Condenser Test Heat Exchanger Assembly	4.2-21
Figure 4.2-2 PANTHERS IC Test Facility Schematic	4.2-22
Figure 4.2-3 TRACG Nodalization for Simulation of PANTHERS IC Test	4.2-23
Figure 4.2-4 Comparison of TRACG and PANTHERS for Steady-State Tests	4.2-24
Figure 4.2-5 Comparison of TRACG and PANTHERS Inlet Pressure Transient for Test T12	4.2-25
Figure 4.2-6 Comparison of TRACG and PANTHERS Heat Transfer for Test T12	4.2-25
Figure 4.2-7 Comparison of TRACG and PANTHERS Inlet Pressure Transient for Test T13	4.2-26
Figure 4.2-8 Comparison of TRACG and PANTHERS Heat Transfer for Test T13	4.2-26
Figure 4.2-9 Comparison of TRACG and PANTHERS for Pool Level Test	4.2-27

**List of Figures**  
(continued)

	<u>Page</u>	
Figure 4.3-1	TRACG Model of the PANDA PCCS as Modified for the Steady-State Tests	4.3-18
Figure 4.3-2	TRACG Model of the PANDA PCCS Inlet Pipe as Modified for the Steady-State Tests	4.3-18
Figure 4.3-3	TRACG Model of the PANDA PCCS Secondary Side	4.3-19
Figure 4.3-4	Comparison of TRACG Calculations of Condenser Efficiency with PANDA Measurements (Steam-Air Tests)	4.3-20
Figure 4.3-5	Comparison of TRACG Calculations of Condenser Inlet Pressure with PANDA Measurements (Pure-Steam Tests)	4.3-20
Figure 4.4-1	Pressure Suppression Test Facility - Test 5707 Series	4.4-11
Figure 4.4-2	Pressure Suppression Test Facility - Test 5807 Series	4.4-12
Figure 4.4-3	TRACG Component Layout	4.4-13
Figure 4.4-4	TRACG Modeling of Eight Degree WW Section	4.4-14
Figure 4.4-5	TRACG Modeling of Vent System	4.4-15
Figure 4.4-6	TRACG Suppression Pool Nodalization	4.4-16
Figure 4.4-7	Temperature Profile of Volume 5 - Test 5707-01	4.4-17
Figure 4.4-8	Temperature Profile of Volume 1 - Test 5807-29	4.4-18
Figure 4.4-9	Temperature Profile of Volume 2 - Test 5807-29	4.4-19
Figure 4.4-10	Temperature Profile of Volume 3 - Test 5807-29	4.4-20
Figure 4.4-11	Temperature Profile of Volume 4 - Test 5807-29	4.4-21
Figure 4.4-12	Temperature Profile of Volume 5 - Test 5807-29	4.4-22
Figure 4.4-13	Temperature Profile of Volume 6 - Test 5807-29	4.4-23

— VOLUME 2 —

Figure 5.0-1	SBWR LOCA Phases and Major Test Coverage	5.1-3
Figure 5.1-1	GIST Facility	5.1-21
Figure 5.1-2	GIST Facility - Major Flow Paths	5.1-22
Figure 5.1-3	GIST Facility -Pressure Vessel	5.1-23
Figure 5.1-4	TRACG Nodalization of GIST RPV	5.1-24
Figure 5.1-5	Nodalization of GIST Containment	5.1-25
Figure 5.1-6	TRACG Nodalization of GIST Steamlines	5.1-25
Figure 5.1-7	TRACG Nodalization for GDCS Line Calibration	5.1-26
Figure 5.1-8	GIST RPV Blowdown	5.1-27
Figure 5.1-9	Comparison of RPV Pressures (Bottom Drain Line LOCA-A07)	5.1-28
Figure 5.1-10	Comparison of Upper Drywell Pressure (Test A07)	5.1-28
Figure 5.1-11	Comparison of Wetwell Pressure (Test A07)	5.1-29
Figure 5.1-12	Comparison of GDCS Flow Rate (Test A07)	5.1-29
Figure 5.1-13	Comparison of Annulus Pressure Drop (Test A07)	5.1-30
Figure 5.1-14	Comparison of Core Pressure Drop (Test A07)	5.1-30
Figure 5.1-15	Comparison of Bypass Pressure Drop (Test A07)	5.1-31
Figure 5.1-16	Comparison of Standpipe Pressure Drop (Test A07)	5.1-31
Figure 5.1-17	Comparison of RPV Pressure (Test B01)	5.1-32
Figure 5.1-18	Comparison of RPV Pressure (Test B07)	5.1-32
Figure 5.1-19	Comparison of RPV Pressure (Test C01A)	5.1-33
Figure 5.1-20	Comparison of RPV Pressure (Test D03A)	5.1-33
Figure 5.1-21	Comparison of GDCS Flow (Test B01)	5.1-34

**List of Figures**  
(continued)

	<u>Page</u>
Figure 5.1-22 Comparison of GDCS Flow (Test B07)	5.1-34
Figure 5.1-23 Comparison of GDCS Flow (Test C01A)	5.1-35
Figure 5.1-24 Comparison of GDCS Flow (Test D03A)	5.1-35
Figure 5.1-25 Comparison of Annulus Pressure Drop (Test B01)	5.1-36
Figure 5.1-26 Comparison of Annulus Pressure Drop (Test B07)	5.1-36
Figure 5.1-27 Comparison of Annulus Pressure Drop (Test C01A)	5.1-37
Figure 5.1-28 Comparison of Annulus Pressure Drop (Test D03A)	5.1-37
Figure 5.1-29 Comparison of Core Pressure Drop (Test B01)	5.1-38
Figure 5.1-30 Comparison of Core Pressure Drop (Test B07)	5.1-38
Figure 5.1-31 Comparison of Core Pressure Drop (Test C01A)	5.1-39
Figure 5.1-32 Comparison of Core Pressure Drop (Test D03A)	5.1-39
Figure 5.1-33 Calculated Annulus Level (Test B07)	5.4-40
Figure 5.1-34 Comparison of Rod Temperatures (Test B07)	5.4-41
Figure 5.1-35 Calculated Core Axial Void Profile (Test B07)	5.4-42
Figure 5.2-1 GIRAFFE Facility Layout	5.2-34
Figure 5.2-2 TRACG Nodalization of the Vessel Component	5.2-35
Figure 5.2-3 TRACG Nodalization of the Individual Vessels	5.2-36
Figure 5.2-4 PCC Nodalization	5.2-37
Figure 5.2-5 The RPV and Piping	5.2-38
Figure 5.2-6 Suppression Chamber and Piping	5.2-39
Figure 5.2-7 GDCS Pool and Piping	5.2-40
Figure 5.2-8 Drywell and Drywell Piping	5.2-41
Figure 5.2-9 H1: Drywell and Wetwell Pressure	5.2-42
Figure 5.2-10 H1: RPV and PCC Power	5.2-42
Figure 5.2-11 H1: PCC Mass Flow Rate	5.2-43
Figure 5.2-12 H1: PCC Nitrogen Partial Pressure	5.2-43
Figure 5.2-13 H1: DW Nitrogen Partial Pressure	5.2-44
Figure 5.2-14 H1: WW Nitrogen Partial Pressure	5.2-44
Figure 5.2-15 H1: DW and WW Pressure - Sensitivity to Increased PCC Heat Transfer Area	5.2-45
Figure 5.2-16 H1: PCC Nitrogen Partial Pressure - Sensitivity to Increased PCC Heat Transfer Area	5.2-45
Figure 5.2-17 H2: Drywell and Wetwell Pressure	5.2-46
Figure 5.2-18 H2: DW and WW Pressure - Simulated Helium Updraft from LDW	5.2-46
Figure 5.2-19 H2: RPV and PCC Power - Simulated Helium Updraft from LDW	5.2-47
Figure 5.2-20 H2: PCC Mass Flow Rate - Simulated Helium Updraft from LDW	5.2-47
Figure 5.2-21 H2: PCC Helium Partial Pressure - Simulated Helium Updraft from LDW	5.2-48
Figure 5.2-22 H2: DW Helium Partial Pressure - Simulated Helium Updraft from LDW	5.2-48
Figure 5.2-23 H2: WW Helium Partial Pressure - Simulated Helium Updraft from LDW	5.2-49
Figure 5.2-24 H2: DW and WW Pressure - Sensitivity to Specifying all Helium Initially in Top of UDW	5.2-49
Figure 5.2-25 H2: DW and WW Pressure - Sensitivity to 3 Cell -Header	5.2-50
Figure 5.2-26 H2: PCC Helium Partial Pressure - Sensitivity to 3 Cell-Header	5.2-50
Figure 5.2-27 H3: Drywell and Wetwell Pressure	5.2-51
Figure 5.2-28 H3: RPV and PCC Power	5.2-51
Figure 5.2-29 H3: PCC Mass Flow Rate	5.2-52
Figure 5.2-30 H3: PCC Noncondensable Gas Partial Pressure	5.2-52

**List of Figures**  
(continued)

	<b><u>Page</u></b>
Figure 5.2-31 H3: DW Helium Partial Pressure	5.2-53
Figure 5.2-32 H3: WW Helium Partial Pressure	5.2-53
Figure 5.2-33 H4: Drywell and Wetwell Pressure	5.2-54
Figure 5.2-34 H4: RPV and PCC Power	5.2-54
Figure 5.2-35 H4: PCC Mass Flow Rate	5.2-55
Figure 5.2-36 H4: PCC Noncondensable Gas Partial Pressure	5.2-55
Figure 5.2-37 H4: DW Helium Partial Pressure	5.2-56
Figure 5.2-38 H4: WW Helium Partial Pressure	5.2-56
Figure 5.2-39 T2: Drywell and Wetwell Pressure	5.2-57
Figure 5.2-40 T2: RPV and PCC Power	5.2-57
Figure 5.2-41 T2: PCC Mass Flow Rate	5.2-58
Figure 5.2-42 T2: PCC Nitrogen Partial Pressure	5.2-58
Figure 5.2-43 T2: DW Nitrogen Partial Pressure	5.2-59
Figure 5.2-44 T2: DW and WW Pressure - Sensitivity to Increased PCC Heat Transfer Area	5.2-59
Figure 5.3-1 GIRAFFE Facility Layout	5.3-34
Figure 5.3-2 RPV Internals	5.3-35
Figure 5.3-3 TRACG Vessel Nodalization	5.3-36
Figure 5.3-4 The RPV and Piping	5.3-37
Figure 5.3-5 Drywell and Drywell Piping	5.3-38
Figure 5.3-6 Wetwell and Piping	5.3-39
Figure 5.3-7 GDCS Pool and Piping	5.3-40
Figure 5.3-8 IC and PCC Models in TRACG	5.3-41
Figure 5.3-9 GS1 - RPV Dome Pressure	5.3-42
Figure 5.3-10 GS1 - DW Pressure	5.3-42
Figure 5.3-11 GS1 - WW Pressure	5.3-43
Figure 5.3-12 GS1 - RPV Dome Pressure	5.3-44
Figure 5.3-13 GS1 - DW Pressure	5.3-44
Figure 5.3-14 GS1 - WW Pressure	5.3-44
Figure 5.3-15 GS1 - Chimney Collapsed Level	5.3-45
Figure 5.3-16 GS1 - Channel Delta P	5.3-45
Figure 5.3-17 GS1 - Bypass Collapsed Level	5.3-46
Figure 5.3-18 GS1 - Downcomer Collapsed Level	5.3-46
Figure 5.3-19 GS1 - Chimney Collapsed Level	5.3-47
Figure 5.3-20 GS1 - Channel Delta P	5.3-47
Figure 5.3-21 GS1 - Bypass Collapsed Level	5.3-48
Figure 5.3-22 GS1 - Downcomer Collapsed Level	5.3-48
Figure 5.3-23 GS1 - GDCS Flow	5.3-49
Figure 5.3-24 GS1 - GDCS Flow	5.3-49
Figure 5.3-25 GS1 - GDCS - DW Break Flow	5.3-50
Figure 5.3-26 GS1 - RPV - DW Break Flow	5.3-50
Figure 5.3-27 GS1 - GDCS Pool Level	5.3-51
Figure 5.3-28 GS1 - GDCS Flow Volume	5.3-51
Figure 5.3-29 GS1 - GDCLB1 Flow Volume	5.3-52
Figure 5.3-30 GS2 - RPV Dome Pressure	5.3-53
Figure 5.3-31 GS2 - DW Pressure	5.3-53
Figure 5.3-32 GS2 - WW Pressure	5.3-54

**List of Figures**  
(continued)

	<u>Page</u>
Figure 5.3-33	5.3-54
Figure 5.3-34	5.3-55
Figure 5.3-35	5.3-55
Figure 5.3-36	5.3-56
Figure 5.3-37	5.3-56
Figure 5.3-38	5.3-57
Figure 5.3-39	5.3-57
Figure 5.3-40	5.3-58
Figure 5.3-41	5.3-58
Figure 5.3-42	5.3-59
Figure 5.3-43	5.3-59
Figure 5.3-44	5.3-60
Figure 5.3-45	5.3-60
Figure 5.3-46	5.3-61
Figure 5.3-47	5.3-61
Figure 5.3-48	5.3-62
Figure 5.3-49	5.3-62
Figure 5.3-50	5.3-63
Figure 5.3-51	5.3-64
Figure 5.3-52	5.3-64
Figure 5.3-53	5.3-65
Figure 5.3-54	5.3-65
Figure 5.3-55	5.3-66
Figure 5.3-56	5.3-66
Figure 5.3-57	5.3-67
Figure 5.3-58	5.3-67
Figure 5.3-59	5.3-68
Figure 5.3-60	5.3-68
Figure 5.3-61	5.3-69
Figure 5.3-62	5.3-69
Figure 5.3-63	5.3-70
Figure 5.3-64	5.3-70
Figure 5.3-65	5.3-71
Figure 5.3-66	5.3-71
Figure 5.3-67	5.3-72
Figure 5.3-68	5.3-72
Figure 5.3-69	5.3-73
Figure 5.3-70	5.3-73
Figure 5.3-71	5.3-74
Figure 5.3-72	5.3-74
Figure 5.3-73	5.3-75
Figure 5.3-74	5.3-75
Figure 5.3-75	5.3-76
Figure 5.3-76	5.3-76
Figure 5.3-77	5.3-77
Figure 5.3-78	5.3-77
Figure 5.3-79	5.3-78

**List of Figures**  
(continued)

	<b><u>Page</u></b>
Figure 5.3-80	GS4 - Downcomer Collapsed Level 5.3-78
Figure 5.3-81	GS4 - Chimney Collapsed Level 5.3-79
Figure 5.3-82	GS4 - Channel Delta-P 5.3-79
Figure 5.3-83	GS4 - Bypass Collapsed Level 5.3-80
Figure 5.3-84	GS4 - Downcomer Collapsed Level 5.3-80
Figure 5.3-85	GS4 - GDCS Flow 5.3-81
Figure 5.3-86	GS4 - GDCS Flow 5.3-81
Figure 5.3-87	GS4 - GDCS - DW Break Flow 5.3-82
Figure 5.3-88	GS4 - RPV - DW Break Flow 5.3-82
Figure 5.3-89	GS4 - GDCS Pool Level 5.3-83
Figure 5.3-90	GS4 - GDCS Flow Volume 5.3-83
Figure 5.3-91	GS4 - GDCLB1 Flow Volume 5.3-84
Figure 5.3-92	GS3 - No Heat Loss: RPV Pressure 5.3-85
Figure 5.3-93	GS3 - No Heat Loss: DW Pressure 5.3-85
Figure 5.3-94	GS3 - No Heat Loss: WW Pressure 5.3-86
Figure 5.3-95	GS2 - RPV Dome Pressure 5.3-87
Figure 5.3-96	GS2 - DW Pressure 5.3-87
Figure 5.3-97	GS2 - SC Pressure 5.3-88
Figure 5.3-98	GS2 - RPV Dome Pressure 5.3-88
Figure 5.3-99	GS2 - DW Pressure 5.3-89
Figure 5.3-100	GS2 - SC Pressure 5.3-89
Figure 5.3-101	GS2 - Chimney Collapsed Level 5.3-90
Figure 5.3-102	GS2 - Channel Delta-P 5.3-90
Figure 5.3-103	GS2 - Bypass Collapsed Level 5.3-91
Figure 5.3-104	GS2 - Downcomer Collapsed Level 5.3-91
Figure 5.3-105	GS2 - Chimney Collapsed Level 5.3-92
Figure 5.3-106	GS2 - Channel Delta - P 5.3-92
Figure 5.3-107	GS2 - Bypass Collapsed Level 5.3-93
Figure 5.3-108	GS2 - Downcomer Collapsed Level 5.3-93
Figure 5.3-109	GS2 - GDCS Flow 5.3-94
Figure 5.3-110	GS2 - GDCS Flow 5.3-94
Figure 5.3-111	GS2 - GDCS - DW Break Flow 5.3-95
Figure 5.3-112	GS2 - RPV - DW Break Flow 5.3-95
Figure 5.3-113	GS2 - GDCS Pool Level 5.3-96
Figure 5.3-114	GS2 - GDCS Flow Volume 5.3-96
Figure 5.3-115	GS2 - GDCLB1 Flow Volume 5.3-97
Figure 5.3-116	GS1 - Upper DW Air Pressure 5.3-98
Figure 5.3-117	GS1 - Lower DW Air Pressure 5.3-98
Figure 5.3-118	GS1 - WW Air Pressure 5.3-99
Figure 5.4-1	Schematic of the One-Sixth Scale BWR-5 Facility 5.4-11
Figure 5.4-2	TRACG Nodalization Diagram 5.4-12
Figure 5.4-3	Channel at 41-in. Center: Well-Mixed Model 5.4-13
Figure 5.4-4	Channel at 55-in. Middle: Well-Mixed Model 5.4-13
Figure 5.4-5	Channel at 41-in. Periphery: Well-Mixed Model 5.4-14
Figure 5.4-6	Bypass 41-in. Center: Well-Mixed Model 5.4-14
Figure 5.4-7	Bypass 55-in. Middle: Well-Mixed Model 5.4-15

**List of Figures**  
(continued)

	<b><u>Page</u></b>
Figure 5.4-8	Bypass 41-in Periphery: Well-Mixed Model 5.4-15
Figure 5.4-9	Lower Plenum at 14-in.: Well-Mixed Model 5.4-16
Figure 5.4-10	Upper Plenum Center: Well-Mixed Model 5.4-16
Figure 5.4-11	Channel at 41-in. Center: Conservative Model 5.4-17
Figure 5.4-12	Channel at 55-in. Middle: Conservative Model 5.4-17
Figure 5.4-13	Channel at 41-in. Periphery: Conservative Model 5.4-18
Figure 5.4-14	Bypass 41-in. Center: Conservative Model 5.4-18
Figure 5.4-15	Bypass 55-in. Middle: Conservative Model 5.4-19
Figure 5.4-16	Bypass 41-in. Periphery: Conservative Model 5.4-19
Figure 5.4-17	Lower Plenum at 14-in.: Conservative Model 5.4-20
Figure 5.4-18	Upper Plenum Center: Conservative Model 5.4-20
Figure 5.4-19	Non-Dimensional Parameters 5.4-21
Figure 5.5-1	Pressure Suppression Test Facility (PSTF) Schematic 5.5-10
Figure 5.5-2	PSTF TRACG Component Layout 5.5-11
Figure 5.5-3	TRACG Model of PSTF Suppression Pool 5.5-12
Figure 5.5-4	TRACG Vent System Model - PSTF and SBWR 5.5-13
Figure 5.5-5	Drywell Pressure Response - TRACG vs Measured Data, Test 5703-01 5.5-14
Figure 5.5-6	Drywell Pressure Response - TRACG vs Measured Data, Test 5703-02 5.5-15
Figure 5.5-7	Drywell Pressure Response - TRACG vs Measured Data, Test 5703-03 5.5-16
Figure 5.6-1	Pressure Suppression Test Facility Schematic 5.6-13
Figure 5.6-2	TRACG Simulation of PSTF/Mark II 5.6-14
Figure 5.6-3	PSTF Steam Generator and Blowdown Line 5.6-15
Figure 5.6-4	TRACG Nodalization of 4T/Mark II PSTF 5.6-16
Figure 5.6-5	Drywell Pressure Response For Test 5101-34 - TRACG vs Measured Data 5.6-17
Figure 5.6-6	Wetwell Airspace Pressure For Test 5101-34 - TRACG vs Measured Data 5.6-18
Figure 5.6-7	Drywell-to-Wetwell Pressure Differential For Test 5101-34 - TRACG vs Measured Data 5.6-19
Figure 5.7-1	PANDA Test Facility Schematic 5.7-71
Figure 5.7-2	PANDA Vessel Component Nodalization Diagram 5.7-72
Figure 5.7-3	RPV, IC, and Connected Piping Nodalization Diagram 5.7-73
Figure 5.7-4	PCCS (PCC1) Nodalization Diagram 5.7-74
Figure 5.7-5	PCCS and ICS Pools Nodalization Diagram 5.7-85
Figure 5.7-6	Main Vent (DW2 to WW2) Nodalization Diagram 5.7-86
Figure 5.7-7	Vacuum Breaker (DW2 to WW2) Nodalization Diagram 5.7-87
5.7 Attach.	Comparison of TRACG Predictions with PANDA Test Data 5.7A-1 through 5.7A-233/5.7A-234
Figure 6.1-1	Dodewaard RPV with Internals (Left) and with Measurement Equipment (Right) 6.1-13
Figure 6.1-2	TRACG Model for Dodewaard Steady-State and Transient Analysis 6.1-14
Figure 6.1-3	Axial Power Distribution at End of Cycle 23 6.1-15

**List of Figures**  
(continued)

	<u>Page</u>	
Figure 6.2-1	Comparison of the Power-Pressure Path of the February 1992 Startup with a Regular Startup (From [6.2-1])	6.2-33
Figure 6.2-2	TRACG Nodalization Diagram of Dodewaard for Startup Simulation	6.2-34
Figure 6.2-3	Axial Power Distribution Used for Startup Simulation	6.2-35
Figure 6.2-4	Comparison of Measured and Calculated Thermal Power	6.2-36
Figure 6.2-5	Comparison of Measured and Calculated Pressure	6.2-37
Figure 6.2-6	Comparison of Measured and Calculated Steam Flow	6.2-38
Figure 6.2-7	Comparison of Measured and Calculated Water Level	6.2-39
Figure 6.2-8	Comparison of Measured and Calculated Downcomer Local Subcooling	6.2-40
Figure 6.2-9	Comparison of Measured and Calculated Downcomer Velocity	6.2-41
Figure 6.2-10	Comparison of Measured and Calculated Short Range Downcomer Pressure Differences DP1 and DP2	6.2-42
Figure 6.2-11	Comparison of Measured and Calculated Long Range Downcomer Pressure Difference DP3	6.2-43
Figure 6.2-12	Comparison of Measured and Calculated Bypass Temperature	6.2-44
Figure 6.2-13	Comparison of Measured and Calculated Bypass Velocity	6.2-45
Figure 6.2-14	Comparison of Measured and Calculated Sparger Flow	6.2-46
Figure 6.2-15	Calculated Local Subcooling in the Hot Channel (Channel 79) and its Chimney (Ring 2)	6.2-47
Figure 6.2-16	Calculated Void Fraction at the Exit of the Hot Channel	6.2-48
Figure 6.2-17	Calculated Core-and-Bypass-Averaged Void Fraction	6.2-49
Figure 6.2-18	Calculated Liquid Velocity in the Hot Channel (Channel 79 Ring 2)	6.2-50
Figure 6.2-19	Calculated Liquid Velocity at Channel Entrance for all Four Channels	6.2-51
Figure 6.2-20	Calculated Liquid Axial Velocity in the Bypass	6.2-52
Figure 6.2-21	Calculated Void Fractions and Velocities in Channel 81 and Chimney Ring 2 (Zoomed-In 5-Minute Period)	6.2-53
Figure 6.3-1	Schematic Diagram of the CRIEPI Thermal Hydraulic Test Facility	6.3-11
Figure 6.3-2	Schematic Diagram of the Pressure Drop Measurement Location	6.3-12
Figure 6.3-3	Sketch of CRIEPI Circulation Flow for Various Values of Inlet Subcooling	6.3-13
Figure 6.3-4	TRACG Model of CRIEPI Test Facility	6.3-14
Figure 6.3-5	Channel Inlet Pressure Drop (Region 1,2)	6.3-15
Figure 6.3-6	Channel Exit Pressure Drop (Region 5,6)	6.3-15
Figure 6.3-7	Chimney (lower part) Pressure Drop (Region 7)	6.3-16
Figure 6.3-8	Chimney (exit ) Pressure Drop (Region 8)	6.3-16
Figure 6.3-9	Steady-State Flow Comparison (P = 0.2MPa)	6.3-17
Figure 6.3-10	Steady-State Flow Comparison (P = 0.5MPa)	6.3-17
Figure 6.3-11	Circulation Flow as a Function of Inlet Subcooling	6.3-18
Figure 6.3-12	Power - Inlet Subcooling Stability Map	6.3-18
Figure 6.3-13	Single Flow Peak	6.3-19
Figure 6.3-14	Chimney Void Fraction Distribution	6.3-19
Figure 6.3-15	Chimney Void Fraction Distribution	6.3-20
Figure 6.3-16	Chimney Temperature Distribution (Tl = Liquid Temperature; Ts = Saturation Temperature)	6.3-20
Figure 6.3-17	Chimney Temperature Distribution Tl = Liquid Temperature; Ts = Saturation Temperature)	6.3-21
Figure 6.3-18	Mechanism of Low Pressure Oscillations	6.3-21



**List of Figures**  
(continued)

	<b><u>Page</u></b>	
Figure 6.3-19	Void Fraction at Different Chimney Locations	6.3-22
Figure 6.3-20	Channel Inlet and Chimney Exit Mass Flow Perturbations	6.3-22
Figure 6.3-21	Implicit - Explicit Scheme Comparison	6.3-23
Figure 6.3-22	Time Step Sensitivity	6.3-23
Figure 6.3-23	Node Size Sensitivity	6.3-24
Figure 6.4-1	PANDA RPV Schematic	6.4-12
Figure 6.4-2	Test E1A: Pressure at the Top of the RPV (solid) and in the PCC3 Inlet Line (dash)	6.4-13
Figure 6.4-3	Test E1A: Flow from the RPV to PCC3 (solid) and from PCC3 to the GDCS Pool (dash)	6.4-13
Figure 6.4-4	Test E1B: Pressure at the Top of the RPV (solid) and in the PCC3 Inlet Line (dash)	6.4-14
Figure 6.4-5	Test E1B: Flow from the RPV to PCC3 (solid) and from PCC3 to the GDCS Pool (dash)	6.4-14
Figure 6.4-6	Test E1C: Pressure at the Top of the RPV (solid) and in the PCC3 Inlet Line (dash)	6.4-15
Figure 6.4-7	Test E1C: Flow from the RPV to PCC3 (solid) and from PCC3 to the GDCS Pool (dash)	6.4-15
Figure 6.4-8	Test E2: Pressure at the Top of the RPV (solid) and in the PCC3 Inlet Line (dash)	6.4-16
Figure 6.4-9	Test E2: Flow from the RPV to PCC3 (solid) and from PCC3 to the GDCS Pool (dash)	6.4-16
Figure 6.4-10	Test E3: Pressure at the Top of the RPV (solid) and in the PCC3 Inlet Line (dash)	6.4-17
Figure 6.4-11	Test E3: Flow from the RPV to PCC3 (solid) and from PCC3 to the GDCS Pool (dash)	6.4-17
Figure 6.4-12	Test E3: Liquid Temperature at the Chimney Inlet	6.4-18
Figure 6.4-13	Base TRACG Model of PANDA RPV	6.4-19
Figure 6.4-14	Simplified TRACG Model of PANDA RPV	6.4-20
Figure 6.4-15	TRACG Simulation of Test E1C: 1) PCC3 Flow (solid); 2) Steam Flow into the Steam Dome (dash)	6.4-21
Figure 6.4-16	TRACG Simulation of the Test E1C: RPV Pressure at 1) Top; 2) Bottom	6.4-21
Figure 6.4-17	TRACG Simulation of the Test E1C: Liquid temperature at 1) Channel Inlet; 2) Chimney Inlet	6.4-22
Figure 6.4-18	TRACG Simulation of the Test E2: 1) PCC3 Flow (solid); 2) Steam Flow into the Steam Dome (dash)	6.4-22
Figure 6.4-19	TRACG Simulation of the Test E2: RPV Pressure at 1) Top; 2) Bottom	6.4-23
Figure 6.4-20	Flow Dependency on Inlet Subcooling (K) for Test E1C: 1) 0.6; 2) 0.4; 3) 0.15; 4) -0.6; 5) -1.35; 6) -1.4	6.4-23
Figure 6.4-21	Circulation Flow for Test E2	6.4-24
Figure 6.5-1	Measured CRIEPI Circulation Flow (P = 0.2 MPa, q = 2.5 kW/chan, Inlet subcooling = 5.1 K)	6.5-13
Figure 6.5-2	Measured CRIEPI Chimney Inlet Temperature (P = 0.2 MPa, q = 2.5 kW/chan, Inlet subcooling = 5.1 K)	6.5-13

**List of Figures**  
(continued)

		<u>Page</u>
Figure 6.5-3	Measured CRIEPI Upper Chimney Void Fraction (P = 0.2 MPa, q = 2.5 kW/chan , Inlet subcooling = 5.1 K )	6.5-14
Figure 6.5-4	TRACG Simulation: 1 - Nondimensional Circulation Flow; 2 - Nondimensional Chimney Inlet Temperature; 3 - Chimney Exit Void Fraction	6.5-14
Figure 6.5-5	Measured Chimney Inlet Temperature for PANDA Exploratory Test E1C	6.5-15
Figure 6.5-6	CRIEPI Data: Stability Maps at Various System Pressures	6.5-15
Figure 6.5-7	TRACG Simulation: Dependence of Subcooling Number on Phase Change Number at the Upper Boundary of the Oscillatory Region	6.5-16
Figure 6.5-8	CRIEPI Data: Dependence of Subcooling Number on Phase Change Number at the Upper Boundary of the Oscillatory Region	6.5-16
Figure 6.5-9	TRACG Simulation: Sensitivity of Circulation Flow to Chimney Height at Zero Inlet Subcooling	6.5-17
Figure 6.5-10	TRACG Simulation: Dependence of the Flow Oscillation Period on Flashing Number	6.5-17
Figure 6.5-11	TRACG Simulation: Sensitivity of Circulation Flow to System Pressure at Zero Inlet Subcooling	6.5-18
Figure 6.5-12	TRACG Model with Five Channel-Chimney Regions	6.5-19
Figure 6.5-13	Core Flow Calculated with Multiple Channel TRACG Model	6.5-20
Figure 7.2-1	SBWR Boron Concentrations Estimated Using TRACG Models	7.2-6
Figure 7.2-2	TRACG SBWR Drywell Model	7.2-7
Figure 8.1-1	Evolution of SBWR/TRACG Nodalization for LOCA/ECCS and Transients	8.1-23
Figure 8.1-2	Schematic of the LOCA/ECCS Model Showing the RPV and the Containment Nodalization	8.1-24
Figure 8.1-3	SBWR RPV Nodalization for LOCA/ECCS	8.1-25
Figure 8.1-4	Nodalization of an SBWR Fuel Channel	8.1-26
Figure 8.1-5	Nodalization of GDCS Piping	8.1-27
Figure 8.1-6	Nodalization of SBWR Steamline System for LOCA/ECCS	8.1-28
Figure 8.1-7	Nodalization for SBWR Feedwater System	8.1-29
Figure 8.1-8	Nodalization of Steam Separators	8.1-29
Figure 8.1-9	Nodalization for SBWR IC and DPV System	8.1-30
Figure 8.1-10	Nodalization of Main Steamline System for SBWR Transients	8.1-31
Figure 8.2-1	TRACG Model of SBWR Containment -RPV	8.2-24
Figure 8.2-2	TRACG Model of SBWR Containment - IC and PCC	8.2-25
Figure 8.2-3	TRACG Model of SBWR Containment - DW and GDCS	8.2-26
Figure 8.2-4	TRACG Model of SBWR Containment - WW	8.2-27
Figure 8.2-5	TRACG Model of SBWR Containment - Configured for Main Steamline Break	8.2-28
Figure 9.1-1	SBWR Stability Map	9.1-28

## Nomenclature and Abbreviations

### Nomenclature

#### English Letters

Symbols	Description	Units
A	Cross-sectional flow area	m <sup>2</sup>
B	Specific buoyancy flux defined in Eq. 2.1-22b	m <sup>4</sup> /s <sup>3</sup>
C <sub>0</sub>	Drift flux model distribution parameter	*
C	Concentration	*
c <sub>i</sub>	Interfacial shear parameter	*
c <sub>p</sub>	Specific heat at constant pressure	J/kg K
d	Characteristic length	m
D	Diameter	m
D <sub>h</sub>	Hydraulic diameter	m
e	Specific internal energy	J/kg
F/A <sup>2</sup>	Sum of loss coefficients divided by area <sup>2</sup> (Eq. 2.1-24b)	1/m <sup>4</sup>
f	Darcy friction factor	*
f <sub>2</sub>	Parameter defined in Eq. 2.1-4	*
f <sub>3</sub>	Parameter defined in Eq. 2.1-1	*
f <sub>4</sub>	Parameter defined in Eq. 2.1-1	*
f(X <sub>i</sub> )	Designates an arbitrary function of arguments X <sub>i</sub>	*
G	Mass flux	kg/m <sup>2</sup> s
g	Acceleration due to gravity	9.81 m/s <sup>2</sup>
H	Submergence head	m
h	Specific enthalpy	J/kg
h <sub>fg</sub>	Latent heat of vaporization	J/kg
Δh	Specific enthalpy difference	J/kg
h	Heat transfer coefficient	J/m <sup>2</sup> K
h <sub>y</sub>	Heat transfer coefficient with noncondensibles	J/m <sup>2</sup> K
J <sub>j</sub>	Volumetric flow rate	m <sup>3</sup> /s
J <sub>o</sub>	Volumetric injection flow rate in pool	m <sup>3</sup> /s
K	Form loss coefficient	*
k	Thermal conductivity	J/ m K
k <sub>μ</sub>	Coefficient in Eq. (2.1-22a)	*
L	Pipe or pipe segment length	m
L	Hydrostatic or gravity head	m
L <sub>0</sub>	Characteristic length	m
L/A	Sum of pipe segment lengths divided by area (Eq. 2.1-25b)	m <sup>-1</sup>
n	Number of free or wall jets	*
ΔP	Pressure difference	Pa

\* = dimensionless

## Nomenclature and Abbreviations (continued)

$\dot{P}$	Rate of pressure change	Pa/s
$P^*$	Pressure parameter defined in Eq. 2.1-10	Pa
$Q$	Heat rate	W
$R$	Radius	m
$T$	Temperature	K
$\Delta T$	Temperature difference, form defined by Eq. 2.1-6	K
$t$	Time	s
$t_0$	Charateristic time	s
$u$	Fluid velocity	m/s
$u_e$	Characteristic entrainment velocity	m/s
$u_0$	Characteristic transport velocity	m/s
$V_{gj}$	Drift flux velocity	m/s
$v$	Specific volume	m <sup>3</sup> /kg
$W$	Mass flow rate	kg/s
$\Delta W$	Differential mass flow rates between channels	kg/s
$X$	Steam quality	*
$X$	Distance from centerline	m
$y$	Mass fraction	*
$Z$	Characteristic distance from submerged vent	m
$z$	Axial coordinate along flow path	m

### Greek Letters

Symbols	Description	Units
$\alpha$	Void fraction	*
$\Delta\alpha$	Void fraction difference	*
$\beta$	Coefficient of thermal expansion	K <sup>-1</sup>
$\mu$	Viscosity	kg/m s
$\rho$	Density	kg/m <sup>3</sup>
$\sigma$	Surface tension	kg/s <sup>2</sup>
$\tau$	Time constant	s

### Nondimensional Groups

Symbols	Description
$N_{Ku}$	Kutateladze Number, defined by Eq. 2.1-2
$N_{Bi} = h d/k_s$	Biot Number
$N_{Fr}$	Froude Number, defined by Eq. 2.1-16
$N_{fl}$	Flashing Number, defined in Section 6.2.3
$N_{Gr}$	Grashof Number, defined by Eq. 2.1-19

## Nomenclature and Abbreviations

(continued)

$N_{Nu} = h d/k$	Nusselt Number
$N_{Nu,dlt}$	Droplet Nusselt Number, defined by Eq. 2.1-13
$N_{Nu,fb,low\ flow}$	Film Boiling Nusselt Number at low flow
$N_{Pr} = c_p \mu/k_f$	Prandtl Number
$N_{PCH}$	Phase change Number, defined by Eq. 2.1-17
$N_{Nu,fb,dist. dlt}$	Film Boiling Nusselt Number, form given in Table 2.1-1
$N_{Eu}$	Euler Number, form defined by Eq. 2.1-9b
$N_\rho = \rho_g/\rho_l$	Density Ratio Number
$N_{Re} = \rho V D_h/\mu$	Reynolds Number
$N_{sub}$	Subcooling Number, defined by Eq. 2.1-18
$N_{We,dlt}$	Droplet Weber Number, defined by Eq. 2.1-14
$N_{Ra} = N_{Gr} N_{Pr}$	Rayleigh Number
$N_{Ri}$	Richardson Number, defined by Eq. 2.1-9
$\Pi_{GM}$	Nondimensional group, defined by Eq. 2.1-1
$\Pi_{IN}$	Inertia pressure number, defined by Eq. 2.1-26
$\Pi_P$	Nondimensional group, defined by Eq. 2.1-1
$\Pi_V$	Nondimensional group, defined by Eq. 2.1-1
$\Pi_{PCH,stored}$	Phase change group-heat stored in structures, defined by Eq. 2.1-3
$\Pi_{PCH,decht}$	Phase change group-core decay heating, defined by Eq. 2.1-7
$\Pi_{Q,stored}$	Heat addition group-heat stored in structures, defined by Eq. 2.1-4
$\Pi_{Q,misc}$	Heat addition group-miscellaneous sources
$\Pi_{Q,decht-losses}$	Heat addition group-net core decay heating, defined by Eq. 2.1-8
$\Pi_t$	Time scale group, defined by Eq. 2.1-3
$\Pi_{sub}$	Subcooling group, form defined by Eq. 2.1-5
$\Pi_{subm}$	Submergence pressure number, defined by Eq. 2.1-23
$\Pi_W$	Inventory addition group, form defined by Eq. 2.1-11
$\Pi_{Wh}$	Enthalpy flow group, form defined by Eq. 2.1-12
$\Pi_{mech}$	Mechanical compression group, form defined by Eq. 2.1-10
$\Pi_{loss}$	Pressure loss number, defined by Eq. 2.1-25
$\Pi_{hyd}$	Hydrostatic head group, defined by Eq. 2.1-24
$\Pi_{bj}^S$	Free buoyant jet mixing time ratio, defined by Eq. 2.1-21a
$\Pi_{bl}^S$	Wall buoyant jet mixing time ratio, defined by Eq. 2.1-21b

### Subscripts

avg	Average value
BP	Bypass
bj	Free buoyant jet
bl	Wall buoyant jet
c	Core

## Nomenclature and Abbreviations

(continued)

ch	Chimney
DW	Drywell
DC	Downcomer
decht	Decay heat
decht-losses	Decay heat less heat losses
dlt	Droplet
GDCS	Gravity-Driven Cooling System
GT	Guide tube
G,g	Gas phase
EQ	Equalization line
FW	Feedwater
f	Fluid
fg	Phase change
fb	Film boiling
fuel	Fuel
hx	Heat exchanger
LP	Lower Plenum
L,l	Liquid phase
L/G	Change from Liquid to Gas
leak	Leakage flow
i	Refers to component or location "i"
j	Refers to component or location "j"
MV	Main Vent
max	Maximum value
mod	Model (Test Facilities)
N/C	Noncondensibles
o	Initial value
0	Characteristic value
PCC	Passive Containment Cooling Condenser
p	Prototype (SBWR)
ppm	Parts per million
rest	Restriction
RPV	Reactor Pressure Vessel
SRV	Safety-Relief Valve
r	Refers to a reference quantity
SL	Steam Line
sat	Saturation
sep	Separator
sub	Vent submergence
sp	Spray
UTP	Upper Tie Plate
VB	Vacuum Breaker
W	Wall

## Nomenclature and Abbreviations

(continued)

WW	Wetwell
wall	Wall of structure
y	Refers to heat transfer coefficient in gas with N/C
$\infty$	Refers to temperature away from wall

Additional subscripts are defined in the text or are self-explanatory

### Superscripts

'	Denotes derivative with respect to pressure
.	Denotes derivative with respect to time
+	Nondimensional variable normalized to its initial value
◦	Nondimensional parameter normalized to reference value
S	Specific (for a well defined geometry)

### Abbreviations

ADS	Automatic Depressurization System
ADW	Annular Drywell
ALPHA	Advanced LWR Passive Heat Removal and Aerosol Program
ATLAS	Fuel bundle thermal hydraulic test facility at GE
ATWS	Anticipated Transients Without Scram
ATRAC	Computer input deck generator for TRACG
BAF	Bottom of Active Fuel
BDL	Bottom Drain Line
BDLB	Bottom Drain Line Break
BT	Boiling Transition
BWR	Boiling Water Reactor
CANDU	Canadian Deuterium Uranium reactor
CHF	Critical Heat Flux
CCFL	Counter Current Flow Limiting
CRD	Control Rod Drive
CRGT	Control Rod Guide Tube
CRIEPI	Central Research Institute for Electric Power Industry
DBA	Design Basis Accident
DPV	Depressurization Valve
DRF	Design Record File
DSA	Double sided heat Slabs
DW	Drywell
ECCS	Emergency Core Cooling System
ECPR	Experimental Critical Power Ratio
ENEA	Italian national agency for new technology, energy and environment
EOC	End of Cycle

## Nomenclature and Abbreviations

(continued)

EQL	Equalization Line
EBWR	Experimental Boiling Water Reactor
FIST	Full Integral Simulation Test
FRIGG	Facility used for fuel channel thermal-hydraulic tests in Sweden
GDC	Gravity-Driven Cooling
GDCS	Gravity-Driven Cooling System
GDCL	GDCS Line
GDLB	GDCS Line Break
GE	General Electric Company
GIRAFFE	Gravity-Driven Integral Full-Height Test for Passive Heat Removal
GIST	GDCS Integrated Systems Test
GTBP	Guide Tube Bypass
HPCS	High Pressure Core Spray
H2TS	Hierarchical Two-Tier Scaling
HVL	Horizontal Vent Line
IC	Isolation Condenser
ICS	Isolation Condenser System
IST	Integral System Test
I.D.	Inner Diameter
JAPC	Japan Atomic Power Company
JPI	Jet Pump Injection
KEMA	Dutch company for engineering and consultancy services
KSP	Kuhn-Schrock-Peterson correlation
LDW	Lower Drywell
LOCA	Loss-of-Coolant Accident
LWRSIM	Light water reactor simulation code used by the Dutch
L/D	Length to Diameter ratio
ln()	Natural logarithm with base $e=2.718282$
MDW	Middle Drywell-center, annular section of DW
MIT	Massachusetts Institute of Technology
MPR	Minimum Pressure Regulator
MSL	Main Steam Line
MSLB	Main Steam Line Break
MSIV	Main Steam line Isolation Valve
NB	No-Break
NDT	Nondestructive Test
NRC	Nuclear Regulatory Commission
N/C	Noncondensibles
O.D.	Outer Diameter
OHT	Ontario Hydro Technologies
PANACEA	BWR core simulator code
PANDA	Passive Nachwarmeabfuhr-und Drueckabbau-Testanlage
PANTHERS	Performance Analysis and Testing of Heat Removal Systems



## Nomenclature and Abbreviations

(continued)

PCC	Passive Containment Condenser
PCCS	Passive Containment Cooling System
PCT	Peak Clad Temperature
PCV	Primary Containment Vessel
RHR	Residual Heat Removal
PIRT	Phenomena Identification and Ranking Table
RSA	Control rod drive flow
PSI	Paul Scherrer Institute
PSTF	Pressure Suppression Test Facility
RPV	Reactor Pressure Vessel
RWCU	Reactor Water Cleanup
RZS	Reactor water cleanup flow
SBWR	Simplified Boiling Water Reactor
SC	Pressure Suppression Chamber
SET	Separate Effects Test
SDC	Shutdown Cooling
SLCS	Standby Liquid Control System
SIET	Societa Informazioni Esperienze Termoidrauliche
SIT	Systems Interaction Tests
SP	Suppression Pool
SPERT	Reactivity insertion transient test facility at Idaho National Laboratory
SRV	Safety-Relief Valve
SSAR	Standard Safety Analysis Report
TAF	Top of Active Fuel
TAPD	SBWR Test and Analysis Program Description
TCS	Turbine Control Valve
TCV	Turbine Stop/Control Valves
TLTA	Two Loop Test Apparatus
TRACG	Transient Reactor Analysis Code, GE version
TSV	Turbine Stop Valve
UCB	University of California at Berkeley
UDW	Upper Drywell
VB	Vacuum Breaker
WL	Water Level
WW	Wetwell
1-D	One-dimensional
Π-group	Refers to a nondimensional group in text

## EXECUTIVE SUMMARY

### Introduction

This report describes the qualification of the TRACG computer code performed for the Simplified Boiling Water Reactor (SBWR). TRACG is the GE version of the Transient Reactor Analysis Code (TRAC) developed originally by the Los Alamos National Laboratory. TRACG has been extensively assessed for operating BWRs. The objective of this qualification effort is to extend the range of assessment to cover various classes of SBWR events. TRACG is being used for the analysis of SBWR loss-of-coolant accidents (LOCAs) with respect to performance of the Emergency Core Cooling Systems (LOCA/ECCS), and containment pressure and temperature response (LOCA/containment), anticipated transients, anticipated transients without scram (ATWS) and stability. From a thermal-hydraulic perspective, the SBWR differs from the Advanced Boiling Water Reactor (ABWR) in its use of natural circulation for core flow, and passive safety systems for inventory makeup in the reactor pressure vessel and long-term decay heat removal from the containment. A number of test programs have been conducted to study the performance of SBWR LOCAs. Additionally, other tests, while not specifically performed for the SBWR, provide valuable data to assess individual TRACG models used in the calculation of SBWR performance. The present report compiles results of all qualification studies specific to the SBWR in one document. It supplements the material in the generic TRACG Qualification report (NEDE-32177P, Rev. 2). The objectives of this report are to document the results of the qualification studies and, thereby, to demonstrate that TRACG has been adequately assessed, and the model bias and uncertainties have been quantified, for application to the SBWR.

GE is following a systematic and rigorous approach to qualifying TRACG for application to the SBWR. The Qualification Strategy is discussed in Section 2. For each class of events, key safety parameters and important physical phenomena were established. Phenomena Identification and Ranking Tables (PIRT) were developed for SBWR LOCA, transients, ATWS and stability. A comprehensive list of TRACG qualification studies was developed to provide qualification coverage of all the highly ranked SBWR PIRT phenomena.

The TRACG Assessment Plan is summarized in the form of an “assessment matrix”. The highly ranked PIRT phenomena, for which test data are needed, are displayed in rows, and the test facilities that provide applicable data are listed in columns. The assessment matrix reflects knowledge gained through the experimental programs.

Sections 3, 4, 5 and 6 describe the qualification studies performed in accordance with the assessment plan. In each section, the applicability of the data to the SBWR is established in terms of the coverage of the highly ranked PIRT phenomena identified for the test, and the range of the test variables in relation to the applicable SBWR range. The TRACG model and comparisons with data are presented and the deviations between data and calculations are quantified.

The key results of the qualification studies for the separate effects tests, component tests and integral systems tests are summarized below.

## **Separate Effects Tests**

Section 3 pertains to the Separate Effects Tests (SETs). The majority of the TRACG qualification studies in this category were performed prior to the SBWR-specific test program and reported in the generic TRACG qualification report. These studies are applicable to all BWRs and relate to basic (generic) phenomena such as interfacial shear, wall heat transfer and critical flow. The present report includes two additional separate effects tests: (1) void fraction measurements in large diameter pipes performed at Ontario Hydro, and (2) void fraction tests at low pressure performed at Toshiba. The first is relevant to the SBWR partitioned chimney region, and the second to rod bundles under accident conditions. The basic phenomena for which TRACG was assessed are void fraction in rod bundles and large diameter pipes, critical flow, bundle frictional pressure drop, natural circulation flow and the onset of hydrodynamic oscillations. The results of the SET comparisons demonstrate the capability of the TRACG models to calculate the highly ranked basic phenomena with acceptable accuracy.

## **Component Tests**

Section 4 covers the SBWR component tests. The SBWR-specific studies include Passive Containment Condenser (PCC) and Isolation Condenser (IC) performance tests at PANTHERS and the steady-state PCC performance tests at PANDA. Tests performed to examine the temperature stratification of the suppression pool have also been included in this section. All these tests provide data for evaluation of the SBWR containment performance in a LOCA. Additionally, IC performance is important during main steamline isolation events.

### **PANTHERS PCC**

[

Redacted

]

[

Redacted

]

### **PANDA Steady-State PCC Tests**

[

Redacted

]

### **PANTHERS IC**

The PANTHERS IC facility consisted of a prototype IC module, a steam supply vessel which simulates the SBWR reactor vessel, a vent volume, and associated piping sufficient to establish IC thermal-hydraulic performance. The IC test unit was one module of a full-scale, two-module vertical tube heat exchanger. The IC was installed in a water pool with dimensions appropriate for one SBWR IC module.

The comparison of test data and TRACG calculations shows that the heat transfer was calculated accurately in a pure-steam environment over the full range of SBWR transient and accident conditions.

[

Redacted

]

### **Suppression Pool Stratification Tests**

Two series of tests were undertaken, prior to the SBWR program, to investigate how thermal stratification of the suppression pool affected the performance of the Mark III horizontal vent system. One set of tests was performed with full-size vents and the other set using one-third area-scaled vents. For TRACG evaluation, one test from each of these sets was selected.

[

Redacted

]

[

Redacted

]

## **Integral Systems Tests**

Integral Systems Tests are discussed in Section 5. This section covers all the relevant SBWR-specific LOCA tests (GIST, GIRAFFE and PANDA). In addition, prior BWR containment tests have been added for the early blowdown transient. These Mark III and Mark II tests characterize the early blowdown into the drywell, and through the main vents into the suppression pool. An analysis of a boron mixing test performed in the 1/6<sup>th</sup> scale facility at the Vallecitos Nuclear Center addresses an identified qualification need for the ATWS scenario.

### **GIST**

The GIST facility is a full-height, 1/508 volumetric scale model of the March 1987 SBWR conceptual design and simulates the response to LOCAs, focusing on the effectiveness of the GDCS. In spite of significant differences in configuration between the GIST facility and the current SBWR design, GIST provided an adequate simulation of the key phenomena related to RPV blowdown and GDCS injection. The governing phenomena for top-down scaling of reactor inventory and pressure were preserved in GIST. The test conditions were varied over a sufficiently wide range to assess TRACG accuracy for various break locations, break sizes and GDCS flow rates.

TRACG calculated the performance of the GIST facility with acceptable accuracy over the full range of break sizes and initial conditions. The calculations included system pressures (RPV, drywell and wetwell), regional mass distribution of the two-phase fluid within the vessel, the minimum water level in the downcomer annulus, the GDCS onset time and the GDCS flow rate.

### **GIRAFFE SIT**

The GIRAFFE test facility is operated by Toshiba Corporation in Kawasaki, Japan and is a 1/400 scale model of the SBWR (1:1 in height and 1:400 in cross-sectional area). The test facility simulates the current 1996 SBWR configuration and includes the IC and PCC systems, which were not present in GIST. The SIT study pertains to a series of four LOCA tests conducted at the GIRAFFE facility, to provide a database on the performance of the SBWR ECCS during the late blowdown/early GDCS phase of a LOCA, with specific focus on potential systems interaction effects.

The TRACG analysis calculated all the important test parameters (pressures, levels, core coverage, GDCS flow) for all four System Interaction Tests with acceptable accuracy.

### **GIRAFFE Helium**

The purpose of the GIRAFFE Helium test program was to demonstrate the operation of the Passive Containment Cooling System (PCCS) in the post-accident containment environment in

the presence of both lighter-than-steam and heavier-than-steam noncondensable gases. The results provide data relevant to SBWR containment thermal-hydraulic performance, PCC heat removal capability, and containment pressure response. This study pertains to a series of six tests conducted at the GIRAFFE facility to provide data on the containment performance during the long-term PCCS phase of a LOCA.

For the tests with nitrogen, the peak drywell and wetwell pressures were adequately calculated by TRACG. The drywell pressure varies in a narrow range between the early peak pressure and the wetwell pressure, and can be bounded between these values. The noncondensable distributions in the lower drywell, upper drywell and wetwell were calculated well. Within the PCC, TRACG calculated very little nitrogen holdup, while the data (inferred from the temperature measurements) showed nitrogen at the bottom of the tubes. This is consistent with the conservative bias in the TRACG calculation of PCC heat transfer, which means that a smaller amount of surface was needed for condensation.

[

Redacted

]

## **PANDA**

The PANDA test facility included all of the features of the SBWR containment required for an integral system simulation of long-term LOCA response. Most notably, the PANDA facility included a detailed representation of the PCCS utilized for long-term decay heat removal.

The facility was designed to model the long-term cooling phase of a LOCA for the SBWR. It was a 1/25 volume-scaled, full-height simulation of the SBWR primary system and containment. Included in the facility were the major components necessary to model the SBWR system response during the long-term phase of the LOCA. These components include the containment drywell (DW), the wetwell (WW) or suppression chamber, the reactor pressure vessel (RPV) including the core, and those safety systems that would operate during the long-term phase of the LOCA. The PANDA DW and WW are represented by pairs of vessels, connected by large pipes. This double-vessel arrangement permits improved simulation of spatial distribution effects within the containment volumes. Important passive safety systems modeled in PANDA

include the Passive Containment Cooling System (PCCS), Isolation Condenser System (ICS) and GDCS.

The PANDA transient test matrix comprised a series of ten integral system tests intended, primarily, to simulate the long-term cooling phase of the post-LOCA transient. Parametric variations considered in the tests included (1) alternatives for configuring and refilling the PCC and IC pools, (2) asymmetric distributions of steam and air in the DW, (3) system interactions associated with parallel operation of the PCCS and ICS, (4) a direct bypass of steam from the DW to the WW air space, and (5) PCCS startup and operation from a condition representing the upper limit of initial DW air inventory. One test also examined PCCS performance during the portion of the post-LOCA transient extending from the early GDCS injection phase into the long-term cooling phase.

[

Redacted

]

### **1/6<sup>th</sup> Scale Boron Mixing Facility**

The boron mixing study is applicable to ATWS events. In order to study this mixing phenomenon, a series of tests was carried out in a facility that was a mockup of a BWR-5 at one-sixth linear scale (1/216 in volume). One test in this series was chosen as being representative of the conditions in a SBWR. This test had no forced circulation of the coolant in the system and the Standby Liquid Control System (SLCS) injection was in the periphery of the upper plenum. This configuration is close to that in SBWR, which has boron injection in the upper portion of the peripheral bypass region.

[

Redacted

]

### **PSTF Mark III Tests**

Three series of large-scale demonstration tests were conducted in the Pressure Suppression Test Facility (PSTF) in support of the horizontal vent pressure suppression system used in the Mark III containment design. In these tests, the emphasis was on investigation of vent-clearing phenomena associated with the horizontal vent system during a LOCA. One of these test series was selected to assess and demonstrate the adequacy of TRACG to calculate the early containment pressure response and the vent-clearing process for the horizontal vent pressure suppression system.

The calculations show that TRACG adequately simulates the vent-clearing process for the horizontal vent system. The calculated vent-clearing times for all three vents are comparable and consistent with the measured data for each test. The TRACG calculated value of the DW short-term peak pressure is on the conservative side of the test data.

### **4T Mark II Tests**

A series of blowdown tests was performed specifically to investigate pool dynamic phenomena in the Mark II containment concept, and to provide data for the evaluation of the vertical vent pressure suppression geometry used in the Mark II containment design.

This test series utilized the steam generator and drywell of the PSTF, and the Temporary Tall Test Tank (4T) as a combination suppression pool and wetwell air space. These tests are of particular interest in assessing TRACG capability for calculating pressure response of a containment design with the closed wetwell configuration used in the SBWR. Seven tests with the closed wetwell configuration were chosen and analyzed with TRACG.

The TRACG calculation results and their comparison with the measured data show that TRACG adequately simulates the interactions between the blowdown flow, the drywell, the wetwell and the vent system. TRACG calculates drywell pressure responses which match well with the measured data and are on the conservative side. Also, TRACG adequately models and calculates steam condensation on the drywell walls.

The TRACG calculations of the 4T/Mark II data demonstrate the adequacy of TRACG for calculating containment response with the closed wetwell design used in the SBWR.

### **Natural Circulation and Low Pressure Flow Oscillation Tests**

Tests related to natural circulation and low pressure flow oscillations are described in Section 6. These consist of Dodewaard steady-state operation and startup, CRIEPI flow oscillation tests and PANDA exploratory tests.

#### **Dodewaard**

[

Redacted

]



[

Redacted

]

Startup data are available for the Dodewaard plant and were also analyzed with TRACG. During the startup of February 15 and 16, 1992, measurements were performed at various stages of the startup process. No oscillations were observed during this or any of the earlier startups in Dodewaard.

[

Redacted

]

### **CRIEPI Test Facility**

Tests were conducted at CRIEPI to investigate the potential for flow oscillations in a natural circulation system at low pressure. The CRIEPI test loop consisted of two electrically heated channels, chimney, separator (upper plenum), downcomer, preheater and subcooler. The total length of the downcomer section is approximately 30m. The tests were conducted at three pressures: 0.2 MPa, 0.35 MPa, and 0.5 MPa.

Results of TRACG computer simulation were compared with the CRIEPI data for the steady-state and oscillatory regimes. Good agreement between TRACG results and experimental data was shown. The modes of oscillations and the mechanism were analyzed. The Inlet Subcooling - Heat Flux stability map obtained with TRACG (at a system pressure 0.2 MPa) was in a good agreement with the experimental stability map. Based on these comparisons, it was concluded that TRACG has the capability to accurately calculate low-pressure flow oscillations.

### **PANDA Exploratory Tests**

A series of five exploratory tests was performed at the PANDA facility to characterize the oscillations seen in the RPV steam flow and downcomer level. These tests provide useful data for assessing the capability of TRACG to calculate low pressure oscillations in a natural circulation system. Four of the tests were performed with a mixture of air and RPV steam going to the PCC, while the fifth test had no air injection. The four tests with air injection showed small oscillations in the RPV pressure, accompanied by larger oscillations in the steam flow. When the condenser operated with pure steam, the steam flow oscillations were not present, but there were sinusoidal variations in the downcomer level and temperature.

The TRACG analysis calculated the oscillations seen in the tests. The calculated period was close to the observed period of 240s. The calculated oscillations were sensitive to the downcomer level position as observed in the tests. The post-test analysis led to the conclusion that the governing phenomenon was related to the propagation of enthalpy up the channel and flashing in the chimney.

## **Evaluation of Results and Conclusions**

The results and findings from the qualification studies are consolidated in Sections 7, 8 and 9. Section 7 summarizes the limitations in the TRACG models and shows that they are either unimportant or can be addressed by bounding models. Section 8 discusses the implications of the findings from the qualification studies on the choice of an appropriate nodalization for the SBWR. Requirements for nodalization of different regions (reactor vessel, drywell, wetwell) and components (PCC IC, etc.) based on the test simulations are factored into the final nodalization scheme for the SBWR plant. Section 9 summarizes the comparisons between data and the TRACG calculations in terms of the bias and uncertainty in the calculation of the key parameters. This discussion is categorized in terms of transients, LOCA/ECCS, LOCA/containment, stability, and plant startup (natural circulation and low pressure flow oscillations). The assessment plan defined in Section 2 is revisited to confirm that data used for TRACG qualification covered the appropriate SBWR range for all the key PIRT phenomena.

The overall performance of the SBWR for LOCAs can be evaluated with very little uncertainty. The core does not uncover for any of the postulated breaks and there is no core heatup. The containment pressure can be calculated on a global thermodynamic basis; the primary effect is the compression of the wetwell gas space resulting from the purging of the noncondensibles from the drywell, augmented later by the vapor pressure of steam as the suppression pool heats up because of the blowdown energy and decay heat over the first few hours. The plant response and the performance of the key safety systems has been confirmed by test results (PANTHERS, GIST, GIRAFFE, PANDA and Mark III and Mark II containment early blowdown response tests) which were accurately calculated by TRACG. The key safety parameters (peak cladding temperature and peak containment pressure) are easily predicted and have large design margins. Some of the details related to the mixing of gases in the drywell and the unequal sharing of the PCC heat load by the three PCCs were not accurately calculated by TRACG. In such cases, the detailed behavior was either not important to the overall response, or it could be bounded by a modified calculation procedure.

For operational transients, the governing physical phenomena are similar to operating BWRs. TRACG has been qualified against data from the Peach Bottom turbine trip tests, Hatch MSIV closure tests and Hatch flow coastdown tests. The safety parameters (RPV pressure and neutron flux response) are accurately calculated by TRACG. The SBWR transient response differs from operating plants in the magnitude of level swings caused by void changes in the tall chimney. These differences have been addressed by separate effects tests on level changes and by void fraction measurements in large pipes. These tests were calculated well by TRACG.

ATWS events involve the same physical phenomena as for operational transients. In addition, steam is discharged to the suppression pool through Safety/Relief Valves, and shutdown of the nuclear reaction is achieved by delivery of boron to the core. All the important

phenomena were covered under TRACG qualification for LOCA and transients, except for mixing and stratification of the injected borated water solution in the RPV inventory. [

Redacted

]

In conclusion, the qualification results documented in this report demonstrate that TRACG has been satisfactorily assessed over the defined assessment matrix, and is qualified for application to the SBWR over the intended range of applications. TRACG can, therefore, be used for licensing analysis of transient and accident events, in conjunction with an appropriate application methodology. The details of the application methodology will be documented in a separate TRACG Application Report.

# 1. Introduction

This report describes the qualification of the TRACG computer code performed specifically for the Simplified Boiling Water Reactor (SBWR). It supplements the material in the TRACG Qualification report (NEDE-32177P, Rev. 2) [1-1]. The term “Computer Code Qualification” has been in use at GE Nuclear Energy for many years and incorporates the process of validation of the code against data or other engineering calculations. The validation studies are the subject of this report. Here, the terms “code qualification” and “code validation” are used interchangeably. Validation is part of the process of “qualifying” the computer code for design application. Other parts of the process include independent design verification and configuration control. Independent design verification is performed by a Design Review Team which reviews the required documentation, the software test plan and test results, and any other information deemed necessary for the review. These activities are covered under GE Nuclear Energy quality assurance requirements and are not discussed in this report.

## 1.1 Relationship to Generic TRACG Qualification Report

Reference 1-1 includes a comprehensive collection of TRACG qualification studies applicable to BWR-related separate effects, component, integral system and reactor tests. Reference 1-1 will be referred to as the “generic TRACG qualification report”. These tests cover a wide range of phenomena and configurations representative of BWR conditions for loss-of-coolant accidents (LOCAs), operational transients and density wave oscillation. Most of these data are also applicable to the SBWR, as discussed in the SBWR Test and Analysis Program Description (TAPD) [1-2]. A detailed listing of the tests applicable to SBWR and the specific qualification objective is provided in Section 2.1 of this report.

Reference 1-2 developed a comprehensive list of TRACG qualification studies needed to support the SBWR program. This list (Tables 5.1-1a through 5.4-1b of Reference 1-2) includes many of the tests covered in the generic report as well as additional data required (Table 6.1.1 of Reference 1-2) to provide coverage of all the highly ranked SBWR PIRT phenomena. (PIRT denotes the Phenomena Identification and Ranking Tables, which have been developed for SBWR LOCA, transients, ATWS and stability in Reference 1-2). The present report compiles results of all the qualification studies relevant to the SBWR in one document. These studies comprise primarily the SBWR-specific tests. Qualification studies reported in the generic TRACG qualification report are referenced but have not been repeated here; hence, this report is intended to be used in conjunction with the generic TRACG qualification report. Quantitative estimates of the data uncertainties and TRACG prediction deviations have been listed for all relevant tests, including those from the generic TRACG qualification report.

## 1.2 Relationship to Other Documents Needed for TRACG Application

This report is one of several documents that provide the information necessary for the validation of the TRACG computer code and its application for SBWR design analysis. The relationship of this report to the generic TRACG qualification report [1-1] was explained in the previous section. The other pertinent reports are the various Test Reports (see Reference 1-3 for a complete list), Scaling of the SBWR Related Tests [1-4], TRACG Model Description [1-5], the SBWR Test and Analysis Program Description [1-2], and Application of TRACG Model to SBWR Licensing Safety Analysis [1-6]\*. The purpose of this section is to describe these documents, their relationships to each other, and their roles in providing the information needed for the validation and application of TRACG.

TRACG is being qualified for SBWR licensing analyses for LOCA-ECCS, LOCA-containment, operational transients, ATWS and stability applications. A detailed description of the application methodology is provided in Reference 1-6. While there are differences in the application approach for the different types of events, the relationships between the various documents can be described in the framework of the Code Scaling, Applicability and Uncertainty (CSAU) methodology [1-7]. GE is following the CSAU methodology for LOCA-ECCS and operational transients. For LOCA-containment applications, a similar approach is being followed which embodies most of the elements of the CSAU process. However, bounding models have been utilized for drywell mixing and suppression pool stratification. For ATWS events and stability analysis, a formal CSAU process is not being followed, although a number of the CSAU steps (such as the development of PIRTs and assessment requirements) have been included.

Figure 1.2-1 shows the various elements of the CSAU process as defined in Reference 1-7. Some of the details in this figure are different for the specific TRACG applications to the SBWR. However, this figure is used as a reference because it identifies all the steps needed for the documentation, validation and application of a computer code for safety analysis, starting from the selection of the application (e.g., LOCA) scenario and the “frozen” code. The term “frozen code” refers to a fixed, controlled version of the code which is used for the validation studies and analysis. The CSAU framework consists of three major elements comprising 14 steps. The first element relates to requirements and code capabilities. This is the process of defining the transient scenario to be analyzed (Step 1), selecting the nuclear power plant (Step 2), and development of the Phenomena Identification and Ranking Tables (PIRT) (Step 3). A frozen version of the code is selected (Step 4) and documentation is provided on the models in the code (Step 5). Comparison of the model capabilities with the phenomena to be modeled establishes the applicability of the code in Step 6. Element 2 is termed Assessment and Ranging of Parameters. The major steps in this element are to establish the assessment matrix (Step 7), perform assessment of the code against Separate Effects Tests (SETs) and Integral Systems Tests (ISTs) to determine the appropriate nodalization to be used (Step 8), and to determine code biases and uncertainties (Step 9). In addition, any bias and uncertainty due to the effect of scale is determined (Step 10). The third

---

\* For the ESBWR, this report is not relevant and is replaced by the ESBWR Application Report.

element consists of sensitivity and uncertainty analyses. Uncertainties in the estimation of key reactor input parameters and operating state are evaluated in Step 11. Calculations are then performed (Step 12) to determine the sensitivity of key code prediction variables to the various biases and uncertainties identified in Steps 9-11. These biases and uncertainties are combined in Step 13 to determine the total uncertainty for the transient under consideration (Step 14).

[

Redacted

]

[

Redacted

]

The TRACG models are described in the TRACG Model Description [1-5], which was revised to expand the description of the models and correlations. The range of applicability of the correlations and individual bias and uncertainty with respect to the database are addressed. This report specifically addresses Step 5 in Figure 1.2-1. Other supporting documentation on the use of TRACG is contained in the TRACG User's Manual [1-8].

Step 8 of the CSAU Methodology defines the plant nodalization based on the assessment of the code against relevant SET and IST. The major SBWR test facilities (GIST, GIRAFFE, PANTHERS and PANDA) are described in various test reports. A listing of these test reports can be found in the SBWR Testing Summary Report [1-3], which describes key features of the tests and the results obtained. The scaling report [1-4] establishes the fidelity of the test facilities to scale the major SBWR phenomena and the applicability of the test data to the SBWR. Step 8 allows for feedback from lessons learned in the assessment process on the plant nodalization. Changes in nodalization needed to calculate the experiments accurately are reflected in the plant nodalization.

The present report (TRACG Qualification for SBWR) starts by refining the assessment matrix (Step 7). This report and the generic TRACG qualification report describe the assessment of TRACG through comparisons with SETs, component tests, ISTs and BWR plant data. In this report, a distinction is made between "separate effects tests" and "component performance tests" in the SETs category. Similarly, the ISTs have been divided into "Integral Systems Tests" and "Plant Tests". The comparison of the TRACG calculations with test data establishes guidelines for the nodalization to be used for reactor and containment analysis. In the GE methodology, a once-through process is followed, wherein all refinements to the nodalization resulting from the findings in the calculations are implemented into the plant nodalization at the end of the assessment. In some cases, the plant nodalization differs from the test nodalization. Differences are justified in the individual sections describing the qualification study. Where appropriate, sensitivity to nodalization differences is presented.

The results of the assessment lead to evaluations of the model bias and uncertainty in the calculation of various parameters (Step 9). Step 9 of the CSAU process defines the code and experimental uncertainty. Here, code uncertainty is evaluated by a direct comparison of data with code calculations. Data accuracy is addressed in the individual descriptions of the tests. The contribution due to data uncertainty is not explicitly identified in the statistical evaluation of the comparisons between data and calculations; it will be implicitly included in the differences between data and calculations. This is discussed in more detail in Section 2. Thus, the qualification reports address Steps 8 and 9.

GE interprets the CSAU Step 9 as providing two categories of information on the model uncertainties. The first kind is the total uncertainty in the calculation of certain key parameters such as reactor water level, containment pressure, etc. These are directly obtained from the differences between calculations and test data, as discussed above. The second kind is the uncertainty in individual highly ranked PIRT phenomena, which cover more basic parameters such as condensation heat transfer and void fraction (interfacial shear). These uncertainties are mostly obtained from the TRACG Model Description [1-5]. A detailed discussion of how representative values of these uncertainties are derived will be provided in the Application Report. Thus, Figure 1.2-1 also shows Step 9 within the dashed boundary of the Application Report. Uncertainties in the highly ranked PIRT phenomena are propagated through the TRACG code to arrive at overall code uncertainty in Step 13 of the CSAU process.

Analysis of data from test facilities at different scales provides information on the scaleup capabilities of the code. However, formal discussion of any impacts on the pertinent safety parameters as a result of the scaleup to plant size (Step 10) has been deferred to the Application report as indicated in Figure 1.2-1 in the lowest dotted box that contains Step 10.

[

Redacted

]

Reference 1-6, Application of TRACG Model to SBWR Licensing Safety Analysis, is intended to address the remaining steps in the CSAU methodology (Steps 11 through 14). The uncertainties in the highly ranked PIRT phenomena are defined, together with uncertainties in the plant initial and boundary conditions. The values of these parameters are varied over a representative range to establish the sensitivity in the key safety parameters being evaluated. The effects of the significant parameters are then either combined statistically using a Monte Carlo process, or incorporated through the use of conservative values or models. The Application Report addresses the application of TRACG for operational transients, ATWS, LOCA/ECCS and LOCA/containment analysis.



**Table 1.2-1**  
**Versions of TRACG used for Qualification Studies**

[

Redacted

]

**Table 1.2-1**  
**Versions of TRACG used for Qualification Studies**  
**(continued)**

[

Redacted

]

**Table 1.2-1**  
**Versions of TRACG used for Qualification Studies**  
**(continued)**

[

Redacted

]

**Table 1.2-1**  
**Versions of TRACG used for Qualification Studies**  
**(continued)**

[

Redacted

]

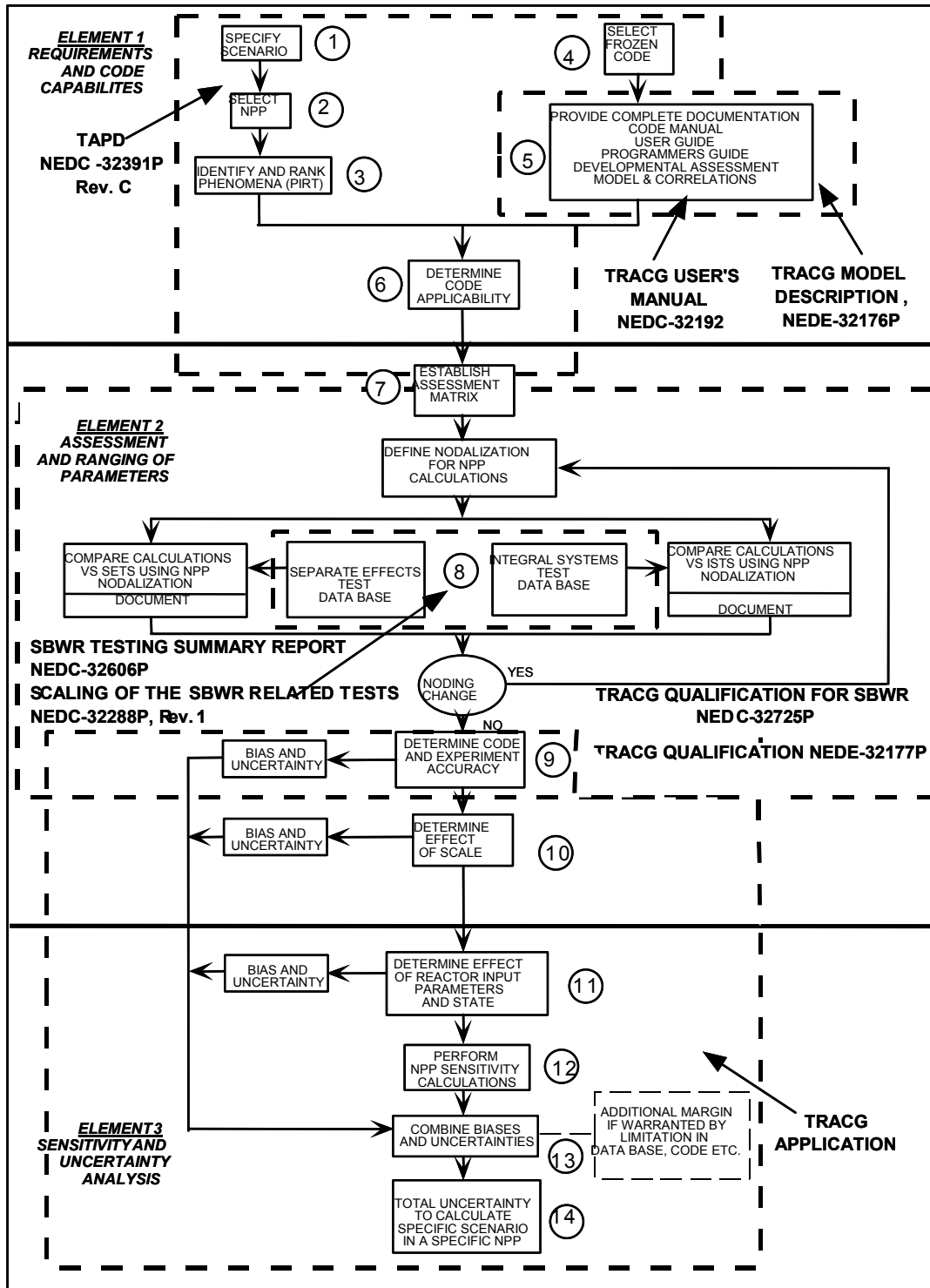


Figure 1.2-1 Road Map of SBWR TRACG Related Documentation

### 1.3 Report Road Map

This section describes how the contents of the report have been organized. Figure 1.3-1 shows a road map through the report, and provides the rationale for its structure. It also indicates the topics covered in the various report sections.

As indicated on the left side of the figure, the report can be divided into four parts. The first part, as presented in Section 2, defines the **Assessment Plan** or Qualification Strategy. The second part consists of the **Qualification Studies** defined in the Assessment Plan. This material is contained in Sections 3, 4, 5 and 6. An **Evaluation of the Results** is performed in Sections 7, 8 and 9. Section 7 evaluates the shortcomings in the TRACG models, their impact, and procedures to bound their effects. Section 8 describes the TRACG nodalization that has been qualified by the process described and documented in this report. This nodalization will be used in the TRACG SBWR Application Report to be issued separately. Section 9 summarizes and consolidates the results of Sections 3 through 6 so that conclusions regarding TRACG qualification are readily apparent. Finally, the **Conclusions** related to the adequacy of TRACG qualification are given in Section 10.

The right side of Figure 1.3-1 shows a more detailed flow path through the report. A detailed assessment plan was developed in TAPD Section 5 for validation of TRACG for the SBWR. Since then, LOCA test programs have been completed at several large-scale SBWR test facilities [1-3]. In Section 2.1, the information from Reference 1-3 is utilized to modify the rankings of a few LOCA PIRT phenomena. The output is the updated PIRT tables for LOCA, which are used in the subsequent portions of the report. The updated PIRT has been incorporated into the final assessment plan in Section 2.1 and shows the coverage of the highly ranked PIRT phenomena by a matrix of separate effects, component and integral systems tests.

Sections 3, 4, 5 and 6 describe the qualification studies performed in accordance with the assessment plan. Section 3 pertains to the Separate Effects Tests. The majority of the TRACG qualification studies in this category were performed earlier and were reported in Reference 1-1. These studies are applicable to all BWRs and relate to basic (generic) phenomena such as interfacial shear, wall heat transfer and critical flow. These studies are not repeated in the present report. However, statistics on the data uncertainty and prediction errors for each test are reported. The present report includes two SETs specifically for the SBWR: (1) void fraction in large diameter pipes and (2) void fraction at low pressures. The first is relevant to the SBWR partitioned chimney region, and the second to rod bundles at post-blowdown conditions. Section 4 covers the SBWR component tests. As for the SETs, qualification studies reported in the earlier generic TRACG qualification report are not repeated here. The new SBWR studies include PCC and IC performance tests at PANTHERS and PANDA. Tests performed to examine the temperature stratification of the suppression pool have also been included. Integral System Tests are discussed in Section 5. All relevant SBWR LOCA tests (GIST, GIRAFFE and PANDA) have been included in this category. In addition, prior BWR containment tests have been added for the early blowdown transient. These Mark III and Mark II tests characterize the early blowdown into the drywell, and through the main vents into the suppression pool. An analysis of a boron mixing test performed in the 1/6<sup>th</sup> scale facility at the Vallecitos Nuclear Center (VNC) addresses an identified qualification need for the ATWS scenario. Tests related to

natural circulation and low pressure flow oscillations have been segregated in Section 6. These consist of the Dodewaard steady-state operation and startup, CRIEPI low pressure flow oscillation tests and PANDA exploratory tests.

Each qualification section is organized as follows:

- Introduction
  - General description and purpose of tests; tests selected for post-test analysis; purpose of post-test analysis
- Test Facility/Test Matrix
  - Brief description of test facility; summary of test matrix
- Applicability of Data to SBWR
  - Aspects of SBWR scenario addressed by the test with reference to PIRT phenomena; range of relevant test parameters vs. SBWR
- TRACG Model
  - Nodalization of test facility; comparison with SBWR containment model nodalization
- Test Simulation
  - Method of simulating the test with TRACG; initial and boundary conditions
- Results of Post-Test Calculations
  - Comparison between the test data and TRACG results; discussion of comparisons (key features of test behavior and TRACG predictions); sensitivity studies
- Summary and Conclusions
  - Overall assessment of adequacy of TRACG predictions; specific assessment with respect to key PIRT phenomena; implications for TRACG simulation of SBWR

The results and findings from the qualification studies are consolidated in Sections 7, 8 and 9. Section 7 reviews areas where the TRACG models were found to have some deficiencies. It is shown that these deficiencies do not detract from the qualification objectives. In some cases, the limitations in TRACG are of no consequence in predicting SBWR response. In two areas where the limitations need to be addressed (drywell mixing and suppression pool stratification), the effects can be readily bounded by selecting appropriate input parameters.

Section 8 discusses the implications of the findings from the qualification studies on the nodalization for the SBWR. Requirements for nodalization of different regions (reactor vessel, drywell, wetwell) and components (PCC and PCC pool, etc.) based on the test simulations are factored into the final nodalization scheme for the SBWR plant.

Section 9 summarizes the comparisons between data and the TRACG predictions in terms of the bias and uncertainty in the prediction of key parameters. This discussion covers the major categories of transients: LOCA/ECCS, LOCA/containment, transients, ATWS, stability and plant startup (natural circulation and low pressure flow oscillations). The adequacy of the TRACG models and nodalization is established based on the acceptability of the prediction deviations for SBWR simulation. The qualification coverage is reevaluated in Section 9. The assessment plan defined in Section 2 is revisited to assure that the data used for TRACG qualification covered the appropriate SBWR range for all the highly ranked PIRT phenomena.

Section 10 summarizes the main conclusions from the report and states the overall conclusions regarding the adequacy of the TRACG models and the coverage of the range of scenarios expected in the SBWR analysis.



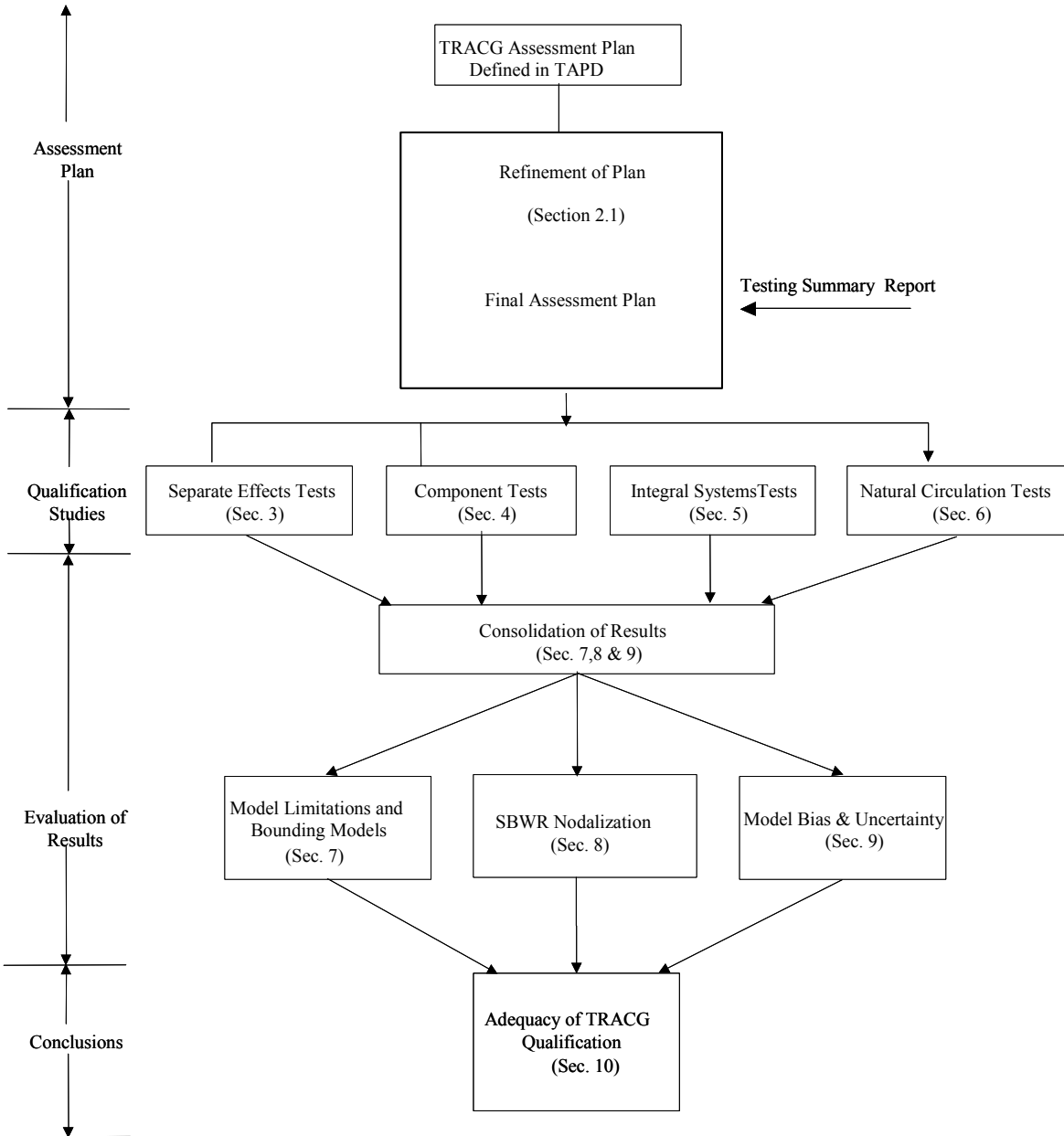


**Figure 1.3-1 Qualification Report Roadmap**

## 1.4 References

- [1-1] *TRACG Qualification*, GE Nuclear Energy, NEDE-32177P, Revision 2, January 2000.
- [1-2] *SBWR Test and Analysis Program Description*, GE Nuclear Energy, NEDE-32391P, Revision C, August, 1995.
- [1-3] *SBWR Testing Summary Report*, GE Nuclear Energy, NEDC-32606P, Rev. 0, August 2002.
- [1-4] *Scaling of the SBWR Related Tests*, GE Nuclear Energy, NEDC-32288P, Revision 1, October 1995.
- [1-5] *TRACG Model Description - Licensing Topical Report*, GE Nuclear Energy, NEDE-32176P Revision 2, December 1999.
- [1-6] *Application of TRACG Model to SBWR Licensing Safety Analysis*, GE Nuclear Energy, NEDE-32178P, Rev. 1 January 1998.
- [1-7] *Quantifying Reactor Safety Margins - Application of Code Scaling, Applicability and Uncertainty Evaluation Methodology for a Large-Break Loss-of-Coolant Accident*, NUREG/CR/5249, EGG-2552, 1989.
- [1-8] *TRACG02V User's Manual*, GE Nuclear Energy, NEDC-32192, December 1992.
- [1-9] S.Z. Kuhn, V.E. Schrock and P.F. Peterson, *Final Report on U.C. Berkeley Single Tube Condensation Studies*, UCB-NE-4201 Rev. 2, August 1994.
- [1-10] H.K. Forster and N. Zuber, *Dynamics of Vapor Bubbles and Boiling Heat Transfer*, AIChE Journal, pp. 531-535, 1955.

## 2. Qualification Strategy

### Objective

The objective of the TRACG qualification effort is to assess the performance of the code for various classes of SBWR transient and accident events. TRACG modeling applicability will be evaluated in terms of its capability to simulate the important phenomena for these transients over a sufficient range and with acceptable accuracy. Specifically, TRACG will be used for licensing analysis of the following categories of SBWR events:

<u>SBWR Application</u>	<u>SBWR SSAR Section</u>
Anticipated Transients	Section 15.1 through 15.5
LOCA/ECCS	Sections 6.3, 15.6
LOCA/Containment	Section 6.2
ATWS	Section 15.8
Stability	Section 4, Appendix 4D

The primary thrust of the TRACG LOCA/Containment analysis is the calculation of the long-term pressure and temperature response. TRACG is not employed to calculate short-term dynamic loads resulting from the early blowdown transient. Empirical correlations and models have been developed, based on a large body of experimental data, for loads due to pool swell, chugging and condensation oscillations. These models have been used to determine the containment dynamic loads for the SBWR. TRACG is also not used to determine the minimum containment pressure resulting from inadvertent spray actuation and for the sizing of vacuum breakers. These design parameters are calculated based on conservative assumptions of one hundred percent condensation efficiency for the spray.

[

Redacted

]

In this section, the tasks involved in the TRACG qualification process are discussed and references are made to the individual sections that cover these tasks. These include identification of important phenomena, compilation of the assessment matrix and definition of model bias and uncertainty. The contributions of experimental uncertainty, nodalization and time step sensitivity to the total uncertainty are discussed. Limitations in the TRACG models and the use of bounding procedures to address these issues are reviewed at the end of this section.

## Identification of Important Phenomena

The qualification of TRACG for the SBWR has followed a systematic and detailed approach. The first step was to identify key safety parameters for each SBWR application. These are the criteria used to judge the performance of the safety systems and the margins in the design. The key safety parameters are listed below for the classes of events for which TRACG is being qualified.

[

Redacted

]

The values of the key safety parameters are determined by the governing physical phenomena. In order to delineate the important physical phenomena, it has become customary to develop Phenomena Identification and Ranking Tables (PIRTs). PIRTs are ranked with respect to their impact on the key safety parameters. For example, the peak containment pressure is determined by phenomena such as the discharge flows from the RPV through the break and ADS valves, the mixing of steam with the noncondensibles in the drywell, the transport of the noncondensibles to the wetwell and the Passive Containment Condenser (PCC) heat removal performance. Detailed PIRTs were developed for the classes of events listed above in Reference 2-2. This was done based on the subjective judgment of a group of experts for each class of transients and accidents.

Top-down (scenario related) and bottom-up (individual system related) approaches were used to ensure that all important phenomena were captured. The highly ranked PIRT phenomena, based on the earlier subjective ranking approach, are tabulated in Section 5 of Reference 2-2. Further insight was gained into the relative importance of individual phenomena as a result of scaling studies [2-3]. Completion of the major SBWR test programs also led to greater understanding of the dominant phenomena. This newly gained knowledge has been factored into the PIRT in Section 2.1 of this report.

## Compilation of Assessment Matrix

The next step in the qualification process was to compile a list of the test data that are available to qualify TRACG for the highly ranked phenomena in the PIRT. As described in the TAPD [2-2], this led to the definition of additional data requirements. Test programs were conducted to obtain the needed data [2-4].

The data were grouped into the following categories:

- Separate Effects Tests:** These are well-controlled tests used to provide information on the basic models and phenomena, including: (1) void fraction and level swell data to assess interfacial shear and subcooled boiling models; (2) heat transfer data (e.g), on the condensation heat transfer in the presence of noncondensibles); (3) flow limitation data such as counter-current flow limitation (CCFL) and critical flow; (4) pressure drop data to assess wall friction; (5) critical power data; (6) rod drop test data from the SPERT test reactor to assess the kinetics models; and (7) thermal hydraulic stability data at operating and startup conditions. The low pressure flow oscillation tests conducted at the Tokyo Institute of Technology have been moved from the Integral Systems Tests (IST) category to the separate effects category. The tests analyzed were forced flow tests and were analyzed without consideration of the downcomer; thus, they fit better into the separate effects category. Qualification studies of separate effects data were mostly presented in the generic TRACG Qualification Report [2-5]. These are summarized in Section 3 of the present report, which also includes two additional post-test analyses: comparison with Ontario Hydro [2-6] and Toshiba void fraction data [2-7].
- Component Performance Tests:** In these tests, the performance characteristics of SBWR components have been evaluated. The data include: (1) steam separator data for phase separation and pressure drop; (2) data for PCC and Isolation Condenser (IC) heat removal; and (3) suppression pool stratification data. The steam separator tests were covered in the generic TRACG Qualification Report [2-5]; the others are discussed in Section 4 of this report. SBWR separators are of same design as BWR/6: namely, the AS2B type. Flow rates induced by natural circulation are lower than BWR/6 flow rates and the inlet quality is somewhat higher, representative of the upper end of the BWR/6 separator operating range.
- Integral System Tests:** These tests consist of scaled simulations of SBWR systems. The primary purpose of these tests is to evaluate the integral system performance and the interaction between the various components in the system, typically for LOCAs. In the early period of reactor blowdown during a LOCA, the key phenomena and system response are similar for all BWRs, and some of the facilities that simulate earlier BWRs also provide useful data for the SBWR. Integral System LOCA tests are discussed in Section 5. Tests that pertain to SBWR natural circulation and startup performance are discussed in Section 6.
- BWR Plant Tests:** This category includes transient and stability tests for operating plants. Obviously, there are no SBWR-specific tests, because the SBWR is not in operation. However, plant data from operating BWRs provide valuable assessment of the reactor response to neutron kinetics and control systems which are also applicable to the SBWR. Qualification against a number of BWR plant tests is described in the Generic TRACG Qualification Report (Reference 2-5).

Table 2.0-1 summarizes the data used for TRACG model development and qualification for SBWR. The test facilities and experiments are listed together with the purpose of each test. Most of the tests are described in Reference 2-5. The table only provides references for the new tests; others are referenced to the generic TRACG Qualification Report.

A matrix was compiled in Reference 2-2 of the highly ranked PIRT phenomena (shown in rows) vs. the test facilities that provide data for coverage of these phenomena (shown in columns). This matrix is termed the “Assessment Matrix” and is shown in Tables 5.1-1a, 5.1-2a, 5.2-1a, 5.2-2a 5.3-1a, 5.3-2a and 5.4-1a of Reference 2-2. The refinement of the PIRT mentioned earlier resulted in minor modifications to the original assessment matrix. The modified assessment matrix is given in Tables 2.1-3a through 2.1-7b in Section 2.1. Thus, Section 2.1 provides the updated TRACG assessment plan for the SBWR.

The individual assessment studies are described in Section 3 for Separate Effects Tests, Section 4 for Component Tests, Section 5 for Integral Systems Tests and Section 6 for Natural Circulation and Flow Oscillation Tests. For each test, the results of the assessment include determination of model accuracy in terms of bias and uncertainty, evaluation of the need for any bounding models, and judgment of the adequacy of the range of qualification coverage compared to the corresponding SBWR range.

### Model Bias and Uncertainty

Model accuracy was determined through calculation of the model bias and uncertainty. For each set of data from a given test facility, a bias is calculated as the mean deviation between the TRACG calculations and test measurements. Model uncertainty is calculated as the standard deviation (unbiased estimate) of the differences about that average. Where there are multiple sets of data (Nsets) for the same parameter, it is assumed that they belong to the same population, and the data sets are combined by weighting the statistics by the number of data points in each set [2-8]. Model bias and uncertainty are calculated as follows:

$$Bias = \frac{\sum_1^{Nsets} (number\ of\ points)_i (mean\ error)_i}{Total\ number\ of\ points} \quad (2.0-1)$$

$$S = \sqrt{\frac{\sum_1^{Nsets} (n_i - 1) S_i^2}{n_{total} - 1}} \quad (2.0-2)$$

where S is the total standard deviation and S<sub>i</sub> is the standard deviation for data set ‘i’, given by

$$S_i = \sqrt{\frac{\sum_1^{n_i} (x_j - \bar{x}_i)^2}{n_i - 1}} \quad (2.0-3)$$

where

$x_j$  = individual deviation between TRACG calculation and measured data point,

$\bar{x}_i$  = bias for set ‘i’,  $n_i$  = number of points in data set ‘i’.

For the separate effects and component tests, the parameters being evaluated are typically determined from steady-state tests (e.g., void fraction, PCC heat removal). For integral tests, evaluations are made of key limits and events, such as minimum water level, peak containment pressure and GDCS initiation time. The way in which these biases and uncertainties are used is different. The calculation deviations from the separate effects tests are used to determine the model uncertainties in the basic TRACG models. In the application methodology, these uncertainties are propagated through a statistical combination process, leading to an overall uncertainty in the TRACG calculation of the key safety parameters. The bias and uncertainty for parameters from the integral systems tests are only utilized as checks on the statistical process. They serve to provide assurance that the statistical process of combining uncertainties in the basic models is providing reasonable results. In this way, the problem of compensating errors, which could be introduced by relying solely on complex integral systems tests to derive overall model bias and uncertainty, is minimized.

[

Redacted

]

### **Scaling Distortions, Nodalization Differences and Time Step Sensitivity**

In each of the qualification sections, issues related to the test scaling basis, and implications of nodalization differences between the test and SBWR are discussed. For the major SBWR test facilities, it was shown in the scaling and summary test reports [2-3, 2-4] that scaling distortions in the tests are acceptable for obtaining data for TRACG qualification for the intended purpose. Nodalization differences between the test facility and SBWR are introduced primarily because of test configuration differences. In some cases, the sensitivity to these differences is explored through sensitivity studies. Uncertainties introduced due to sensitivity to time step size are not considered explicitly in the total model uncertainty. TRACG uses a built-in time step size determination algorithm which is based on specified convergence criteria and rate of change criteria [2-9]. This algorithm has been extensively tested and its effectiveness has been established [2-5, 2-9]. Only the maximum time step can be varied in TRACG; the time step could be reduced based on the internal criteria mentioned above. The TRACG Qualification Report [2-5] shows examples of sensitivity studies performed on the nodalization, time step size and convergence criteria. Nodalization studies were performed for the PSTF Blowdown Test, Marviken break flow test and on the fuel channel void distribution. The effects of time step size and convergence criteria were studied for PSTF. These tests were chosen because the effects of

time step size on key TRACG models related to interfacial shear and critical flow can be tested. The studies for PSTF [2-5] show little sensitivity to time step variation. Nodalization and convergence criteria also have a very small effect as long as reasonable user guidelines are followed [2-36]. This can be seen from the Marviken and PSTF studies. The fuel channel void distribution was also found to be insensitive to the nodalization. The choice of the numerical solution scheme and nodalization are important for stability calculations in order to minimize the effects of numerical damping. Extensive studies have been performed to define the appropriate numerics and cell sizes for both thermal-hydraulic and BWR core models. Examples are shown in Sections 3.7, and 7.4 through 7.7 of Reference 2-5. Differences in the results could also be introduced by the use of different modeling strategies (e.g., use of 1-D vs. 3-D components) etc. This factor has been minimized by the use of consistent modeling guidelines and similarity, to the extent possible, between test and SBWR nodalizations.

**TRACG Limitations and Use of Bounding Models**

[

Redacted

]

**Summary of Assessment Results**

The results of the assessment are summarized in Section 9. The TRACG model biases and uncertainties are reported for the basic models, as well as for the key safety parameters from the integral system tests. The accuracy of the TRACG models was found to be acceptable with respect to uncertainties in the calculation of the safety parameters. The range of qualification coverage was reviewed and found to be sufficient with respect to the desired coverage for the SBWR. The SBWR has large margins to design limits such as peak cladding temperature and containment pressure. This can be shown in spite of using bounding procedures for some phenomena as discussed earlier. Thus, the uncertainties in the TRACG models can easily be tolerated and TRACG predictions of SBWR performance are of acceptable accuracy.



**Table 2.0-1**  
**Database Used to Support TRACG Models and Qualification for SBWR**

[

Redacted

]

## **2.1 Assessment Matrix and Coverage of PIRT Phenomena**

This section defines the assessment matrix to demonstrate coverage of all the highly ranked PIRT phenomena. The matrix was originally developed in Section 5 of Reference 2-2. The tests have been divided into (1) Separate Effects Tests, (2) Component Performance Tests, (3) Integral Systems Tests, and (4) Operating Plant Data. The first two types of tests are suitable for model development or for verifying individual models, the latter two for checking the overall performance of the code.

[

Redacted

]

**Changes Resulting from changes to Highly Ranked Phenomena for Reactor and Core:**

[

Redacted

**Changes Resulting from changes to Highly Ranked Phenomena for Containment**

[

Redacted

]

**2.1.1 Separate Effects Tests**

Separate effects tests (SETs) from various facilities are listed in Tables 2.1-3a and 2.1-3b. These are cross-correlated against the highly ranked PIRT phenomena. Because of the difference in the phenomena tables for the containment, Table 2.1-3a is restricted to the reactor vessel and core; Table 2.1-3b covers the phenomena for the containment. The facilities are listed in Table 2.0-1 where the type of test and data available are also indicated.

An 'X' in the matrix indicates that TRACG qualification against the data has been completed. An "\*" indicates that the data have been used to develop correlations used in TRACG (e.g., UC Berkeley tube condensation data). [

Redacted

]

### 2.1.2 Component Tests

Component tests are listed in Tables 2.1-4a and 2.1-4b. The distinction between component tests and separate effects tests is that the component tests focus on overall component performance.

[

Redacted

]

### 2.1.3 Integral System Response Tests

Integral system response tests model overall behavior of a facility subjected to transients simulating specific accidents or transient events. Tests are performed on a scaled simulation of the reactor system.

This section discusses the integral systems testing of the SBWR. Most of these tests are focused on simulated LOCAs. The different phases of the LOCA transient scenario are shown in Figure 2.1-1.

[

Redacted

]

[

Redacted

]

#### **2.1.4 Plant Operating Data**

The transient response of the SBWR is similar to that of other BWRs for operational transients in many respects. Plant data are very valuable in validating code performance for complex systems involving an interplay between thermal hydraulics, neutron kinetics and control system response.

[

Redacted

]

#### **2.1.5 Summary of Test Coverage**

Sections 2.1.1 through 2.1.4 identified the test facilities and BWR plants from which data have been used for TRACG qualification. This information was tabulated for each of the highly ranked PIRT phenomena, by category of tests (separate effects, component performance, etc.).

[

Redacted

]

[

Redacted

]

**Table 2.1-1 PIRT Phenomena Added or Deleted for LOCA/ECCS**

[

Redacted

]



**Table 2.1-2 PIRT Phenomena Added or Deleted for LOCA/Containment**

[

Redacted

]

**Table 2.1-3a  
Separate Effects Tests for Highly Ranked Phenomena  
for TRACG Qualification for SBWR - Reactor and Core**

[

Redacted

]

**Table 2.1-3a (cont'd)  
Separate Effects Tests for Highly Ranked Phenomena  
for TRACG Qualification for SBWR - Reactor and Core**

[

Redacted

]

**Table 2.1-3a (cont'd)  
Separate Effects Tests for Highly Ranked Phenomena  
for TRACG Qualification for SBWR - Reactor and Core**

[

Redacted

]

**Table 2.1-3a (cont'd)  
Separate Effects Tests for Highly Ranked Phenomena  
for TRACG Qualification for SBWR - Reactor and Core**

[

Redacted

]

**Table 2.1-3b**  
**Separate Effects Tests for Highly Ranked Phenomena**  
**for TRACG Qualification for SBWR - Containment**

[

Redacted

]

**Table 2.1-3b (cont'd)**  
**Separate Effects Tests for Highly Ranked Phenomena**  
**for TRACG Qualification for SBWR – Containment**

[

Redacted

]

**Table 2.1-4a**  
**Component Tests for Highly Ranked Phenomena for**  
**TRACG Qualification for SBWR - Reactor and Core**

[

Redacted

]



**Table 2.1-4a (cont'd)**  
**Component Tests for Highly Ranked Phenomena for**  
**TRACG Qualification for SBWR - Reactor and Core**

[

Redacted

]

**Table 2.1-4a (cont'd)**  
**Component Tests for Highly Ranked Phenomena for**  
**TRACG Qualification for SBWR - Reactor and Core**

[

Redacted

]

**Table 2.1-4b**  
**Component Tests of Highly Ranked Phenomena for**  
**TRACG Qualification for SBWR – Containment**

[

Redacted

]

**Table 2.1-4b (cont'd)**  
**Component Tests of Highly Ranked Phenomena for**  
**TRACG Qualification for SBWR - Containment**

[

Redacted

]

**Table 2.1-5a**  
**Integral System Tests for Highly Ranked Phenomena for**  
**TRACG Qualification for SBWR - Reactor Vessel and Core**

[

Redacted

]

**Table 2.1-5a (cont'd)**  
**Integral System Tests for Highly Ranked Phenomena for**  
**TRACG Qualification for SBWR - Reactor Vessel and Core**

[

Redacted

]

**Table 2.1-5b**  
**Integral System Tests for Highly Ranked Phenomena for**  
**TRACG Qualification for SBWR – Containment**

[

Redacted

]

**Table 2.1-5b (cont'd)**  
**Integral System Tests for Highly Ranked Phenomena for**  
**TRACG Qualification for SBWR - Containment**

[

Redacted

]



**Table 2.1-6a**  
**BWR Plant Data for Highly Ranked Phenomena for**  
**TRACG Qualification for SBWR - Reactor Vessel and Core**

[

Redacted

]

**Table 2.1-6a (cont'd)**  
**BWR Plant Data for Highly Ranked Phenomena for**  
**TRACG Qualification for SBWR - Reactor Vessel and Core**

[

Redacted

]

**Table 2.1-6a (cont'd)  
BWR Plant Data for Highly Ranked Phenomena for  
TRACG Qualification for SBWR - Reactor Vessel and Core**

[

Redacted

]

**Table 2.1-6a (cont'd)  
BWR Plant Data for Highly Ranked Phenomena for  
TRACG Qualification for SBWR - Reactor Vessel and Core**

[

Redacted

]

**Table 2.1-7a**  
**Overall TRACG Qualification Coverage of Highly Ranked Phenomena for SBWR -**  
**Reactor Vessel and Core**

[

Redacted

]

**Table 2.1-7a (cont'd)**  
**Overall TRACG Qualification Coverage of Highly Ranked Phenomena for SBWR -**  
**Reactor Vessel and Core**

[

Redacted

]

**Table 2.1-7b**  
**Overall TRACG Qualification Coverage of Highly Ranked Phenomena for SBWR –**  
**Containment**

[

Redacted

]

**Table 2.1-7b (cont'd)**  
**Overall TRACG Qualification Coverage of Highly Ranked Phenomena for SBWR -**  
**Containment**

[

Redacted

]



[

Redacted

]

**Figure 2.1-1 SBWR LOCA Phases and Major Test Coverage**

## 2.2 References

- [2-1] *Stability and Dynamic Performance of the GE BWR*, NEDO-21506, January 1977.
- [2-2] B.S. Shiralkar, et al., *SBWR Test and Analysis Program Description*, NEDC-32391P, Rev. C, August 1995.
- [2-3] R.E. Gamble, et al., *Scaling of the SBWR Related Tests*, NEDC-32288P, Rev.1, October 1995.
- [2-4] P.F. Billig, et al., *SBWR Testing Summary Report*, NEDC-32606P, Rev. 0, August 2002.
- [2-5] J.G.M. Andersen, et al., *TRACG Qualification*, NEDE-32177P, Rev. 2, January 2000.
- [2-6] A.C. Chan, M. Kawaji and H. Hasanein, *Basic Study on Two-Phase Flow in Large Diameter Vertical Piping*, Joint Study Program Final Report, General Electric Company and Japan Atomic Power Company, April 1995.
- [2-7] S. Morooka, T. Ishizuka, M. Iizuka and K. Yoshimura, *Experimental Study on Void Fraction in a Simulated BWR Fuel Assembly (Evaluation of Cross-Sectional Averaged Void Fraction)*, Nuclear Engineering and Design **114**, pp. 91-98, 1989.
- [2-8] M.G. Ortiz and L.S.Ghan, *Uncertainty Analysis of Minimum Vessel Liquid Inventory During a Small-Break LOCA in a B&W Plant - An Application of the CSAU Methodology Using the RELAP5/MOD3 Computer Code*, NUREG/CR-5818, EGG-2665, December 1992.
- [2-9] J.G.M Andersen et. al., *TRACG Model Description*, NEDE-32176P, Rev. 2, December 1999.
- [2-10] W.R. Usry, *Single Tube Condensation Test Program*, GE Nuclear Energy NEDC-32301, Class 2, March 1994.
- [2-11] S.Z. Kuhn, V.E. Schrock and P.F. Peterson, Final Report on U. C. Berkeley Single Tube Condensation Studies, UCB-NE-4201, Rev. 1, August. 1994.
- [2-12] *PANDA Steady State Data Transmittal Report*, Paul Scherrer Institut, Document No. ALPHA-609-0, May 1996.
- [2-13] S. Botti and R. Silverii, *Thermal-Hydraulic Data Report of PANTHERS-PCC Tests*, SIET Report 00393RP95, April 1995.
- [2-14] R. Silverii, *PANTHERS-IC Test Report*, SIET Report 00458RP95, April 1996.
- [2-15] *Backflow Leakage from the Bypass region for ECCS Calculations*, General Electric Company Analytical Model for Loss-of-Coolant Analysis in Accordance with 10CFR50 Appendix K, NEDE-20566-5P, June 1978.
- [2-16] *Supplemental Information for Plant Modifications to Eliminate Significant In-Core Vibrations*, NEDE-21156, January 1976.

- [2-17] *Test Report for SBWR Depressurization Valve Operational and Flow Rate Test*, WYLE Report #41152-0, September 1990.
- [2-18] *SBWR Vacuum Breaker (VB) Prototype Experimental Qualification General Test Report*, Compes Report ED45913, October 1994.
- [2-19] *Mark III Confirmatory Test Program, 1/3 Scale Condensation and Stratification Phenomena, Test Series 5807*, NEDE-21596P, March 1977.
- [2-20] *GIRAFFE SBWR System Interaction Test Report*, NEDC-32504P, June 1996.
- [2-21] *Mark II Pressure Suppression Test Program Phase II and II Tests*, NEDE-13442P-01, May 1976 and NEDO-13468, October 1976.
- [2-22] *Full-Scale Mark III Tests*, Test Series 5707, NEDE-21853-P, August 1978.
- [2-23] *PANDA M Series Data Transmittal Report*, Paul Scherrer Institut, Document Nos. ALPHA-613-0, ALPHA-615-0, ALPHA-616-0, ALPHA-617-0, ALPHA-618-0, ALPHA-619-0, ALPHA-620-0, ALPHA-621-0 ALPHA-622-0, June/July 1996.
- [2-24] M. Herzog, *GIRAFFE SBWR Helium Series Test Report*, NEDC-32608P, June 1996.
- [2-25] F. Inada, M. Furiya, A. Yasuo, H. Tabata, Y. Yoshioka and H.T. Kim, *Thermo-hydraulic Instability of Natural Circulation BWRs at Low Pressure Start-up: Experimental Estimation of Instability Region with Test Facility Considering Scaling Law*, ICONE3 paper, April 1995.
- [2-26] Internal communication, letter from J.E.Torbeck to Distribution, *PANDA Exploratory Tests*, DRF A10-00070, GEP 9514, May 1995.
- [2-27] *BWR-5 - 1/6 scale Boron Mixing Tests*, NEDE-22267.
- [2-28] *Pressure Suppression Test Program*, Pacific Gas and Electric Co., Bodega Bay Atomic Park Unit 1 Exhibit C, Preliminary Hazards Summary Report, December 1962.
- [2-29] C.H. Robbins, *Tests of the Humboldt Bay Pressure Suppression Containment*, GEAP-3596, November 1960.
- [2-30] *Steady-State Thermal Hydraulic Analysis Report for the GKN Upgrade Project*, GEGKN-93-0103, NEDC-32299P, May 1994.
- [2-31] Nissen, W.H.M., Voet, J. van der, Karuza, J. (1994). *The startup of the Dodewaard natural circulation BWR - experiences*. Nuclear Technology, **107**, pp.93-102, July 1994.
- [2-32] W.J. Oosterkamp and G. Koopmans, *Start-up of Natural Circulation BWRs*, paper presented at ICONE-1, Tokyo, September 1991.
- [2-33] Letter from P.W. Marriott, GE to R. W. Borchardt, *NRC Requests for Additional Information (RAIs) on the Simplified Boiling Water Reactor (SBWR) Design*, MFN No. 128-94, October 1994.

- [2-34] J.F. Briesmeister, editor, *MCNP - A General Monte Carlo N-Particle Transport Code*, Version 4A, LA-12625, Los Alamos National Laboratory, 1994.
- [2-35] S.O.Akerlund et. al., *The GESTR-LOCA and SAFER Models for the Evaluation of the Loss-Of-Coolant Accident*, Vol I, NEDO-23785-1-A, February 1985.
- [2-36] J.G.M.Andersen, Y.K.Cheung and J.C.Shaug, TRACG02V User's Manual, NEDC-32192 (GE Proprietary Report), December 1993.
- [2-37] J. S. Post and A. K. Chung, *ODYSY Application for Stability Licensing Calculations*, NEDC-32992P-A, July 2001.

### 3. Separate Effects Tests

[

Redacted

]

#### References

[3.0-1] *TRACG Model Description, Licensing Topical Report*, NEDE-32176, Rev.2, December 1999.

[3.0-2] *TRACG Qualification*, NEDE-32177P, Rev.2, January 2000.

#### 3.1 Toshiba Low Pressure Void Fraction Tests

##### 3.1.1 Introduction

The separate effects database used for TRACG qualification of interfacial shear models (void fraction data) is mostly at high pressure. The Toshiba tests [3.1-1, 3.1-2] were added to extend the qualification basis to lower pressures. The Toshiba void fraction data are for a 16-rod bundle at 0.50 and 1.00 MPa.

##### 3.1.2 Test Facility and Test Matrix

The tests were performed at the Isogo Engineering Center of Toshiba Corporation. Void fraction measurements were conducted in a vertical 4x4 rod bundle using an X-ray CT scanner. Figure 3.1-1 shows the cross-section of the test bundle. The test section consists of electrically heated rods in a square 4x4 array. Grid spacers were used to maintain rod-to-rod and rod-to-channel spacing. The heated length was 3.7m, and the rod diameter of 12.3 mm and rod-to-rod spacing of 16.2 mm were typical of BWR fuel bundles. The axial power shape was uniform, and the four corner rods had a higher power level to provide a corner peaked local (radial) power distribution. Figure 3.1-2 shows an external view of the test section. The rod bundle is inside the test vessel. An X-ray CT scanner was placed on a stand that could be moved in the vertical direction. Figure 3.1-3 shows the void measuring section. The void fraction was measured at an elevation about 45 mm above the end of the heated length (180 mm above the top spacer). The

pressure vessel was made of aluminum to minimize X-ray attenuation in the structural material. In addition, the rods and channel wall were constructed with beryllium at the measurement elevation, also to minimize X-ray attenuation.

The X-ray CT scanner consisted of an X-ray tube and 8 detectors, which carried out a linear scan over the cross-section. The void fraction distribution was reconstructed from the chordal scan data, yielding a detailed map of the local void fraction across the cross-section. This information was integrated to obtain “subchannel” and cross-sectional average values of the void fraction.

Data were obtained at two pressures (0.50 and 1.00 MPa) and two mass fluxes (833 and 1390 kg/m<sup>2</sup>-s). The equilibrium quality at the exit of the heated bundle ranged from 0 to 12%. Inlet flow was measured by a turbine flow meter. Ungrounded chromel-alumel thermocouples, 3.2 mm in diameter, were used to measure the fluid inlet temperature. Diaphragm type transducers were used to measure the system pressure. These signals were recorded on a mini-computer. Reference 3.1-1 provides the following table of estimated measurement accuracies:

Quantity	Accuracy (%)
Pressure	$\pm 0.38$
Flow Rate	$\pm 0.73$
Power	$\pm 0.88$
Inlet fluid temperature	$\pm 0.47$
Cross-sectional averaged void fraction %	$\pm 2$

The uncertainties in the measurement of pressure, flow rate, power and inlet temperature are shown as percent of the measured values. The uncertainty in the measurement of void fraction is an absolute 2%.

**3.1.3 Applicability of Data to SBWR**

[

Redacted

]

[

Redacted

]

**3.1.4 TRACG Model**

[

Redacted

]

**3.1.5 Test Simulation**

[

Redacted

]

[

Redacted

]

**3.1.6 Results of Calculations**

[

Redacted

]

**3.1.7 Summary and Conclusions**

[

Redacted

]



### 3.1.8 References

- [3.1-1] S. Morooka, T. Ishizuka, M. Iizuka and K. Yoshimura, *Experimental Study on Void Fraction in a Simulated BWR Assembly (Evaluation of Cross-Sectional Averaged Void Fraction)*, Nuclear Engineering and Design **114**, pp. 91-98 (1989).
- [3.1-2] T. Mitsutake, S. Morooka, K. Suzuki, S. Tsonoyama and K. Yoshimura, *Void Fraction Estimation within Rod Bundles Based on Three-Fluid Model and Comparison with X-Ray CT Void Data*, Nuclear Engineering and Design **120**, pp. 203-212 (1990).
- [3.1-3] J.G.M. Andersen, et al., *TRACG Qualification*, NEDE-32177P, Rev.2, January 2000.

**Table 3.1-1**  
**Comparison of Range of Parameters for Toshiba Tests and SBWR**

[

Redacted

]

**Table 3.1-2**  
**Comparison of Toshiba Void Data with TRACG Calculations**

[

Redacted

]

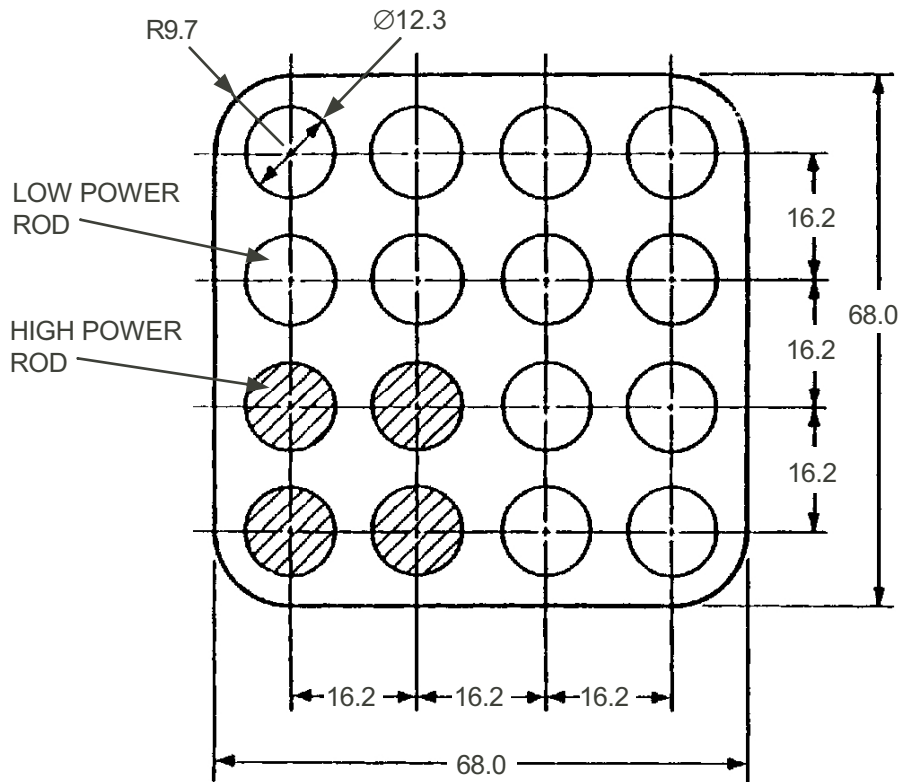


Figure 3.1-1 Test Bundle Cross-Section [3.1-1]

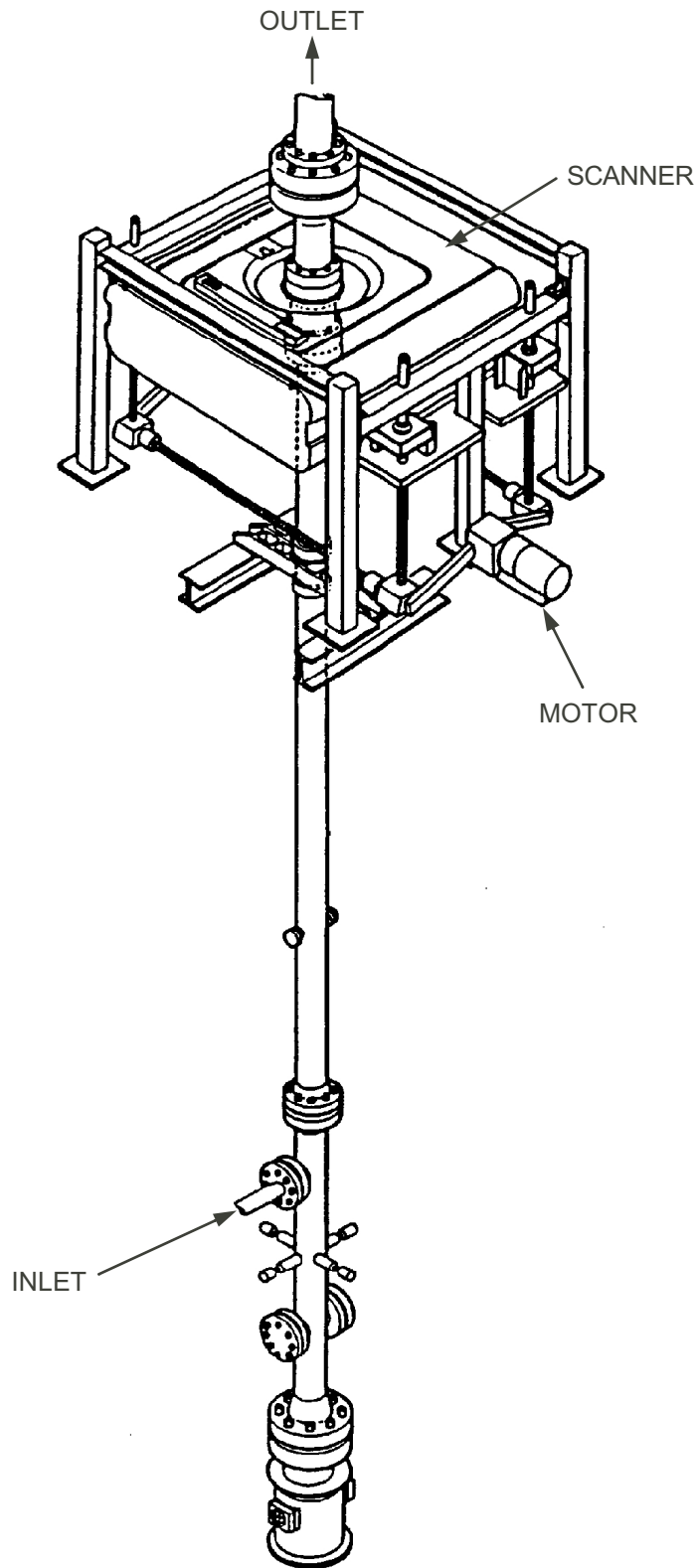


Figure 3.1-2 External View of Test Section [3.1-1]

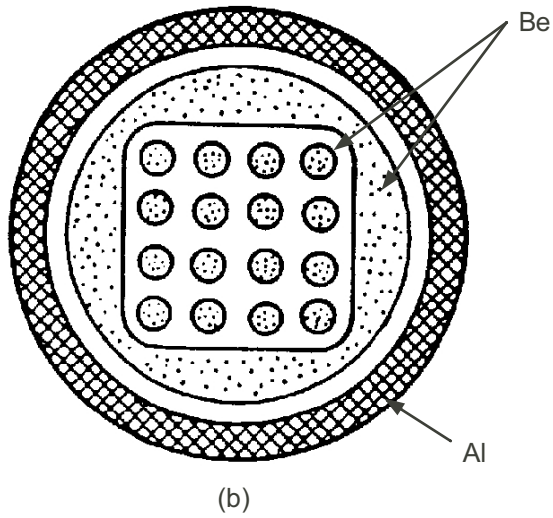
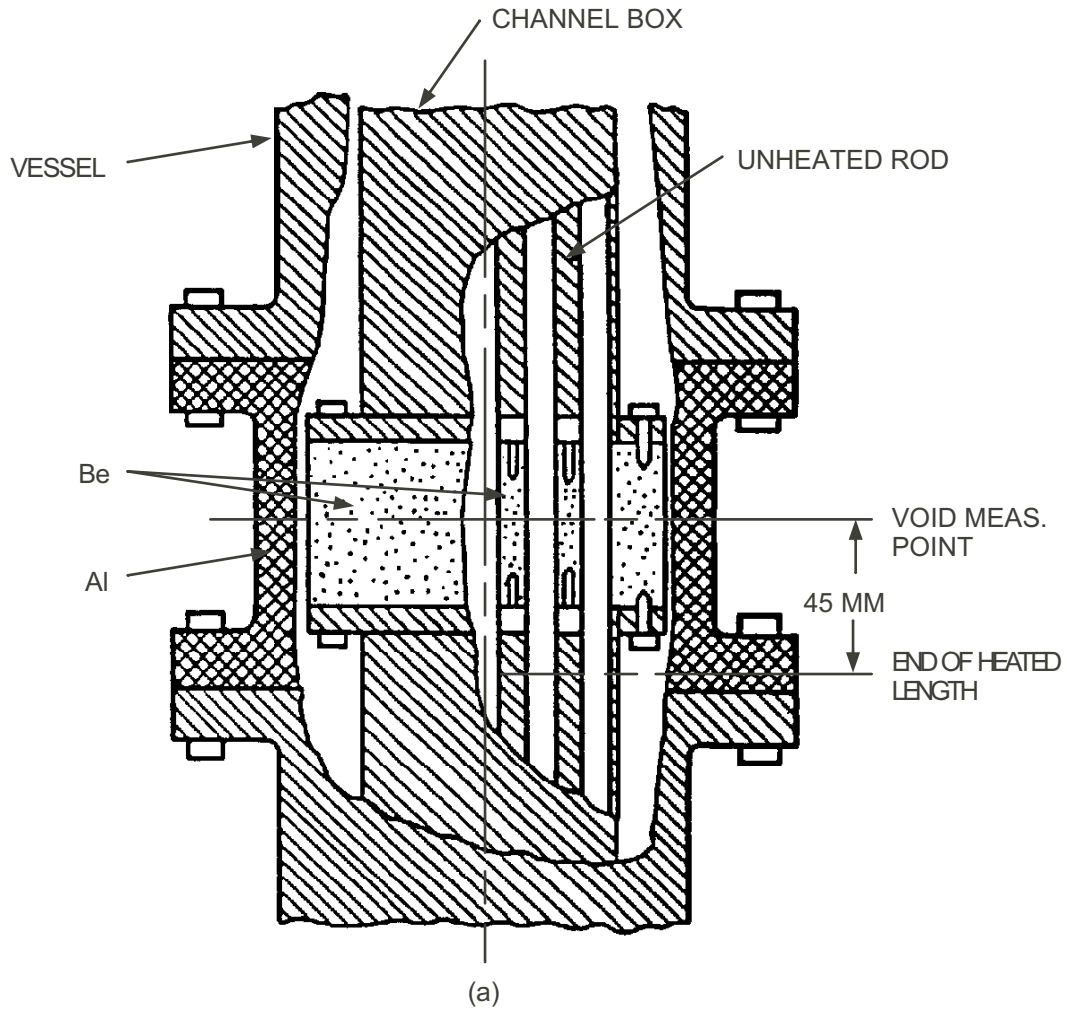


Figure 3.1-3 Void Measurement Section [3.1-1]

[

Redacted

]

**Figure 3.1-4 TRACG Model for Toshiba Test**

[

Redacted

]

**Figure 3.1-5 TRACG Calculations of Toshiba CT Void Data  
(1.00 MPa and 1390 Kg/m<sup>2</sup>-s )**

[

Redacted

]

**Figure 3.1-6 TRACG Calculation of Toshiba CT Void Data  
(1.00 MPa and 833 Kg/m<sup>2</sup>-s)**



[

Redacted

]

**Figure 3.1-7 TRACG Calculation of Toshiba CT Void Data  
(0.50 MPa and 1390 Kg/m<sup>2</sup>-s )**

## 3.2 Ontario Hydro Void Fraction Tests

### 3.2.1 Introduction

In the Simplified Boiling Water Reactor (SBWR), the core flow depends on the net driving head between the downcomer and chimney. The chimney in the SBWR design [3.2-1] is divided into approximately 90 cm square sections. These square partitions are about 6.5m long. The void fraction in the chimney has a strong influence on core flow. During 1994, void data in a 24-in. (61-cm O.D.) vertical pipe under high temperature and high pressure were obtained using the pump test facility of Ontario Hydro Technologies (OHT) in Canada [3.2-2]. This section describes the TRACG simulation of the OHT void fraction tests. The purpose of this simulation is to assess the uncertainty of the TRACG calculation of void fraction in a chimney cell under SBWR operating conditions.

### 3.2.2 Description of Ontario Hydro Void Fraction Tests

The OHT Pump Test Loop with a full-scale CANDU reactor pump was used to perform the void fraction test. The pump is a vertical, single suction and double volute centrifugal pump. The configuration of the OHT Test Loop is shown schematically in Figure 3.2-1. The loop has three parallel, vertical inverted-U branches, connecting the suction and discharge headers. Each branch features a flow control valve and a venturi flow-meter. The loop branches were fabricated using 24-in. (61.0 cm O.D., 51.8 cm I.D.) carbon steel pipes and the suction and discharge headers were made out of 36-in. (91.4 cm O.D.) carbon steel pipes. The height of all the branches was about 12m, which represents a length-to-diameter ratio of about 24. The loop is designed for operation up to 9.4 MPa and 280°C in pressure and temperature, respectively.

The test section was the riser of the branch closest to the pump. Figure 3.2-2 shows a schematic of the test section and the instruments involved. The suction and discharge headers were closed and the other two inverted-U branches were valved off during the void tests. The test section is a 12.4m long, 24-in. (51.8 cm I.D.) carbon steel pipe. The riser features a perforated stainless steel plate type flow straightener located inside the pipe at about 2.0m from its inlet above the discharge header and a venturi-meter near the top of the pipe. The flow through the test section could be controlled using a flow control valve located at the downcomer of the branch. A specially designed multi-detector gamma densitometer and a five-tap Pitotmeter for local void fraction and velocity heads measurements were located at about 7.2m from the riser inlet. Pressure and differential pressure transducers were also installed to measure the pressure drop along the length of the test section.

The gamma densitometer was specially designed to measure void fraction and phase distributions in large diameter, thick-walled steel pipes. A Cesium-137 gamma source with a principal photon energy of 0.662 MeV was used. Lead collimators with four internal partitions were provided on both sides on the pipe to define the beam cross-section and to divide the pipe into five sections for chordal-average void fraction measurements. The void fraction was determined from the attenuated gamma intensities using the following expression:

$$\alpha_j = \frac{\ln[N(\alpha_j) / N(0)]}{\ln[N(1) / N(0)]} \quad (3.2-1)$$

where:

- $N(\alpha_j)$  = attenuated gamma intensity for a given void fraction  $\alpha_j$  in the test pipe
- $N(0)$  = attenuated gamma intensity when the test pipe is filled with liquid only
- $N(1)$  = attenuated gamma intensity when the test pipe is filled with vapor only

Five chordal-average void fraction measurements ( $\alpha_j$ , where  $j=1$  to 5) were thus obtained using Equation 3.2-1.

The OHT multi-detector gamma densitometer was calibrated statically using a piece of pipe identical to the test pipe and air/water at room temperature. In the calibration, the pipe was closed at the bottom and “simulators” of different shapes and sizes were used to simulate the different void and flow patterns. Details of the static calibration were described in Reference 3.2-3. It was found that the measured void fractions compared very well with the actual void fractions in the test pipe with a maximum deviation of about 5% void. The ability of the multi-detector gamma densitometer to identify phase distributions for different cross-section average void fractions was also demonstrated in Reference 3.2-3.

Five Celesco differential pressure transducers (Model DP 30) were connected to the stainless steel tubes to measure the velocity heads for the five Pitot tubes (Figure 3.2-2). The transducers had a range of 0 to 34 kPa and were bled regularly to ensure that the connecting lines were free from vapor bubbles.

The dynamic head in two-phase flows is given by:

$$\Delta P = \frac{1}{2} [\alpha \rho_s u_s^2 + J(1 - \alpha) \rho_f u_f^2] \quad (3.2-2)$$

where:

- $\alpha$  = Local void fraction
- $\rho_s$  = Steam density
- $\rho_f$  = Water density
- $u_s$  = Local steam velocity
- $u_f$  = Local water velocity
- $J$  = A momentum exchange factor ranging in value from 1 to 2 and being a strong function of the void fraction.

In the void data analysis,  $J$  was assumed to have a constant value of 1.0. The local dynamic pressure heads as measured by the Pitotmeter can thus be written as:

$$\Delta P_j = \frac{1}{2} [\alpha_j \rho_s u_{s,j}^2 + J(1 - \alpha_j) \rho_f u_{f,j}^2], \quad (3.2-3)$$

where  $j$  takes the values from 1 to 5.

Assuming no slip between the two phases (i.e.,  $u_f = u_g$ ), the local mass flux can be given by:

$$G_j = \sqrt{2\Delta P_j[\alpha_j\rho_s + (1-\alpha_j)\rho_f]} \quad (3.2-4)$$

where  $\Delta P_j$  and  $\alpha_j$  are measured using the Pitotmeter and multi-detector gamma densitometer, respectively. The total mass flux is obtained from the local mass fluxes using the following expressions:

$$G_r = \frac{\sum_{j=1}^5 G_j A_j}{A_r} \quad (3.2-5)$$

and

$$A_r = \sum_{j=1}^5 A_j, \quad (3.2-6)$$

where  $A_r$  is the total flow area of the test pipe, and  $A_j$  is the cross-section area of the local pipe segment associated with measuring volume  $j$ .

The methodology used to measure two-phase mass fluxes was verified both in vertical and horizontal two-phase flows using 4 in. Sch. 80 pipes. Detailed descriptions of the calibration loops can be found in Reference 3.2-4. In both loop configurations, reasonable agreement (within 15%) between the measured and actual total two-phase mass fluxes was obtained.

Two Celesco differential pressure transducers (Model DP 30) were used to measure the pressure drop along the length of the test section above the Pitotmeter, as shown in Figure 3.2-2. The transducers had the same range as those used in the annubar (i.e., 0-34 kPa). The axial pressure drop measurements were also used to deduce the average void fraction in the test section, assuming the axial acceleration and friction pressure drops were negligible. The average void fraction,  $\alpha_{\Delta h}$ , can thus be expressed as:

$$\overline{\alpha_{\Delta h}} = \frac{\rho_f}{\rho_f - \rho_s} - \frac{\Delta P_t}{(\rho_f - \rho_s)gh} \quad (3.2-7)$$

where:

- $\Delta P_t$  = Pressure drop along the length of the test section
- $g$  = Gravitational acceleration
- $h$  = The distance over which the pressure drop was measured

The average void fraction as obtained from Equation 3.2-7 can be compared with the average void fraction measured directly by the multi-detector gamma densitometer using the following expression:

$$\overline{\alpha}_{rD} = \frac{\sum_{j=1}^5 \alpha_j A_j}{A_r} \quad (3.2-8)$$

where  $\alpha_{rD}$  is the average void fraction obtained from the gamma densitometer measurements.

The nominal operating conditions in the test loop were controlled by heat addition from the pump and heat removal by an air-cooled heat exchanger. The test loop temperature was controlled using a bypass flow to a 6-MW water-to-air heat exchanger. The bypass flow was taken at a location between the universal venturi tube and the flow control valve. During the heatup phase in preparation for the tests, the bypass flow to the heat exchanger was valved off so that the test loop could be heated up from room temperature to 280°C in about two and one-half hours. After the test loop attained the desired temperature, a bypass flow through the heat exchanger was established to maintain the loop temperature constant. The bypass flow through the heat exchanger was adjusted continually during the test as the pump motor power dropped off under two-phase flow operation. Typically, the loop temperature could be held to within 5°C of the target value.

Two-phase flow and void fraction in the test loop were created by draining water from the loop into a storage tank. The void fraction in the test section was monitored by the gamma densitometer during the tests. Draining was interrupted several times to maintain a constant void fraction in the test section. The flow through the test section could then be varied by adjusting the flow control valve in the test section slowly and in steps. Three test section void fractions at 25%, 50% and 75% were attempted during the tests to study the effect of varying mass flow rates on two-phase flow behavior in the test pipe. The two-phase mass flux in the test section was varied from about 600 to 2200 kg/m<sup>2</sup>s during the tests.

During the test, the two-phase flow conditions in the test loop and the test section were varied slowly, and the loop temperature was held to within 5°C of the target value. It may be assumed that quasi-steady-state conditions prevailed during the test and useful two-phase flow test data could also be obtained while the loop was being drained.

The test procedure also provided in-situ calibration for the gamma densitometer in each test. At the beginning of the test, full pipe conditions with water at the test temperature were obtained for all the five detectors. Empty pipe conditions with steam at the same test temperature were obtained at the end of the test. Uncertainties in void fraction measurements could thus be reduced significantly.

The measured void distributions across the diameter of the test pipe were plotted at different times during the transient and shown in Figure 3.2-3. The measured void distribution in the pipe is symmetrical with respect to the pipe center and is relatively flat in profile for all void fractions.

Axial pressure drops at two locations along the test section were measured downstream of the Pitotmeter and gamma densitometer (Figure 3.2-2). The two measurements behaved essentially the same, as expected. Since the frictional and acceleration pressure drops are negligible in the present tests, these axial pressure drops can be used to calculate the average void fraction in the test section. Figure 3.2-4 shows the comparison of the average void fractions in the test section calculated from the axial pressure drop measurements (using Equation 3.2-7) with the corresponding values obtained using the gamma densitometer (using Equation 3.2-8). In general, the average void fractions based on pressure drop measurements were found to be in good agreement with, but slightly lower than the gamma densitometer measurements. This is due to the fact that the acceleration and frictional pressure drops were not included in the hydrostatic head calculations. This comparison also supports the use of the cross-sectional average of the void measurements for comparison with TRACG results. Furthermore, this comparison also suggests that the axial void distribution along the test section during the transient could be relatively uniform.

Since the test results for different tests at the same nominal temperature were found to be very similar, only two tests, one at each temperature, were analyzed and discussed in Reference 3.2-2. These tests were run at nominal temperatures of 280°C (6.4 MPa) and 230°C (2.8 MPa). For the low-pressure test (230°C), oscillations with large amplitudes in the axial  $\Delta P$  and void fraction were observed at the intermediate void fraction. By studying the  $\Delta P$ -cell and pump head measurements through Fast Fourier Transform in the frequency domain, it was determined that the oscillations observed during the low-pressure test were caused by the dynamic behavior of the pump under two-phase flow conditions and its interaction with the piping system. These oscillations are not a fundamental property of the two-phase flow in the vertical test section. Therefore, the low-pressure data are not included for the TRACG qualification.

### 3.2.3 Applicability of Data to SBWR

[

Redacted

]

[

Redacted

]

### **3.2.4 TRACG Model**

[

Redacted

]

### **3.2.5 TRACG Simulation**

[

Redacted

]

[

Redacted

]

### **3.2.6 Results of Calculations**

[

Redacted

]

#### **3.2.6.1 Accuracy of TRACG Calculations**

[

Redacted

]



[  
Redacted  
]

### 3.2.7 Summary and Conclusions

TRACG simulations of the OHT test (280°C/6.4 MPa) have been performed. The TRACG calculated void fractions compare well with the OHT void data. The uncertainty of TRACG calculated void fraction in a chimney has been established from the results of these comparisons. The key results of this study are summarized in the following:

[  
Redacted  
]

### 3.2.8 References

- [3.2-1] H.A. Upton, J.E. Torbeck, P.F. Billig, J.D. Duncan and M. Herzog, *SBWR Design Update: Passively Safe, Nuclear Power Generation For the Twenty First Century*, 4th JSME/ASME Joint International Conference on Nuclear Engineering, New Orleans, USA, March 1996.
- [3.2-2] H.A. Hasanein, A.M.C. Chan, M. Kawaji and Y. Yoshioka, *Steam-Water Two-phase Flow in Large diameter Vertical Piping at High Pressures and Temperatures*, 4th JSME/ASME Joint International Conference on Nuclear Engineering, New Orleans, USA, March 1996.
- [3.2-3] A.M.C. Chan, *Void Fraction Measurements in Large Diameter Pipes with Thick Metal Walls or Complex Internal Geometries*, Proceedings of the National Heat Transfer Conference, 1992, American Nuclear Society, pp. 236-244.
- [3.2-4] A.M.C. Chan and D. Bzovey, *Measurement of Mass Flux in High Temperature High Pressure Steam-Water Two-Phase Flow using a Combination of Pitot Tubes and a Gamma Densitometer*, *Journal of Nuclear Engineering and Design*, 1990, Vol. 122, pp. 95-104.

**Table 3.2-1**  
**Comparison of Key Parameters in the OHT Test Facility and SBWR Chimney Partitions**

[

Redacted

]

**Table 3.2-2**  
**Comparison of TRACG/OHT Void Fraction During the Time periods of Varying Mass Flow Rate (280°C/6.4 MPa)**

[

Redacted

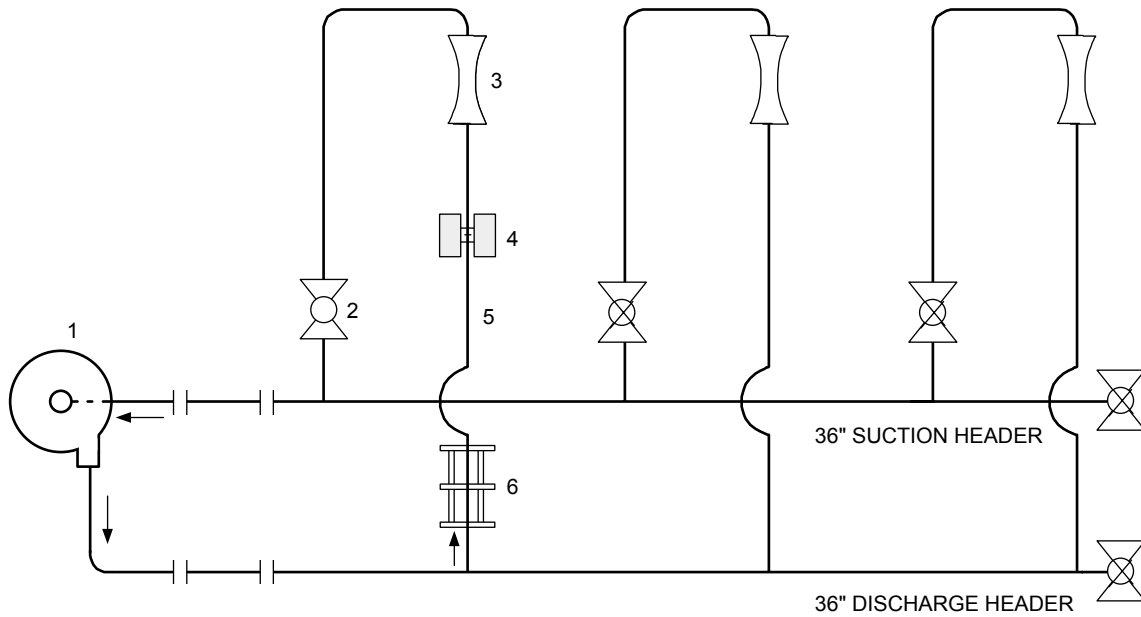
]

**Table 3.2-3**  
**Assessment of TRACG Accuracy for Ontario Hydro Tests**

[

Redacted

]



- 1-PUMP (BRUCENGS 'A' PUMP)
- 2-FLOW CONTROL VALVE
- 3-UNIVERSAL VENTURI TUBE
- 4-GAMMA DENSITOMETER AND FIVE TAP PITOMETER
- 5-24" CARBON STEEL PIPE (12m IN LENGTH)
- 6-PERFORATED S.S. PLATE TYPE FLOW STRAIGHTENING VANE

**Figure 3.2-1 Schematic Diagram of the Test Facility [3.2-2]**

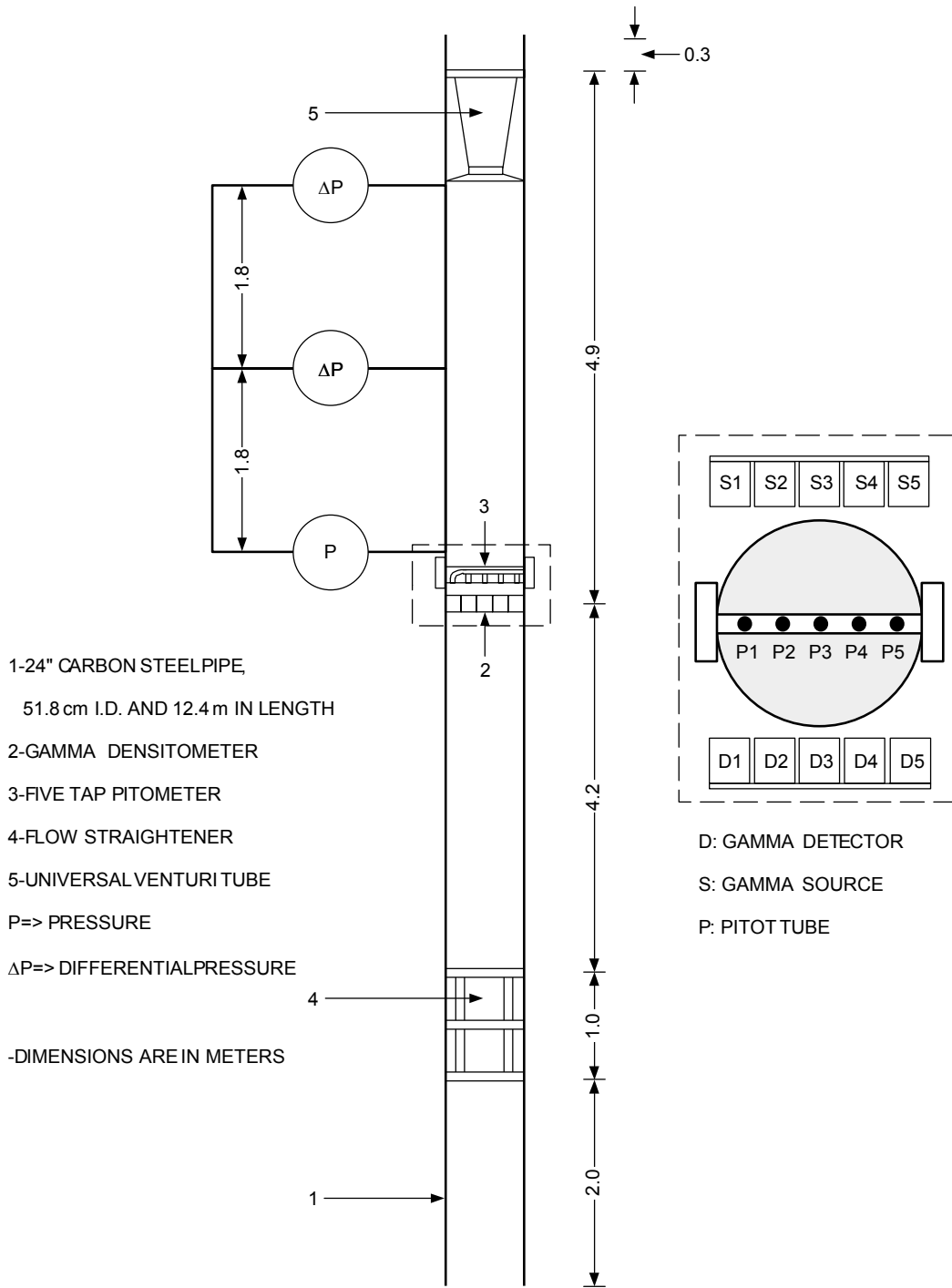
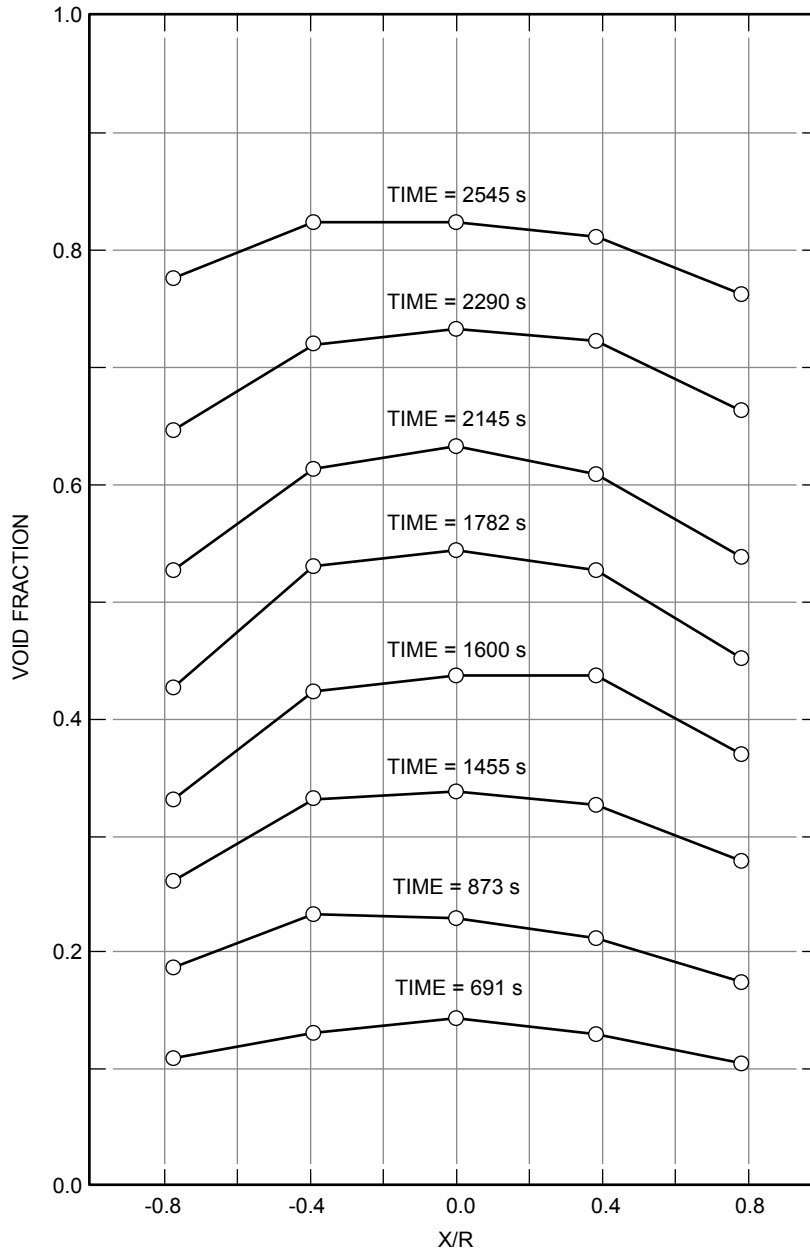
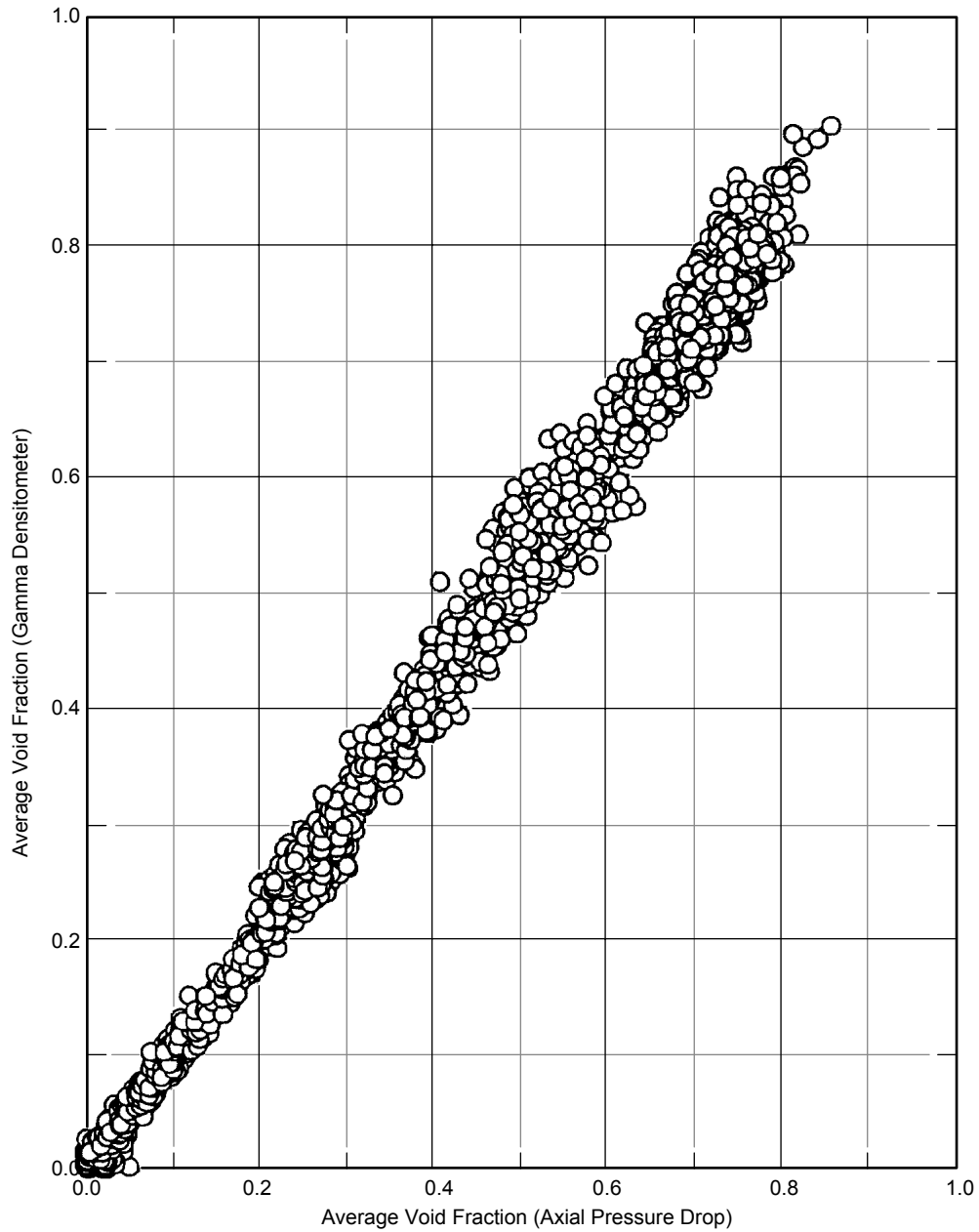


Figure 3.2-2 Schematic Diagram of the Test Section [3.2-2]



NOTE: TIME-AVERAGED DATA WAS USED FOR PLOTTING THIS GRAPH.  
ORIGINAL DATA WAS AVERAGED OVER 36 SECONDS.

**Figure 3.2-3 Radial Void Fraction Distribution at Nominal Temperature of 280°C**



NOTE: TIME-AVERAGED DATA WAS USED FOR PLOTTING THIS GRAPH.  
ORIGINAL DATA WAS AVERAGED OVER 1.0 SECOND.

**Figure 3.2-4 Average Void Fraction as Obtained from the Gamma Densitometer Measurements Versus those Obtained using the Axial Pressure Drop Measurements at Nominal Temperature of 280°C**

[

Redacted

]

**Figure 3.2-5 TRACG Model Description of OHT Test**

[

Redacted

**Figure 3.2-6 Local Void Fluctuations (around 2000 s) at Nominal Temperature of 280°C**

]



[

Redacted

**Figure 3.2-7 Local Void Fluctuations (around 2500 s) at Nominal Temperature of 280°C**

]

[

Redacted

]

**Figure 3.2-8 Comparison of TRACG and Time-averaged Data - Average Void Fraction at Nominal Temperature of 280°C**

### **3.3 Summary of Separate Effects Comparisons**

#### **3.3.1 Void Fraction Data**

[

Redacted

]

[

Redacted

]

### 3.3.2 PSTF Level Swell Tests

[

Redacted

]

[

Redacted

]

**3.3.3 Condensation in the Presence of Noncondensibles - University Tests**

[

Redacted

]

### 3.3.4 Critical Flow

[

Redacted

]

### 3.3.5 Frictional Pressure Drop

[

Redacted

]

[

Redacted

]

### **3.3.6 Critical Power**

[

Redacted

]

#### **3.3.6.1 ATLAS Critical Power Data**

[

Redacted

]



**3.3.6.2 Applicability of GEXL Correlation for Bundles with 2.8m Length**

[

Redacted

]

**3.3.7 SPERT Reactivity Insertion Test**

[

Redacted

]

[

Redacted

]

### **3.3.8 Thermal Hydraulic Stability**

[

Redacted

]

**3.3.9 Flow Oscillations at Low Pressure**

[

Redacted

]

**3.3.10 Humboldt Bay and Bodega Bay Pressure Suppression Test Programs**

[

Redacted

]

[

Redacted

]

### 3.3.11 References

- [3.3-1] H. Christensen, *Power-to-Void Transfer Function*, ANL 6385, July 1961.
- [3.3-2] O. Nylund, R. Eklund and R. Rydalm, OF-64b, *Results of Void Measurements*, FRIGG PM-105, June 1970.
- [3.3-3] J.F. Wilson, R.J. Grenda and J.F. Patterson, *Steam Volume Fraction in a Bubbling Two-Phase Mixture*, Trans ANS 4(2), pp. 356-357, 1961.
- [3.3-4] G.G. Bartolomei, V.A. Suvorov and S.A. Tevlin, *Hydrodynamics of Steam Generation in a Two-Circuit Nuclear Power Plant*, Teploenergetika 10(1), pp. 52-57, 1963.
- [3.3-5] M. Petrick and E.A. Spleha, *Thermal Hydraulic Performance Characteristics of EBWR*, ANL 6693, May 1963.
- [3.3-6] S. Morooka, T. Ishizuka, M. Iizuka and K. Yoshimura, *Experimental Study on Void Fraction in a Simulated BWR Assembly (Evaluation of Cross-Sectional Averaged Void Fraction)*, Nuclear Engineering and Design 114, pp. 91-98 (1989).
- [3.3-7] H.A. Hasanein, A.M.C. Chan, M. Kawaji and Y. Yoshioka, *Steam-Water Two-Phase Flow in Large diameter Vertical Piping at High Pressures and Temperatures*, 4th JSME/ASME Joint International Conference on Nuclear Engineering, New Orleans, USA, March 1996.

- [3.3-8] J.A. Findlay, *BWR Refill-Reflood Program Task 4.8 - Model Qualification Task Plan*, General Electric Company, GEAP-24898, August 1981.
- [3.3-9] S.Z. Kuhn, V.E. Schrock and P.F. Peterson, *Final Report on U.C. Berkeley Single Tube Condensation Studies*, UCB-NE-4201 Rev. 2, August 1994.
- [3.3-10] A.A. Dehbi, M.W. Golay and M.S. Kazimi, *The Effects of Noncondensable Gases on Steam Condensation under Turbulent Natural Conditions*, MIT Report MIT-ANP-TR-004, June 1991.
- [3.3-11] *The Marviken Full-Scale Critical Flow Test - Third Series, Results from Test 24, MXC-224*, Marviken Power Station, Sweden, September 1979.
- [3.3-12] A.R. Edwards and T.P. O'Brien, *Studies of Phenomena Connected with the Depressurization of Water Reactors*, Journal of the British Nuclear Energy Society, 9, pp. 125-135, April 1970.
- [3.3-13] K.H. Chu and B.S. Shiralkar, *Prediction of Critical Power Based on a Two-Fluid and Multi-Field Model*, Fourth International Meeting on Nuclear Thermal Hydraulics, Operation and Safety, 1993.
- [3.3-14] Letter from P.W. Marriott (GE) to R.W. Borchardt (NRC), *NRC Requests for Additional Information (RAIs) on the Simplified Boiling Water Reactor (SBWR) Design*, MFN No. 128-94, Docket No. STN 52-004, October 5, 1994.
- [3.3-15] M. Aritomi, T. Nakahashi, J.H. Chiang, M. Wataru and M. Mori, *Transient Behavior of Natural Circulation for Boiling Two-Phase Flow (Experimental Results)*, 6th Proc. Nuclear Thermal Hydraulics, p.313, November 1990.
- [3.3-16] E. Vial and V.E. Schrock, *A Correlation Based on the Combined UCB and MIT Data Sets for Condensation Inside Tubes with Noncondensable Gas*, UCB-NE-4193, April 1993.
- [3.3-17] B. Matzner and J.E. Casterline, *The Effect of Length and Pressure on Critical Heat Flux for a Closely Spaced 19 Rod Bundle in Forced Convection Boiling*, Columbia University Topical Report No.7, Task XVI of Contract AT(30-3-187), USAEC/AECL Cooperative Program on Heavy Water Moderated Reactors, December 1965.

**Table 3.3-1**  
**Range of Parameters for SBWR Regions**

[

Redacted

]

**Table 3.3-2**  
**Summary of Void Fraction Comparisons**

[

Redacted

]

**Table 3.3-3**  
**TRACG Calculation of Pressure Response and Level Change for PSTF**  
**Level Swell Tests**

[

Redacted

]

**Table 3.3-4  
TRACG Calculation of Critical Flow**

[

Redacted

]

**Table 3.3-5  
TRACG Calculation of Frictional Pressure Drop**

[

Redacted

]

**Table 3.3-6  
Calculation of Natural Circulation Flow and Power for Onset of Stability**

[

Redacted

]



[

Redacted

]

**Figure 3.3-1 Critical Power vs. Length (Columbia Data [3.3-17])**

[

Redacted

]

**Figure 3.3-2 Critical Power Comparisons for 2.8m GE8 Fuel Bundle – GEXL02  
Correlation vs. COBRAG**

## 4. Component Performance Tests

This section describes the TRACG post-test analyses of the component performance tests used to qualify the code for SBWR applications. The component tests included in the post-test evaluation are the PANTHERS PCC Performance Tests (Section 4.1), the PANTHERS IC Performance Tests (Section 4.2), the PANDA PCC Performance Tests (Section 4.3), and the Suppression Pool Stratification Tests (Section 4.4). The first three of these tests were used to qualify TRACG for calculation of PCC and IC heat removal and PCC pressure drop. The Suppression Pool Stratification Tests were used to demonstrate the adequacy of the pool stratification procedure employed in the application of TRACG for calculation of post-LOCA behavior of the SBWR containment. The results of TRACG qualification against separator performance data were reported in the generic TRACG qualification report (J. G. M. Andersen et al., *TRACG Qualification*, NEDE-32177P, Rev. 2, January 2000).

### 4.1 Panthers PCC Performance

#### 4.1.1 Introduction

Section 4.1 describes TRACG qualification based on post-test calculations for tests in the PANTHERS PCC test program. The analysis of these tests was performed by an SBWR analysis team with participation from ENEA (Italy), who also coordinated the testing, JAPC (Japan), and GE. GE managed the post-test analysis activity and provided the final documentation, including the Design Record File (DRF T15-00018). Results of a pre-test analysis of two of the PANTHERS PCC tests were submitted to the NRC in May 1994 [4.1-1].

The PANTHERS PCC test facility utilized a full-scale prototype of the PCC that was designed for the SBWR plant. As such, the PCC test series provided a definitive evaluation of the performance of the condenser component under conditions that are representative of a LOCA in the SBWR. Satisfactory agreement between the test data and the results of TRACG simulations of these tests provides a high degree of confidence that TRACG can be used to simulate the performance of the condensers in a post-LOCA environment.

The overall PANTHERS PCC TRACG qualification activity is summarized in Table A.3-3 of Reference 4.1-2. The first step consisted of “double-blind” pre-test calculations for Tests 15\_1 and 23\_4. A double-blind calculation is one in which neither the exact test conditions nor the test data are available. The results of the pre-test analysis are presented in Reference 4.1-1. The measured PANTHERS PCC condenser efficiencies were predicted with accuracies of 8.4% and 2.2%, respectively, for Tests 15\_1 and 23\_4. The predictions were on the conservative side (lower efficiency) of the test results. Table A.3-3 of Reference 4.1-2 also lists sixteen tests, including the two pre-test cases, for which post-test analyses were to be performed. This set includes three steady-state pure-steam tests, nine steady-state steam-air tests, and four transient tests.

[ Redacted ]

[

Redacted

]

Section 4.1 is organized as follows. Section 4.1.2 presents a description of the PANTHERS PCC test facility and test matrix. Section 4.1.3 discusses applicability of the test data to the SBWR. Section 4.1.4 describes the PANTHERS PCC post-test TRACG models. Section 4.1.5 describes the TRACG simulation of the test procedures for the various types of tests included in the post-test evaluation. Section 4.1.6 presents and discusses the results of the TRACG simulations and their comparison to the measured data. Finally, Section 4.1.7 summarizes the results and presents a set of conclusions from the post-test evaluation. Included in the Section 4.1.7 discussion are specific references to the TRACG “qualification needs” identified in Reference 4.1-2.

## **4.1.2 Test Facility/Test Matrix**

### **4.1.2.1 Test Facility**

PANTHERS/PCC (Passive Containment Condenser) testing was performed as a joint effort between GE, Ansaldo, ENEA, and ENEL at Societa Informazioni Esperienze Termoidrauliche (SIET) in Piacenza, Italy. The test facility consisted of a prototype PCC unit, steam supply, air supply, and vent and condensate volumes sufficient to establish PCC thermal-hydraulic performance.

The PCC condenser was a full-scale, two-module vertical tube heat exchanger designed and built by Ansaldo. Figure 4.1-1 is an outline drawing of the heat exchanger assembly. The heat exchanger was a prototype unit, built to prototype procedures and using prototype materials. Three heat exchanger units (6 modules) are incorporated in the SBWR design. The PCC was installed in a water pool having the appropriate volume for one SBWR PCC assembly.

Figure 4.1-2 is a schematic of the PANTHERS/PCC facility. The primary instrumentation specified is sufficient to ascertain heat exchanger thermal-hydraulic performance by performing mass and energy balances on the facility. Additionally, four heat exchanger tubes were instrumented in such a way that local heat flux information was obtained.

The majority of the PANTHERS/PCC testing was steady-state performance testing. For these tests, the facility was placed in a condition where steam or air/steam mixtures were supplied to the PCC, and the condensed vapor and vented gases were collected. All inlet and outlet flows were measured. The condensate was returned to the steam supply, and the vented gas was released to the atmosphere. Once steady-state conditions were established, data were collected for a period of approximately 15 minutes. The time-averaged data were reported in Reference 4.1-3 and analyzed in Reference 4.1-4.

Steady-state tests using a steam/air mixture were performed as follows. The test loop and PCC condenser were first purged with steam to remove any residual air from the system and to heat the PCC pool to saturation. When the pool was boiling, the required steam flow rate was established, followed by establishment of the required air flow rate to the PCC. The desired

PCC inlet pressure was then established by adjusting the position of the vent tank flow control valve. When steady conditions had been established, data were taken for a period of approximately 15 minutes.

A slightly different procedure was used for the steam-only tests. Originally, the plan was to isolate the vent tank by closing the spectacle flange on the PCC vent line. However, since the measured heat loss from the vent tank was conservatively estimated to be 13 kW [4.1-3, Appendix C], the PCC vent was left open to the tank. Following initial purging of air from the system, the valve from the vent tank to the atmosphere was closed, and the desired steam flow rate was established. The inlet pressure was not controlled, but allowed to stabilize while maintaining full condensation at the fixed steam flow rate. Again, data were acquired for a period of approximately 15 minutes.

PANTHERS/PCC transient condenser performance tests were used to establish noncondensable buildup effects and PCC pool water level effects. The noncondensable buildup tests were designed to examine differences in behavior between heavier-than-steam and lighter-than-steam gases. They were not intended to simulate integral system behavior of the PCCS in the SBWR.

The noncondensable buildup tests were performed as follows. The test conditions were initialized, using the steam-only procedure described above with the spectacle flange on the vent line closed. When steady-state conditions were established, the Data Acquisition System (DAS) was started, and air, helium, or an air/helium mixture was injected at the rate specified. The inlet pressure was allowed to increase as the noncondensable gases accumulated, and the condensation process was degraded by the presence of noncondensable gases in the PCC condensing section. The test was terminated when the PCC heat exchanger reached its design pressure.

For the pool water level tests, the procedure was to establish the initial conditions as described for the steady-state steam or air/steam mixture tests. The vent flow control valve was closed for the steam tests and maintained at a fixed open position for the steam/air tests. The PCC pool water level was allowed to decrease, by either boiloff, draining or a combination of the two. Inlet pressure to the PCC was allowed to rise, consistent with the condensation process. The test was concluded when the desired pool water level range had been investigated.

#### **4.1.2.2 Test Matrix and Data Analysis**

The PANTHERS/PCC Data Report [4.1-3] gives the complete test matrix for all the thermal/hydraulic tests. From that matrix, sixteen tests were chosen for post-test TRACG analysis [4.1-2] in order to demonstrate the capability of TRACG to calculate the heat rejection rate of the PCC over a wide range of conditions. The test conditions chosen for TRACG analysis are discussed below. Section 4.1.3 discusses the applicability of these test conditions to the SBWR.

##### **4.1.2.2.1 Steady-State Performance Tests**

Table 4.1-1 shows the PANTHERS/PCC steady-state performance matrix at 5 kg/s steam flow rate used for TRACG post-test analysis. Test conditions include both pure steam and

air/steam mixtures. Test Conditions 41 and 43 demonstrate the heat exchanger performance with pure saturated steam flow rates at and above rated conditions. Test Conditions 9, 15, 18, and 23 demonstrate the heat rejection rates over a range of air flow rates with the same saturated steam flow as Test Condition 41 in the pure-steam series. Holding steam flow constant at near rated conditions, these tests yield the effect of air (similar to nitrogen in the SBWR) on the condensation process. Test Condition 35 addresses the potential effect of superheat on condenser heat removal at the same rated steam flow condition.

Table 4.1-2 shows the PANTHERS/PCC Steady-State Performance Matrix at Extreme and Intermediate Ranges used for TRACG post-test analysis. Test Conditions 2 and 22 address the effects of air in the low steam flow range at high and low extremes of air flows. Test Conditions 17 and 19 consider the effect of steam flow at a fixed mid-range air flow.

#### 4.1.2.2.2 Transient Tests

Table 4.1-3 shows the PANTHERS/PCC Transient Performance Test Matrix used for TRACG post-test analysis. The tests include noncondensable buildup transients with light and heavy gases and a pool water level transient.

In the noncondensable gas buildup tests, steam was supplied at a constant rate, and steady-state conditions were established in a manner similar to that of the steady-state performance tests. Air, helium, or air/helium mixtures were then injected into the steam supply, with the vent line closed. The transient degradation in heat transfer performance was reflected in an increasing condenser inlet pressure, as a function of the total noncondensable mass injected.

Test Condition 51 provides a baseline condition with air as the only noncondensable. Air is similar to nitrogen in molecular weight, and is heavier than steam. Test Condition 76 repeats Test Condition 51, but utilizes helium as the noncondensable gas instead of air. Helium is lighter than steam, and behaves in a manner similar to hydrogen. The results of Tests 51 and 76 are compared to establish performance differences between lighter-than-steam and heavier-than-steam gases as they build up in the heat exchanger tubes. Test Condition 78 is used to evaluate the effect of an air and helium mixture concurrently flowing into the heat exchanger.

Table 4.1-3 also shows the pool water level effect test condition. GE had originally planned to perform a TRACG post-test analysis of Test 55 [4.1-2]. In Test 55, steam and air were supplied to the PCC heat exchanger, and steady-state conditions were established in a manner similar to the steady-state performance tests. As the water level in the PCC pool dropped and the PCC tubes uncovered, the flow control valve from the vent tank to the atmosphere was held in a fixed open position. As the pool water level decreased, the system pressure increased and the condenser efficiency decreased. The combination of increasing system pressure and decreasing condenser efficiency made the results of the test difficult to interpret and did not clearly elucidate the effect of pool water level on condenser heat transfer. Simulation of Test 55 would have been sensitive to the hydraulic loss of the vent tank flow control valve, which had not been measured.

It was concluded that the ability of TRACG to model the PCC performance with varying pool water level could be evaluated more effectively by simulating Test 54. In Test 54, pure

steam was supplied to the PCC heat exchanger, and steady-state conditions established in a manner similar to the steady-state performance tests. The water level in the PCC pool dropped by boil-off and draining, and the PCC tubes uncovered. Since the vent tank is closed, complete condensation takes place throughout the test. The measured pressure required to maintain complete condensation is compared against TRACG results to evaluate the effect of pool water level on PCC performance.

### **4.1.3 Applicability of Data To SBWR**

#### **4.1.3.1 Scope**

The PANTHERS/PCC test program was a component test of a full-size prototypical SBWR condenser. Boundary conditions consisting of inlet steam flow, air flow, and pressure were imposed, and the performance of the unit was measured. In the TAPD [4.1-2], the applicability of PANTHERS/PCC test data to SBWR is discussed. This section expands on that discussion and shows how actual test conditions used in the TRACG post-test evaluation correspond to potential operating conditions for the PCC in the SBWR.

#### **4.1.3.2 SBWR**

##### **4.1.3.2.1 PCC Operation**

In the SBWR, the post-LOCA function of the PCC is to remove decay heat from the drywell and reject this energy to the atmosphere. This is the major difference between the SBWR and earlier pressure suppression containment designs. In earlier designs, the decay heat is transferred from the drywell to the wetwell via main vent flow, and is subsequently transferred to the ultimate heat sink (UHS) by the Residual Heat Removal (RHR) System.

As in previous pressure suppression containment designs, following the initial vent-clearing transient, the maximum drywell pressure is limited to the wetwell pressure plus the vent submergence head and vent system flow losses. For design basis accidents, the peak long-term drywell pressure occurs when essentially all the noncondensable gases are present in the wetwell and, consequently, the drywell is pure saturated steam. The wetwell pressure is the sum of the partial pressures of nitrogen and water vapor. The resultant drywell pressure is in the range of 300 to 330 kPa.

During a LOCA in the SBWR, the PCCS and the GDCS form a circuit to keep the core covered with water and remove the decay heat. Steam coming off the core leaves the RPV through the DPVs, enters the drywell, and flows to the PCCS. Condensate flow from the PCCS heat exchangers drains to the GDCS pools in the drywell. The GDCS delivers the water to the RPV, where the decay heat of the core converts it to steam and starts the loop again.

##### **4.1.3.2.2 PCC Operational Modes**

The operational modes of the PCC heat exchanger can best be described in terms of the pressure difference across the unit. Figure 4.1-3 illustrates several of a family of possible pressure trajectories along the flow path from the drywell to the suppression pool via the PCC heat exchanger. Note that the drywell-to-wetwell pressure difference can vary only between the

negative value required to open the vacuum breaker and the positive value required to open the main vent. The individual curves in Figure 4.1-3 can be categorized as follows.

### **Reference LOCA Condition**

Curve 1 illustrates the SBWR post-LOCA condition with the PCC carrying the decay heat load. In this case, the drywell pressure is slightly greater than the PCC vent submergence pressure, but less than the LOCA vent submergence pressure. Thus, water is forced out of the PCC vent line, clearing a gas venting path to the suppression pool. The flow is forced through the PCC heat exchanger by the drywell-to-wetwell pressure difference, and noncondensable gases are vented into the suppression pool.

### **PCC Capacity Greater than Decay Heat**

Curves 2 and 3 of Figure 4.1-3 illustrate a situation where most of the noncondensable gases have been vented to the wetwell. These two curves illustrate cases where the drywell is supplying nearly pure steam to the heat exchanger: Curve 3 represents PCCS inlet conditions with less noncondensable gases than Curve 2. As the effects of noncondensable gases degrading the heat transfer process are reduced, the heat exchanger can reject more energy than is supplied to the drywell by decay heat, and the drywell pressure is reduced. The reduced pressure is no longer sufficient to keep the PCC vent open, so suppression pool water partially refills the PCC vent pipe. The flow into the PCC heat exchanger is no longer driven by the drywell-to-wetwell pressure difference, but by the lowered pressure in the heat exchanger tubes due to the condensation process. Typically, this type of operation is limited by Curve 4, where the drywell pressure has fallen below the wetwell pressure by an amount equal to the vacuum breaker opening pressure. (Transiently, the drywell pressure could decrease further, for example, with drywell sprays in operation, but this is not a condition of significance for PCCS operation.) Here, the vacuum breaker opens, returning noncondensable gases to the drywell where they can re-enter the PCCS. When this happens, the capacity of the PCCS to remove energy is temporarily degraded.

### **PCC Capacity Less than Decay Heat**

Finally, Curve 5 of Figure 4.1-3 illustrates the other extreme of PCC operation. In this case, PCC heat transfer is insufficient to reject the decay heat, the drywell pressure rises, and flow is forced through the PCC by the drywell-to-wetwell pressure difference. However, the magnitude of the PCC driving pressure difference is limited by the presence of the main LOCA vents. If the main LOCA vents clear, then mass and energy will flow to the suppression pool via the main vent system to limit the drywell pressure. This pressure difference will determine the parallel flow through the PCCS.

In summary, PCCS performance in the SBWR is characterized by two relatively distinct operating modes: (1) a pressure-driven mode, with the PCC vent cleared to accommodate throughput of a mixture of steam and noncondensable gases; and (2) a condensation-driven mode with the PCC partially filled with water and no throughput to the wetwell. Characteristics of these PCC Operational modes can be summarized and contrasted as follows:



Pressure-Driven Mode

- PCC capacity  $\leq$  core decay heat
- PCC flow is forced by the DW-to-WW pressure difference
- PCC flow includes both steam and noncondensable gas

Condensation-Driven Mode

- PCC capacity  $\geq$  core decay heat
- PCC flow is induced by DW-to-CC pressure difference due to condensation
- PCC flow is essentially pure steam

For completeness, it should be noted that condensation always plays some role in moving a steam-gas mixture through the PCC unit. The distinction is that, in the pressure-driven mode, it is of secondary importance and, by itself would not be able to sustain flow.

4.1.3.2.3 PCC Purge and Vent Process

A PCCS purge event can occur as a result of the system being called upon to remove decay heat after an extended period of inactivity, or by an increase in the mass fraction of noncondensable gas in the region of the drywell from which the system draws its inlet mixture. If the system is starting up after a period of inactivity, the condensers will contain a mixture of steam and noncondensable gas in near thermal equilibrium with the surrounding pool. The partial pressure of the steam will be approximately saturation pressure at the pool temperature and the remainder of the mixture will be noncondensable gas. This mixture must be expelled from the condenser tubes before heat removal can begin. As steam is added to the drywell by the RPV, the drywell pressure will rise until the PCCS vents are cleared and the initial steam/noncondensable gas inventory of the condensers is vented. The movement of the initial inventory out of the condenser tubes will be accompanied by ingestion of a fresh steam/noncondensable gas mixture at the existing drywell conditions in the neighborhood of the PCCS inlets. Depending upon the fraction of noncondensable gas in the inlet mixture, and the decay power, the system may or may not be able to condense steam at the rate it is being added to the drywell by the RPV.

Consider, first, the case where the PCCS heat removal rate at the existing inlet conditions is less than decay power. The situation is the same whether the PCCS is starting up from a period of inactivity or, while operating, is confronted with an increased noncondensable fraction in the inlet mixture. The drywell pressure will rise, thereby increasing the flow rate through the condensers from the drywell to the wetwell. The rise in drywell pressure also slightly increases the condensation rate. Additionally, as steam is continuously added to the drywell by the RPV, and a steam/gas mixture is transported through the condensers, the mass fraction of noncondensable gas in the inlet mixture will start to decrease. At some point, the combination of increasing drywell pressure and decreasing noncondensable inlet mass fraction enables the PCCS heat removal rate to match decay power and the drywell pressure stops rising.

Next, consider the case where PCCS heat removal rate at the existing inlet conditions is greater than decay power. Again, the situation is the same whether the PCCS is starting up from a period of inactivity or, while operating, is confronted with a decreased noncondensable fraction in the inlet mixture. The drywell pressure will start to drop, allowing water to reenter and close the vents. Unless the inlet conditions are pure steam, the PCCS will then start to accumulate noncondensable gas. Gas can accumulate in the vent pipes above the water level, in the headers, and in the condenser tubes. The combination of accumulating noncondensable gas and, to a lesser extent, decreasing drywell pressure results in a decreasing condensation rate. Eventually, the condensation rate will drop below decay power and the drywell pressure will start to rise, initiating a new purge cycle.

The presence of vacuum breakers in the SBWR leads to a potential interaction between PCCS purging and vacuum breaker operation. As discussed above, if the instantaneous PCCS heat removal exceeds decay power, the drywell pressure will decrease. When the difference between DW and WW pressure drops below the submergence head of the PCCS vents, water will enter the vents and noncondensable gas will start to accumulate in the PCCS. The drywell pressure will continue to decrease until the combination of the lower pressure and the noncondensable gas accumulation drops the PCCS heat removal rate below decay power. If the PCCS noncondensable gas inventory when the vents close is relatively small, and the mass fraction of noncondensable gas in the inlet mixture is also small, the drywell pressure can continue to fall until it drops below the wetwell pressure by a sufficient amount to allow the vacuum breakers to open. The noncondensable gas which flows back to the drywell via the vacuum breakers increases the mass fraction of noncondensable gas in the inlet mixture, degrades condenser performance and leads to a new purge cycle. Thus, it can be seen that, depending on the attendant circumstances, a PCCS purge event may or may not lead to a vacuum breaker opening. In discussing these two possibilities, GE has introduced the nomenclature “strong purge” to identify a purge event which leads to opening of a vacuum breaker and “weak purge” to identify one which does not.

### **4.1.3.3 PANTHERS**

#### **4.1.3.3.1 PCC Operation**

The basic feature of PANTHERS/PCC tests is that the PCC test unit is subjected to boundary conditions that determine its performance in a directly analogous manner to the PCC unit in the SBWR. Steam for the tests is supplied by a neighboring power plant. The facility has a condensate tank which collects the condensate from the PCC and returns it to the power plant, thereby performing the function of the GDCS in closing the loop between the PCC and the RPV. The water level in the condensate tank is held at a position corresponding to the top of the loop seal on the drain line in the SBWR. The pressure in the tank is equal to the PCC steam inlet pressure which is similar to the SBWR where the pressure above the GDCS pool is the drywell pressure. The PANTHERS PCC vent configuration differs between the types of tests performed. Figure 4.1-4 shows how the different configurations simulate the two operational modes of the PCC as discussed below.

#### 4.1.3.3.2 Steady-State Tests

As noted in the earlier discussion, the PCC can perform in two distinct modes: pressure-driven and condensation-driven. Both of these conditions are simulated in the PANTHERS/PCC steady-state tests, as discussed below. The pure-steam steady-state tests simulate the condensation-driven mode and the steam-air tests simulate the pressure-driven mode.

##### **Pure Steam Tests**

The pure steam tests, represented by Tests 41, 43, and 49 of the set chosen for post-test analysis, are performed with the PCC vent tank closed. Since there is negligible heat loss from the vent tank, all the steam is condensed within the PCC and steam is drawn into the heat exchanger by the condensation process. These tests simulate the condensation-driven mode. With no noncondensable gases present in the heat exchanger, the pressure is determined as that necessary to maintain complete condensation for the prescribed inlet steam flow.

##### **Air/Steam Mixture Tests - Conditions Early in the LOCA**

In the steam-air steady-state tests, flow is permitted from the vent tank to the atmosphere. The vent tank pressure is controlled such that the PCC inlet pressure matches a specified value at prescribed inlet steam and air flows. These tests simulate the pressure-driven mode. In this case there is flow through the heat exchanger, with the flow rate determined by the difference in pressure between the inlet supply and the vent tank.

The independent variables for the PANTHERS/PCC steady-state steam-air tests are steam flow rate, air flow rate, and PCC inlet pressure. Dependent variables include condenser efficiency (ratio of steam condensed to steam in) and system pressure drop. Figure 4.1-4 illustrates how the test conditions model SBWR post-LOCA conditions.

As noted in the previous discussion of operating modes, with the exception of the main-vent clearing transient which occurs within a few seconds of the LOCA, the pressure drop from the drywell through the PCC heat exchanger to the PCC vent exit cannot exceed a value equivalent to the difference in hydraulic head between the main LOCA vent submergence and the PCCS vent submergence. A larger pressure loss would cause the top main vent to open. This pressure drop limit is approximately 9 kPa.

In PANTHERS, the pressure drop depends on the PCC performance for the prescribed pressure and flow inlet conditions. The PCC pressure drop is one of the dependent variables measured during the testing. Figure 4.1-4 shows that two of the inlet conditions prescribed for Test 23 resulted in an overall pressure drop about equal to the limit at which main vent flow would initiate. These tests represent the upper limit for PCC inlet gas mass fraction at the given steam flow rate. In the SBWR, if the gas mass fraction was higher, a portion of the flow would be diverted to the main LOCA vents.

Test 09 models conditions where a large fraction of the steam is condensed while noncondensable gases are continually vented to the wetwell. The pressure drop through the

system is less than the submergence head between the PCC vent exit and the top main vent, so all of the flow would be through the PCCS.

In the SBWR, as the steaming rate decreases at a relatively constant inlet pressure, the steam in the inlet steam/gas mixture is completely condensed, and the pressure drop through the system is near the lower boundary of the pressure-driven range. (It should be noted that “complete condensation” is used to describe a situation in which the temperature of the gas mixture in the bottom of the condenser is close to the pool temperature. Such a mixture, in direct contact with the condensate film, is likely to contain water vapor at a partial pressure near one bar.) This condition is closely modeled by Test 02, where the efficiency is over 90%. As the fraction of noncondensable gases in the inlet flow approaches zero, the PCC operating mode transitions to the condensation-driven range.

From the above discussion, it can be seen that the PANTHERS PCC test matrix included conditions which produced flows up to the limit of what the unit could experience at any time during the post-LOCA transient. This provides a basis for qualification of the TRACG code for simulation of PCCS performance over the full range of post-LOCA conditions. The only exception is the first few seconds of the LOCA during which the PCCS flow would be dictated by the pressure difference associated with the initial vent-clearing transient. This regime is not important for TRACG qualification, however, because the flow is almost purely noncondensable gas and, consequently, PCCS heat removal is insignificant.

### **Air/Steam Mixture Tests - Conditions after One Hour**

The design basis of the Passive Containment Cooling System (3 heat exchangers) provides the ability to reject all SBWR decay heat at approximately one hour post-LOCA. Figure 4.1-5 compares the range of test conditions for PANTHERS/PCC with the air and steam flow conditions for the SBWR main steam line and GDSC line break scenarios after one hour into a LOCA. The triangles representing the (MSL), bottom drain line (BDL), breaks are constructed as the intersection of a vertical line, bounding the maximum steam flow, and a line drawn from the origin with a slope sufficient to envelope the calculated steam and noncondensable flow rates. The triangles are not one-to-one maps or time histories but, rather, bounds of the steam/noncondensable gas inlet conditions throughout the calculated SBWR LOCA scenario.

The triangles can be used to explain the progression of inlet conditions as the transient proceeds. This progression starts at the origin. In the time period immediately following one hour, subcooled GDSC water is absorbing the decay heat power and there is no flow to the PCCS. This time period is represented by the region near the origin. When the RPV water again reaches saturation, flow to the PCCS resumes and, at first, follows an approximately linear steam/noncondensable gas flow trajectory corresponding to the noncondensable gas mass fraction in the region of the drywell which feeds the PCCS. This initiates the purging process which transports the drywell noncondensable gas to the wetwell via the PCC units. At some point during the purge, the concentration of noncondensable gas in the drywell starts to drop and the steam/noncondensable gas trajectory turns over. The steam flow continues to increase as the noncondensable gas concentration in the inlet mixture decreases. The end of the purging process is represented by the extreme lower right corner of the triangle. The steam flow has now

increased to its maximum value (matching the decay power) and the noncondensable gas flow has dropped to essentially zero. From this point, the steam flow “walks” backward along its axis as the decay power slowly drops.

The difference in the steam/noncondensable gas envelopes for the GDCS line and main steam line break accident scenarios results from the behavior during the GDCS injection phase of the transient. For the main steam line break, a large fraction of the subcooled GDCS water is retained in the pools as the RPV two-phase water level rapidly recovers to the main steam line elevation and equilibrates with the water in the GDCS pools. There is very limited vacuum breaker activation and, accordingly, there is a small noncondensable gas fraction in the drywell at the initiation of PCCS flow. PCCS flow initiates about one hour from the instant of LOCA at a decay power close to its rated heat removal capacity and, as a result of the low drywell noncondensable gas inventory, it rises to match decay power relatively rapidly. For the GDCS break, the pools drain completely and RPV steaming does not resume until about 2.5 hours from the LOCA. During the GDCS injection period, there are multiple vacuum breaker actuations leading to a relatively large noncondensable gas fraction in the drywell when PCCS flow initiates. With the larger noncondensable fraction, PCCS steam flow does not match decay power until about 3.5 hours from the LOCA. Thus, the maximum PCCS steam flow is significantly reduced from the main steam line break case. The bottom drain line break behaves similarly to the GDCS line break.

The information conveyed by Figures 4.1-3 through 4.1-5 can be summarized as follows. Figure 4.1-3 illustrates pressure trajectories from the drywell to the wetwell through the PCCS that are associated with various PCCS operating modes. Specifically, Curves 1 through 4 in Figure 4.1-3 describe a sequence of conditions which could follow a purging transient in which the PCCS heat removal has risen to match decay power. Figure 4.1-4 shows which PANTHERS test conditions correspond to the various PCCS operating regimes. Figure 4.1-5 shows how the SBWR PCCS inlet conditions in the post one-hour LOCA period are covered by the PANTHERS test matrix. The third independent variable, PCC inlet pressure, is not indicated on this figure, but is shown for the various tests in Tables 4.1-1 and 4.1-2. For this same time period, the SBWR would be expected to have a PCC operating pressure near 300 kPa. The steady-state air/steam tests typically have data taken at six pressures, ranging from 200 to 600 kPa, with one pressure near the 300 kPa nominal value.

#### 4.1.3.3.3 Transient Tests

Transient tests are performed to assess two phenomena: (1) the buildup of noncondensable gases in the heat exchanger, and (2) the reduction of PCC pool water level as the inventory is boiled away.

## Noncondensable Gas Buildup Tests

The noncondensable gas buildup tests are initiated by establishing steady-state pure-steam condensation at rated PCCS conditions (i.e., near 5 kg/sec). Air and/or helium, representing heavier-than-steam and lighter-than-steam gases, are then introduced at low volume flow rates. The flow rate is low enough such that the performance may be considered quasi-steady. Noncondensable gases are added until the pressure required for complete condensation is approximately the design pressure of the PCC. These tests do not simulate PCCS operating modes in the SBWR. As described above, any degradation in PCCS performance caused by the presence of noncondensable gases would be quickly relieved by the opening of the PCC vents.

These tests simulate the performance of the PCCS near the boundary of the pressure drop driven range and the condensation pressure driven range. The mixture is almost pure steam compared to the steady-state tests. Complete condensation takes place in the condenser. The spectacle flange on the vent line simulates the blockage of the vent in SBWR by the submergence in the suppression pool. In PANTHERS, the pressure continues to rise as the gases build up in the system. In the SBWR, the pressure would also rise until the water level in the vent reaches the elevation of the vent exit. Then the PCCS would transition to the pressure-drop-driven mode as the gases bubble out and enter the wetwell.

### Water Level Test

The PANTHERS/PCC water level test, T54, begins with similar test conditions to the steady-state steam test, T41. Therefore, the condensation-driven mode is simulated. In this test, through a combination of normal boiloff and draining of the pool, the PCC pool level is lowered through a range that exceeds the SBWR inventory loss over a 72-hour period. The drop in water level is sufficiently slow to yield quasi-steady behavior at any given time.

Data from this test can be used to qualify TRACG for PCC performance over a wide range of water levels. It should be noted that the performance of the unit varies little as the water level drops from normal pool water level to the top of the condenser tubes. This covers the expected water level range for a 72-hour design basis accident.

#### 4.1.3.4 PIRT Phenomena and Coverage

[

Redacted

]

[

Redacted

]

#### 4.1.3.5 Scaling

Since the PANTHERS/PCC tests are conducted with a full-size prototype condenser, there are no scaling distortions to be addressed, except that at PANTHERS the inlet flows (steam and air) of the test unit were held constant in order to time average the data (steady-state tests) or to observe a slow change in performance during a transient.

GE has performed a scaling analysis for the operation of the SBWR PCC [4.1-5] and has concluded that the operation of the PCCS as part of the SBWR can be described as a slow transient. While the operation can become cyclical, the period of the cycles will be long in comparison to the response time of the PCCS. The characteristic response time of the PCC is mainly determined by the transient time of the fluid in the tubes (which is of the order of seconds), and to some extent by the time constant of the tube wall; since these walls are thin, this time constant is also of the order of a few seconds. Thus, the response of the PCC to changes in inlet conditions is much faster than the response of the large SBWR containment volumes. Therefore, the steady-state (and the transient quasi-steady-state) PANTHERS tests provide adequate data to characterize the operation of the SBWR PCCS units.

#### 4.1.3.6 Conclusion

The PANTHERS/PCC tests are conducted with a full-size prototype condenser. The conditions tested are representative of conditions calculated for PCC operation by SBWR containment analyses. Specific statements demonstrating coverage of SBWR PIRT parameters have been provided.

Tests encompassing a broad range of inlet flows, mass fractions, temperatures and pressures were used for the TRACG post-test analysis. The tests capture both pressure-drop-driven and condensation-driven operating modes of the PCC. The steady-state tests simulate the pressure-drop-driven mode from the upper limit of maximum pressure loss through the system (corresponding to flow through the LOCA vent in SBWR) to the transition to the condensation-driven mode. The transient tests demonstrate condensation-driven flows with and without noncondensable gases in the PCC.

The SBWR integrated systems tests (PANDA and GIRAFFE) complete the qualification database by demonstrating the impact of PCC system performance on the total SBWR containment performance.

#### 4.1.4 TRACG Models and Nodalization

[

Redacted

]

##### 4.1.4.1 One-Tube Model

###### 4.1.4.1.1 General Description

[

Redacted

]



[

Redacted

]

4.1.4.1.2 Inlet Line (TEE22)

[

Redacted

]

[

Redacted

]

4.1.4.1.3 Headers (PIPE92 and TEE26)

[

Redacted

]

4.1.4.1.4 Condenser Tubes (PIPE96)

[

Redacted

]

4.1.4.1.5 Drain Line (PIPE46)

[

Redacted

]

[

Redacted

]

4.1.4.1.6 Vent Line (PIPE52)

[

Redacted

]

4.1.4.1.7 Pools (VSSL01 and TEE40)

[

Redacted

]

[

Redacted

]

#### **4.1.4.2 Eight-Tube Model**

[

Redacted

]

**4.1.4.3 Six-Tube Model**

[

Redacted

]

**4.1.4.4 Determination of Hydraulic Loss Factors**

[

Redacted

]

**4.1.4.4.1 Calibration Method**

[

Redacted

]

4.1.4.4.2 Measured Pressure Losses vs. TRACG Calculation

[

Redacted

]

4.1.4.4.3 Discussion of Results

[

Redacted

]

[

Redacted

]

#### **4.1.4.5 TRACG Heat Transfer Correlations**

[

Redacted

]

#### **4.1.5 Test Simulation**

[

Redacted

]

##### **4.1.5.1 Steady-State Tests**

[

Redacted

]

[

Redacted

]

**4.1.5.2 Transient Tests**

[

Redacted

]



[

Redacted

]

**4.1.5.3 Atmospheric Pressure Boundary Condition**

[

Redacted

]

**4.1.6 Results and Discussion**

[

Redacted

]

[

Redacted

]

#### **4.1.6.1 Steady-State Pure-Steam Tests**

[

Redacted

]

##### **4.1.6.1.1 One-Tube Model Results**

[

Redacted

]

##### **4.1.6.1.2 Eight-Tube Model Result**

[

Redacted

]

#### **4.1.6.2 Steady-State Steam-Air Tests**

[

Redacted

]

[

Redacted

]

4.1.6.2.1 One-Tube Model Results

[

Redacted

]

[

Redacted

]

4.1.6.2.2 Eight-Tube Model Result

[

Redacted

]

**4.1.6.3 Transient Tests**

[

Redacted

]

4.1.6.3.1 Transient Gas-Injection Tests

[

Redacted

]

[

Redacted

]

[

Redacted

]

4.1.6.3.2 Transient Water-Level Test

[

Redacted

]

**4.1.6.4 Evaluation of Tube Wall Temperature Data**

[

Redacted

]

[

Redacted

]

4.1.6.4.1 Evaluation of Inside and Outside Film Coefficients

[

Redacted

]

[

Redacted

]



[

Redacted

4.1.6.4.2 Comparison of Measured and Calculated Wall Temperatures

[

Redacted

]

]

[

Redacted

]

[

Redacted

]

4.1.6.4.3 Tube-to-Tube Variations

[

Redacted

]

[

Redacted

]

#### **4.1.6.5 Accuracy of TRACG Calculations**

[

Redacted

]

#### **4.1.7 Summary and Conclusions**

The comparisons between TRACG calculations and PANTHERS PCC test results, presented in Section 4.1.6, support the use of TRACG to model the SBWR Passive Containment Cooling System (PCCS). The post-test evaluation included three steady-state pure-steam tests, nine steady-state steam-air tests, and four transient tests. Each of the steam-air tests consisted of

steady-state runs at several condenser inlet pressures making, in total, forty-eight individual runs covering a wide range of steam flows, inlet air mass fractions, and inlet pressures. It was shown in Section 4.1.3 that these tests covered the range of SBWR post-LOCA conditions and PCCS operating modes.

#### **4.1.7.1 Condenser Performance Under Prototypical Conditions**

The model-data comparisons for the steady-state tests used condenser heat removal and pressure drop as the primary evaluation variables. For the steady-state pure-steam tests, the comparison was made in terms of condenser inlet pressure. This method of comparison is consistent with the way these tests were run. The steam flow was prescribed and the inlet pressure was allowed to reach the level required to condense all of the steam. For the steam-air tests, the inlet pressure was prescribed and the heat removal comparison was made in terms of condenser efficiency, defined as the ratio of steam condensed to total steam flow. [

Redacted

]

#### **4.1.7.2 Condenser Performance under Non-Prototypical Conditions**

Three of the four transient tests included in the post-test evaluation (T51, T76, and T78) were run to examine differences in heat transfer degradation caused by the accumulation of heavier-than-steam and lighter-than-steam gases. These tests were conducted with the vent pipe closed by a spectacle flange. This transient condition does not simulate the SBWR, where the vent pipe is always free to open in response to an increasing difference between drywell and wetwell pressure. The fourth transient test (T54) examined the effect of an extreme reduction in the PCC pool water level, again not prototypical of post-LOCA conditions in the SBWR.

Each of the transient tests was initiated by establishing a steady state with pure-steam inlet conditions (nominally 5 kg/s). In three of the tests, the transient was caused by adding noncondensable gas (air, helium, or an air-helium mixture) to the inlet steam flow at a nominally constant flow rate. In the remaining test, the transient was caused by reducing the water level in

the PCC pool. In all cases, the primary response variable was the inlet pressure, which adjusted, as necessary, to maintain condensation of the prescribed steam flow.

[

Redacted

]

#### **4.1.7.3 Evaluation of TRACG Qualification Needs**

[

Redacted

]

##### **4.1.7.3.1 PCC Flow/Pressure Drop (PC1)**

[

Redacted

]

[

Redacted

]

4.1.7.3.2 Condensation/Condensation-Degradation on Primary Side (PC2)

[

Redacted

]

4.1.7.3.3 Secondary-Side Heat Transfer (PC3)

[

Redacted

]

[

Redacted

]

4.1.7.3.4 Parallel PCC Tube and Module Effects (PC4 and PC5)

[

Redacted

]

**4.1.8 References**

- [4.1-1] MFN No. 078-94, *PANTHERS Pre-Test Calculation*, 31-May 1994.
- [4.1-2] *SBWR Test and Analysis Program Description*, GE Nuclear Energy, NEDC-32391P, Revision C, Class 3, August 1995.
- [4.1-3] S. Botti, and R. Silverii, *Thermal-Hydraulic Data Report of PANTHERS-PCC Tests*, SIET Document No. 00393RP95, 7-April 1995.



- [4.1-4] R. Silverii, *PANTHERS-PCC Data Analysis Report*, SIET Document No. 00394RA95, 21-June-1995.
- [4.1-5] *Scaling of the SBWR Related Tests*, GE Nuclear Energy, NEDC-32288P, Class 3, October 1995.
- [4.1-6] J.G.M. Andersen, Y.K. Cheung, and J.C. Shaug, *TRACG02V User's Manual*, GE Nuclear Energy, NEDC-32192, Class 2, December 1993.
- [4.1-7] W.R. Usry, *Single Tube Condensation Test Program*, GE Nuclear Energy, NEDC-32301, Class 2, March 1994.
- [4.1-8] S.Z. Kuhn, V.E. Schrock and P. F. Peterson, *Final Report on U. C. Berkeley Single Tube Condensation Studies*, UCB-NE-4201, Rev. 1, August 1994.
- [4.1-9] J.G.M. Andersen, et al, *TRACG Model Description*, NEDE 32176P, Rev. 2, Class 3, December 1999.
- [4.1-10] R. Silverii, *Technical Specification for IC and PCC Instrument Installation*, SIET Document No. 00157ST92, 17-February 1994.
- [4.1-11] A.J. Illich, *Post-Test Analysis for GIRAFFE Helium Tests*, NEDC 32600, June 1996.

**Table 4.1-1  
PANTHERS/PCC Steady-State Performance Matrix at 5 kg/s Steam Flowrate for TRACG  
Post-Test Analysis**

<b>Test Condition Number</b>	<b>Steam Flow [kg/s]</b>	<b>Air Flow [kg/s]</b>	<b>Inlet Pressure [kPa]</b>	<b>Superheat [°C]</b>
T41_1	5.08	0	N/A	7.4
T43_2	6.58	0	N/A	5.8
T49_1	4.96	0	N/A	28.4
T09_1	5.00	0.076	296	9.0
T09_6	5.00	0.076	385	7.2
T09_7	4.96	0.077	703	4.6
T09_8	4.96	0.077	782	4.7
T09_9	4.98	0.076	549	6.2
T09_10	5.03	0.076	330	7.8
T15_1	5.01	0.167	300	7.5
T15_2	5.00	0.167	329	4.7
T15_3	5.07	0.166	500	6.4
T15_5	5.06	0.165	648	5.7
T15_6	5.07	0.167	790	7.2
T15_7	5.10	0.166	441	7.5
T18_1	5.02	0.4	300	7.0
T18_2	5.04	0.4	328	6.7
T18_3	5.02	0.4	467	6.1
T18_4	5.08	0.4	284	5.5
T18_5	5.01	0.4	599	4.6
T18_6	4.99	0.4	641	5.3
T23_1	5.03	0.87	437	7.3
T23_2	5.02	0.86	505	7.7
T23_3	5.02	0.86	584	6.2
T23_4	4.99	0.86	296	5.6
T23_5	4.97	0.86	329	8.5
T23_6	4.99	0.85	298	7.0
T35_1	4.96	0.86	298	20.7
T35_2	5.06	0.86	359	20.7
T35_3	5.04	0.86	436	19.1
T35_4	5.01	0.86	499	20.1
T35_5	5.02	0.86	587	18.3
T35_6	5.00	0.86	270	20.5

**Table 4.1-2  
PANTHERS/PCC Steady-State Performance Matrix at Extreme and Intermediate  
Ranges for TRACG Post-Test Analysis**

<b>Test Condition Number</b>	<b>Steam Flow [kg/s]</b>	<b>Air Flow [kg/s]</b>	<b>Inlet Pressure [kPa]</b>	<b>Superheat [°C]</b>
T02_1	1.40	0.015	299	9.5
T02_2	1.41	0.015	201	7.4
T02_3	1.41	0.015	179	7.1
T17_1	2.43	0.41	606	7.1
T17_2	2.56	0.41	520	6.4
T17_3	2.48	0.41	453	7.1
T17_4	2.47	0.41	362	8.0
T17_5	2.48	0.41	275	8.1
T19_1	5.75	0.41	295	7.7
T19_2	5.79	0.41	384	5.4
T19_3	5.79	0.41	472	7.0
T19_4	5.76	0.41	567	7.5
T19_5	5.75	0.41	665	6.3
T22_1	1.43	0.86	198	8.1
T22_2	1.40	0.86	261	6.5
T22_3	1.40	0.86	322	7.1
T22_4	1.40	0.86	389	7.1
T22_5	1.39	0.86	463	6.6

**Table 4.1-3  
PANTHERS/PCC Transient Performance Matrix for TRACG Post-Test Analysis**

<b>Type</b>	<b>Test Condition Number</b>	<b>Steam Flow [kg/s]</b>	<b>Air Flow [g/s]</b>	<b>Helium Flow [g/s]</b>
Air Buildup	T51	5.0	4.4	0
Helium Buildup	T76	5.0	0	0.7
Air/Helium Buildup	T78	5.0	4.4	1.2
Pool Water Level Effect	T54	5.0	0	0

**Table 4.1-4**  
**PANTHERS/PCC TRACG One-Tube Model Components and Junction Elevations**

[

Redacted

]

**Table 4.1-5**  
**Heat Transfer Correspondence Between Condenser Tube Cells and PCC Pool Cells**

[

Redacted

]

**Table 4.1-6**  
**PANTHERS PCC TRACG Eight-Tube Model Components**

[

Redacted

]

**Table 4.1-7**  
**TRACG Calculated Pressure Losses for Test 15\_1 Compared with PANTHERS DP**  
**Measurements**

[

Redacted

]

**Table 4.1-8**  
**Functions of TRACG Components for Specifying PANTHERS/PCC Test Boundary**  
**Conditions**

[

Redacted

]

**Table 4.1-9**  
**TRACG Input Flow Rates and Properties for Noncondensable Gas Accumulation Tests**

[

Redacted

]

**Table 4.1-10  
PANTHERS/PCC Tests Included in Post-Test Evaluation**

<b>Test Number</b>	<b>Test Type</b>	<b>Data Comparison</b>
41	SS - pure steam	inlet pressure/heat transfer rate
43	SS - pure steam	inlet pressure/heat transfer rate
49	SS - pure steam	inlet pressure/heat transfer rate
9	SS - steam/air	condensation efficiency, $\Delta p$
15	SS - steam/air	condensation efficiency, $\Delta p$
18	SS - steam/air	condensation efficiency, $\Delta p$
23	SS - steam/air	condensation efficiency, $\Delta p$
2	SS - steam/air	condensation efficiency, $\Delta p$
17	SS - steam/air	condensation efficiency, $\Delta p$
19	SS - steam/air	condensation efficiency, $\Delta p$
22	SS - steam/air	condensation efficiency, $\Delta p$
35	SS - steam/air	condensation efficiency, $\Delta p$
51	TR - nc buildup	inlet pressure vs. air inventory
76	TR - nc buildup	inlet pressure vs. helium inventory
78	TR - nc buildup	inlet pressure vs. air/helium inventory
54	TR - water level	inlet pressure vs. water level

**Table 4.1-11  
Test Conditions for Steady-State Pure-Steam Tests Included in Post-Test Evaluation**

<b>Test No.</b>	<b>Steam Flow Rate (kg/sec)</b>	<b>Inlet Temperature (°C)</b>
T41_1	5.08	144
T43_2	6.58	149
T49_1	4.96	164



**Table 4.1-12  
Test Conditions for Steady-State Steam-Air Tests Included in Post-Test Evaluation**

<b>Test No.</b>	<b>Steam Flow (kg/sec)</b>	<b>Air Flow (kg/sec)</b>	<b>Air Mass Fraction</b>	<b>Inlet Pressure (kPa)</b>	<b>Inlet Temp. (°C)</b>
2	1.40 - 1.41	0.015	0.011	179 - 299	124 - 143
9	4.96 - 5.00	0.076-0.077	0.015	296 - 782	142 - 174
15	5.00 - 5.10	0.165-0.167	0.032	300 - 790	140 - 176
17	2.43 - 2.56	0.41	0.138-0.144	275 - 606	135 - 162
18	4.99 - 5.08	0.40	0.073-0.074	284 - 641	135 - 165
19	5.75 - 5.79	0.41	0.066-0.067	295 - 665	139 - 168
22	1.39 - 1.43	0.86	0.376-0.382	198 - 463	118 - 144
23	4.97 - 5.03	0.85 - 0.87	0.146-0.148	296 - 584	135 - 160
35	4.96 - 5.06	0.86	0.145-0.148	270 - 587	147 - 172

**Table 4.1-13  
Comparison of Results from 8-Tube and 1-Tube TRACG Input Models for Steady-State  
Steam-Air Tests**

[

Redacted

]

**Table 4.1-14**  
**Comparison of Inferred PANTHERS Film Coefficients with TRACG Calculations for**  
**Pure-Steam Tests**

[

Redacted

]

**Table 4.1-15a**  
**Test Conditions for Evaluation of Tube-to-Tube Variations**

[

Redacted

]

**Table 4.1-15b**  
**Axial Average Wall Temperature Difference for Four Instrumented Tubes**

[

Redacted

]

**Table 4.1-15c**  
**Axial Variation of External Tube Wall Temperatures for Test 09\_9**

[

Redacted

]

**Table 4.1-16**  
**Assessment of TRACG Accuracy for PANTHERS PCC SS Steam-Air Tests**

[

Redacted

]

**Table 4.1-17**  
**Assessment of TRACG Accuracy for PANTHERS PCC SS Pure-Steam Tests**

[

Redacted

]

**Table 4.1-18**  
**Maximum Measurement Uncertainties**

[

Redacted

]

**Table 4.1-19**  
**Maximum Measurement Uncertainty for Condenser Efficiency**

[

Redacted

]

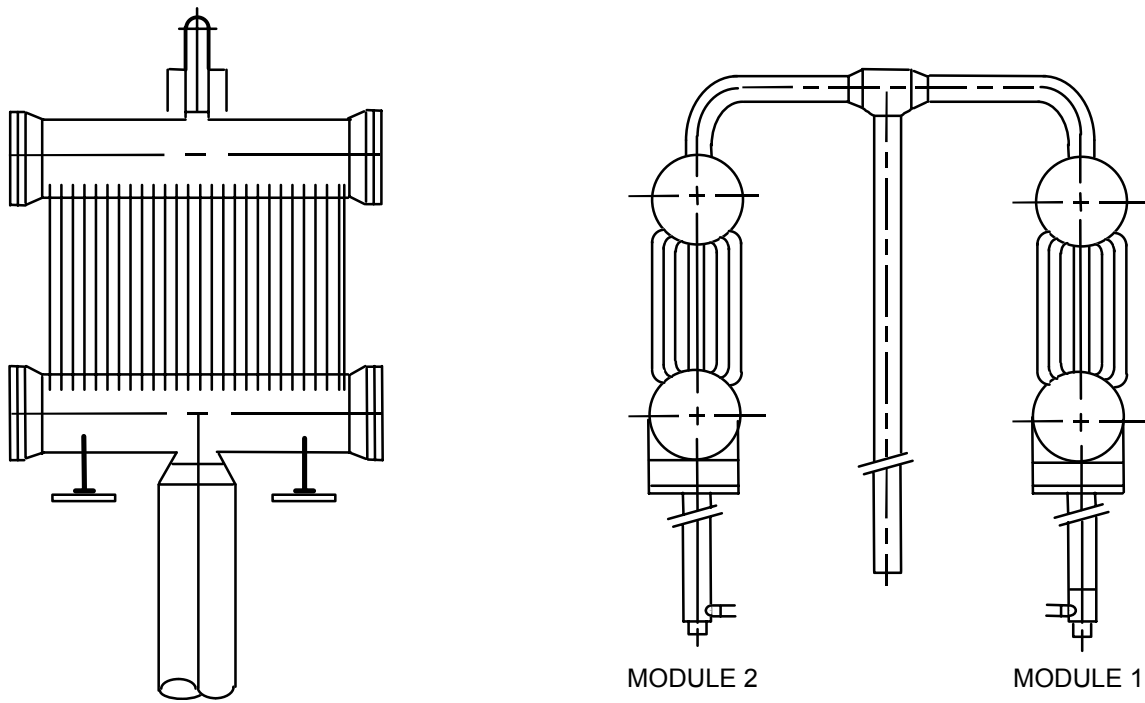


**Figure 4.1-1 Passive Containment Condenser Test Article**

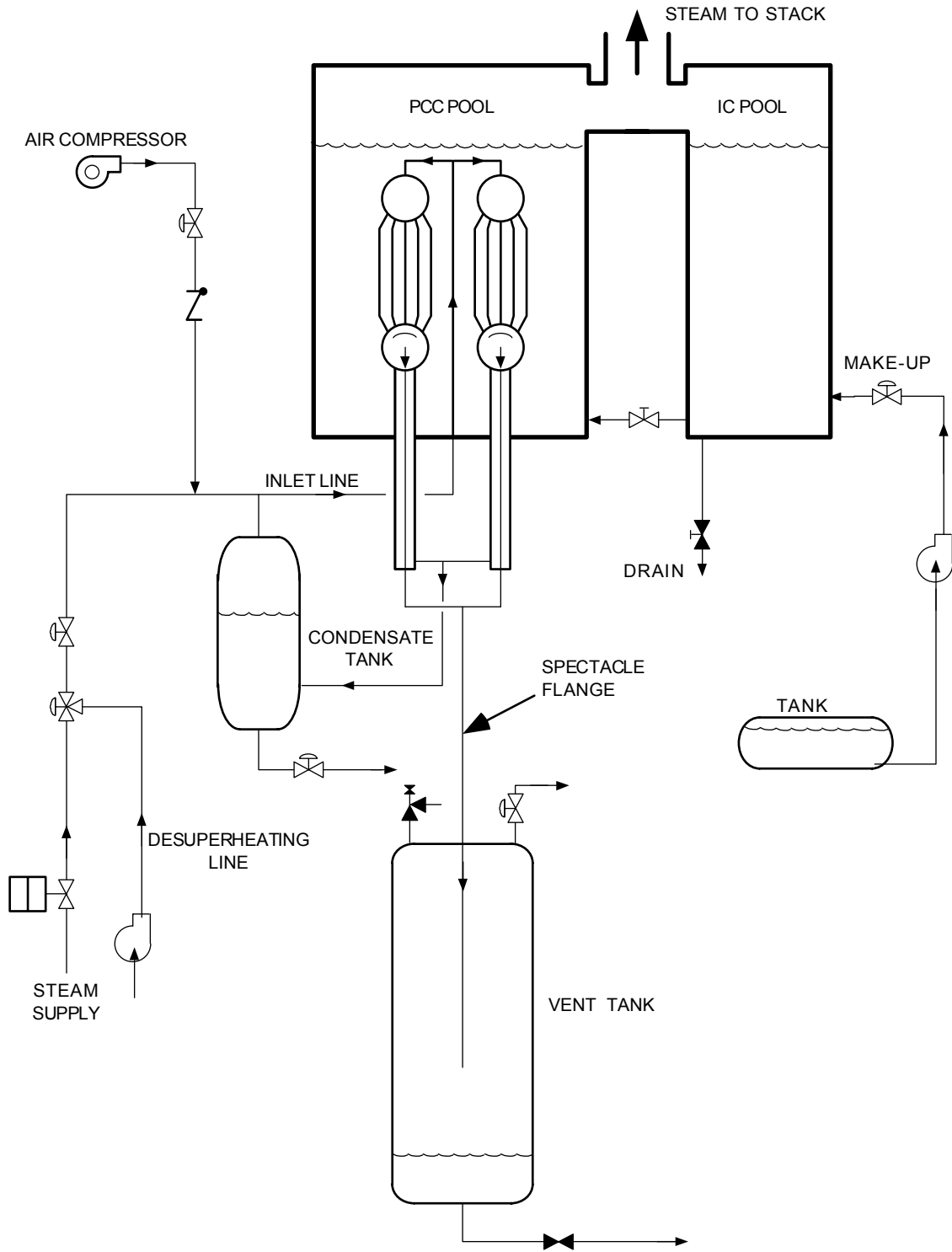
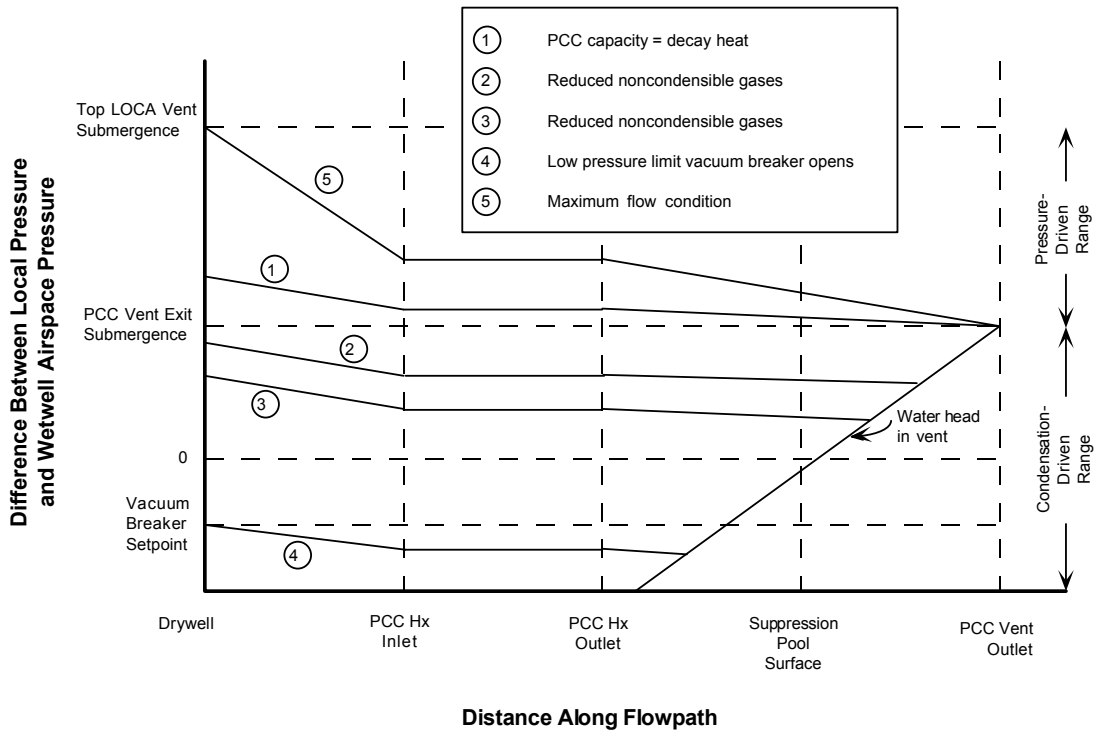


Figure 4.1-2 PANTHERS/PCC Test Facility Schematic





**Figure 4.1-3 PCC Operational Modes**

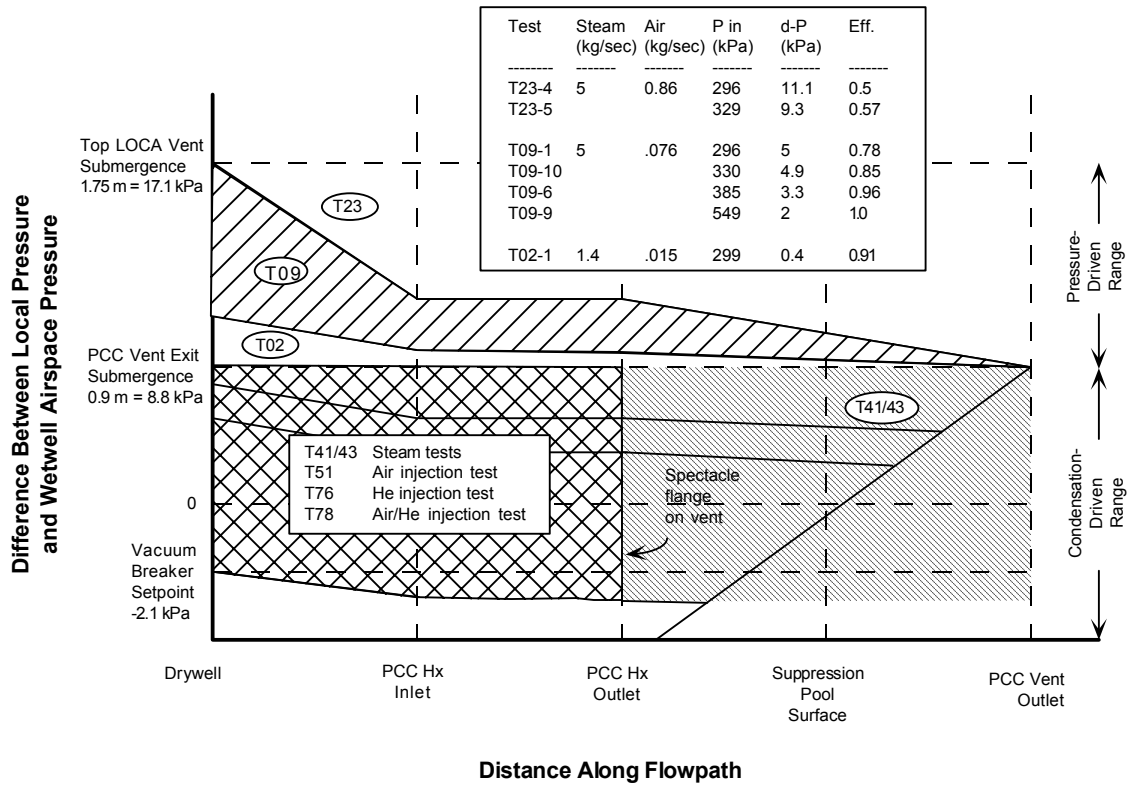


Figure 4.1-4 PANTHERS Representation of PCC Operational Modes

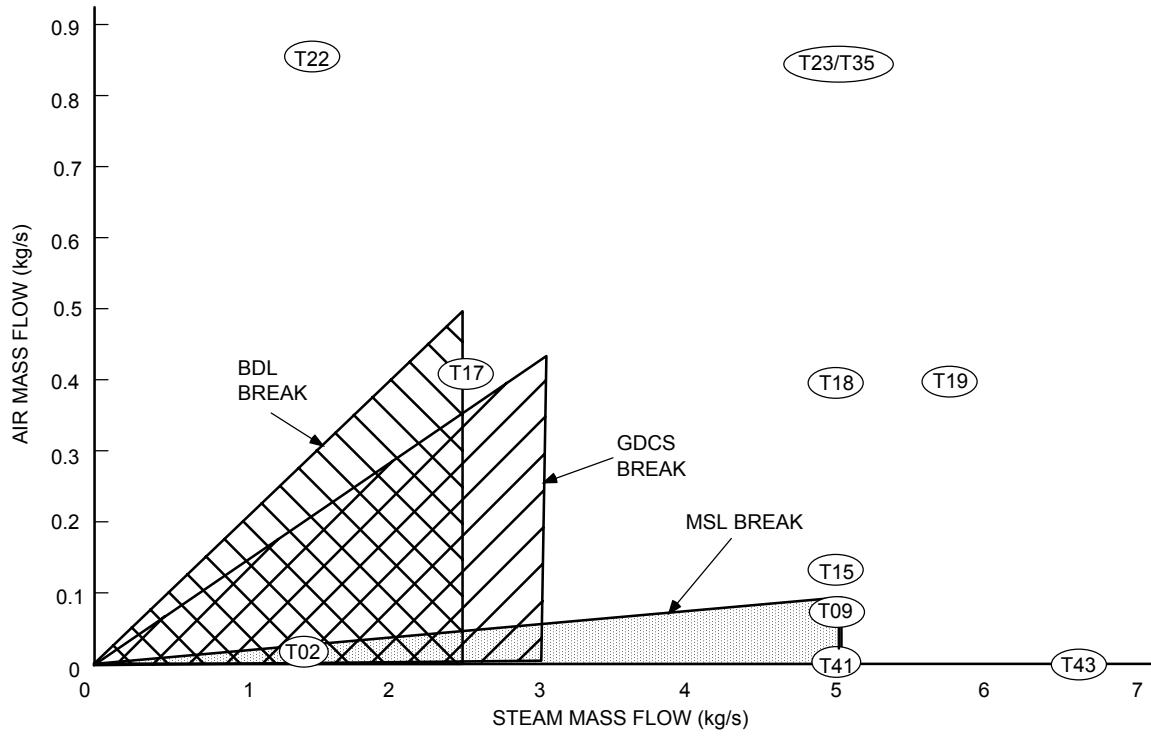


Figure 4.1-5 TRACG PANTHERS/PCC Qualification Points

[

Redacted

]

**Figure 4.1-6 Schematic of TRACG PANTHERS/PCC One-Tube Input Model**

[

Redacted

]

**Figure 4.1-7 Nodalization of Inlet Line (TEE22)**

[

Redacted

]

**Figure 4.1-8 Nodalization of Upper (PIPE92) and Lower (TEE26) Headers**

[

Redacted

]

**Figure 4.1-9 Nodalization of PCC Tubes (PIPE96)**

[

Redacted

]

**Figure 4.1-10 Nodalization of Drain Line (PIPE46)**



[

Redacted

]

**Figure 4.1-11 Nodalization of Vent Line (PIPE52)**

[

Redacted

]

**Figure 4.1-12 Nodalization of Pools (VSSL01 and TEE40)**

[

Redacted

]

**Figure 4.1-13 Nodalization of the PANTHERS/PCC Eight-Tube TRACG Model**

[

Redacted

]

**Figure 4.1-14 Comparison of TRACG and PANTHERS Inlet Pressure for Pure-Steam Tests**

[

Redacted

]

**Figure 4.1-15 Comparison of TRACG and Panthers Condensation Efficiency and Pressure Drop for Test 9**

[

Redacted

]

**Figure 4.1-16 Comparison of TRACG and PANTHERS Condensation Efficiency and Pressure Drop for Test 15**

[

Redacted

]

**Figure 4.1-17 Comparison of TRACG and PANTHERS Condensation Efficiency and Pressure Drop for Test 18**

[

Redacted

]

**Figure 4.1-18 Comparison of TRACG and PANTHERS Condensation Efficiency and Pressure Drop for Test 23**



[

Redacted

]

**Figure 4.1-19 Comparison of TRACG and PANTHERS Condensation Efficiency and Pressure Drop for Test 2**

[

Redacted

]

**Figure 4.1-20 Comparison of TRACG and PANTHERS Condensation Efficiency and Pressure Drop for Test 17**

[

Redacted

]

**Figure 4.1-21 Comparison of TRACG and PANTHERS Condensation Efficiency and Pressure Drop for Test 19**

[

Redacted

]

**Figure 4.1-22 Comparison of TRACG and PANTHERS Condensation Efficiency and Pressure Drop for Test 22**

[

Redacted

]

**Figure 4.1-23 Comparison of TRACG and PANTHERS Condensation Efficiency and Pressure Drop for Test 35**

[

Redacted

]

**Figure 4.1-24 Comparison of TRACG and PANTHERS Condensation Efficiency and Pressure Drop for Test 2 with Heat Transfer Between Vent Line and Drain Line**

[

Redacted

]

**Figure 4.1-25 Comparison of TRACG and PANTHERS Inlet Pressure for Test 51**

[

Redacted

]

**Figure 4.1-26 Comparison of TRACG and PANTHERS Inlet Pressure for Test 76**



[

Redacted

]

**Figure 4.1-27 Comparison of TRACG and PANTHERS Inlet Pressure for Test 78**

[

Redacted

]

**Figure 4.1-28 Comparison of TRACG and PANTHERS Inlet Pressure for Test 54**

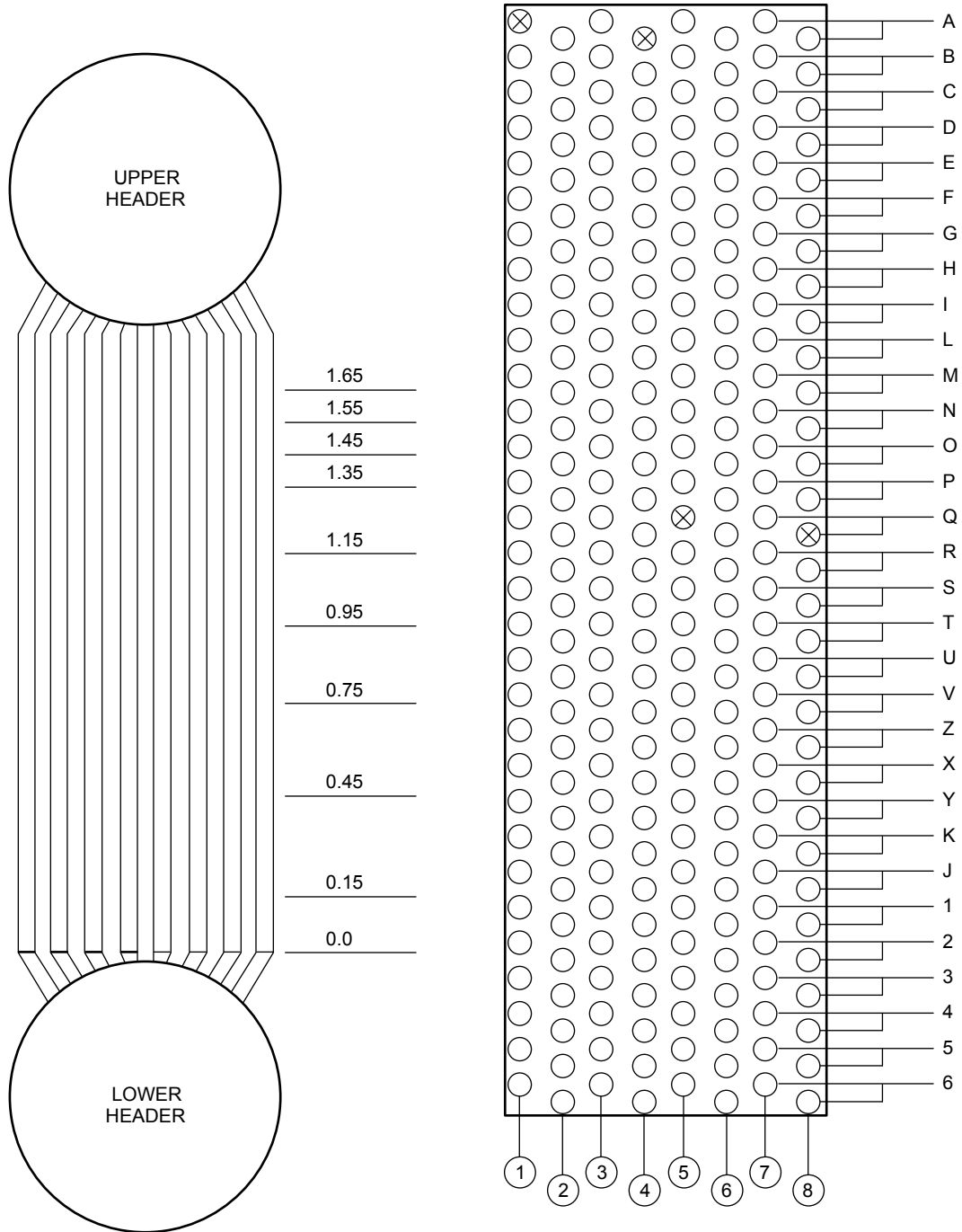


Figure 4.1-29 Location of the PCC Instrumented Tubes and Thermocouples

[

Redacted

]

**Figure 4.1-30 Comparison of Average Tube Wall Temperature Measurements to TRACG Calculations - PANTHERS Test T15\_1**

[

Redacted

]

**Figure 4.1-31 Comparison of Average Tube Wall Temperature Measurements to TRACG Calculations - PANTHERS Test T43\_2**

## 4.2 PANTHERS IC Performance

### 4.2.1 Introduction

As part of the validation effort for application of the TRACG code to the SBWR, pre- and post-test calculations for tests in the PANTHERS IC (Isolation Condenser) test program have been performed. The PANTHERS IC testing was performed at SIET S.p.A. in Piacenza, Italy, utilizing a full-scale prototype IC module. The TRACG model for pre- and post-test calculations was developed at GENE. The purpose of Section 4.2 is to present and discuss the results of the post-test analysis.

[

Redacted

]

The remainder of Section 4.2 is organized as follows. Section 4.2.2 presents a brief description of the PANTHERS IC test facility and test matrix. Section 4.2.3 discusses applicability of the test data to the SBWR. Section 4.2.4 describes the PANTHERS IC post-test TRACG models. Section 4.2.5 describes the TRACG simulation of the procedures and boundary conditions employed to run the various types of tests included in the post-test evaluation. Section 4.2.6 presents and discusses the results of the TRACG simulations. Finally, Section 4.2.7 presents a set of conclusions and a summary for the post-test evaluation. References are listed in Section 4.2.8.

### 4.2.2 Test Facility and Test Matrix

#### 4.2.2.1 Test Facility

PANTHERS IC (Isolation Condenser) testing was performed at Societa Informazioni Esperienze Termoidrauliche (SIET) in Piacenza, Italy. The facility consisted of a prototype IC module, a steam supply vessel which simulates the SBWR reactor vessel, a vent volume, and associated piping sufficient to establish IC thermal-hydraulic performance.

The IC tested was one module of a full-scale, two-module vertical tube heat exchanger designed and built by Ansaldo S.p.A. (Genoa and Milan, Italy). Only one module was tested because of the high energy rejection rate of the IC unit, and inherent limitations of facility and steam supply size. Figure 4.2-1 is an outline drawing of the heat exchanger assembly. The IC was a prototype unit, built to prototype procedures and using prototype materials. Six modules (three heat exchanger units) of the type tested are used in the SBWR. The IC was installed in a water pool having one half the appropriate volume for one SBWR IC assembly.

Figure 4.2-2 is a schematic of the PANTHERS IC facility. The primary instrumentation specified is sufficient to ascertain heat exchanger thermal-hydraulic performance by performing mass and energy balances on the facility. Table 4.2-1 shows maximum measurement uncertainties [4.2-3] for measurements used in the comparisons between TRACG calculated results and test results. The uncertainties in steam flow vary from test to test because the uncertainty is given as a fixed percentage of the measured flow rate. This is further reflected in the uncertainties in heat rejection rate, which is calculated from the measured steam and condensate flow rates. The uncertainty in inlet pressure differs for Test T11 because a lower range instrument was used for that test.

PANTHERS IC testing procedures were specific to the type of test being performed.

### **Steady-State Tests**

Prior to the start of a test, the IC heat exchanger and the steam supply vessel were filled with water to purge air from the system. The test was initiated by supplying steam to the IC inlet via the steam vessel and opening the IC drain valve. Steam supply to the steam vessel was regulated such that the vessel pressure stabilized at the desired value. Data were acquired for a period of approximately 30 minutes. The steam supply was then either increased or decreased to gather data at a different operating pressure, or testing was terminated. Flow into the IC was natural circulation driven, as is the case for the SBWR.

### **Noncondensable Gas Transient Tests**

**Noncondensable gas tests began similarly and proceeded until the pressure stabilized at the desired value.** For this case, a mixture of nitrogen and helium was injected into the IC supply line at a very low flow rate. The ratio of nitrogen to helium in the injected flow was 3.5:1, simulating the composition of radiolytic gases. Gas injection continued until the IC inlet pressure increased to 7.75 MPa (1110 psig) or stopped increasing. The noncondensable flow rate was approximately 5 g/s. The lower IC vent was then opened, and the IC vented until the pressure returned approximately to the initial operating pressure. After closing the lower vent, the IC top vent was opened and the performance monitored until venting was complete. The test was then terminated.

### **Water Level Transient Tests**

Water level tests also began with the IC in stable operation at the desired initial inlet pressure. The IC pool water level was then reduced and the IC performance monitored. The water level was reduced until the IC inlet pressure reached 8.72 MPa. The water level was then increased as the IC performance returned to normal. The test was then terminated.

#### **4.2.2.2 Test Matrix and Data Analysis**

The PANTHERS IC Data Report [4.2-3] gives the complete test matrix for all the tests. From that matrix, six tests were chosen for post-test TRACG analysis [4.2-1] in order to demonstrate the capability of TRACG to calculate the heat rejection rate of the IC over a wide

range of conditions. The test conditions chosen for TRACG analysis are discussed below. Section 4.2.3 discusses the applicability of these test conditions to the SBWR.

#### 4.2.2.2.1 Steady-State Performance Tests

Table 4.2-2 shows the PANTHERS IC Steady-State Performance Matrix used for TRACG post-test analysis. Test conditions represent high (T02), intermediate (T06), and low (T11) operating pressures. These data establish the IC heat rejection rate as a function of inlet pressure.

#### 4.2.2.2.2 Transient Test Conditions

Table 4.2-3 shows the PANTHERS IC Transient Performance Test Matrix used for TRACG post-test analysis. The tests include two noncondensable gas buildup transients and a pool water level transient.

In the noncondensable gas buildup tests, steam was supplied at a constant rate, and steady state conditions were established in a manner similar to that of the steady-state performance tests. A nitrogen/helium mixture was then injected into the steam supply. The transient degradation in heat transfer performance was reflected in an increasing condenser inlet pressure, as a function of the total noncondensable mass injected.

The two noncondensable gas buildup tests analyzed represent conditions at both low (T12) and high (T13) steam flow rates. In T12, gas injection continued until the condenser pressure reached 7.8 MPa. After steady operation for a few minutes, the lower header vent line was opened until the pressure reduced to approximately the initial test pressure. In T13, gas injection was halted when it was seen that the condenser pressure was no longer increasing. Although the steam inlet flow was held constant, the condenser pressure began to decrease, indicating that noncondensable gases were being swept out with the condensate. After a few minutes, the lower header vent line was opened until the pressure reduced to approximately the initial test pressure. In both tests, the upper vent line was later opened to remove any residual gases from the upper region of the condenser. Since all or nearly all of the gases were removed by the lower vent, and no appreciable change was seen in the condenser performance by venting from the upper header, the upper header venting was not modeled by TRACG.

Table 4.2-3 also shows the Pool Water Level Effect Test Condition (TI5). In this test, steam was supplied to the IC heat exchanger, and steady-state conditions established in a manner similar to the steady-state performance tests. The water level in the IC pool dropped by boiloff and draining, and the IC tubes uncovered. The measured pressure required to maintain complete condensation is compared against TRACG results to evaluate the effect of pool water level on IC performance.

### 4.2.3 **Applicability of Data to SBWR**

#### 4.2.3.1 **Steady-State Tests**

The independent variable for the PANTHERS IC steady-state tests is the IC inlet pressure, which is equal to the steam vessel pressure. The isolation condenser is a natural circulation unit.



[

Redacted

]

#### **4.2.3.2 Transient Tests**

[

Redacted

]

The PANTHERS IC tests were not system tests. The purpose of the transient tests was to measure the change in performance of the IC with (a) a known quantity of noncondensable gas present or (b) a change in pool water level. Although the test facility was similar to the arrangement found in the SBWR, with the steam supply and condensate return lines connected to a large pressure vessel, the transient tests did not exactly match the conditions an IC would experience in the SBWR. For example, the operation of the heat exchanger in PANTHERS differed from the conditions it would encounter in the plant (i.e., steam and noncondensable gases are “metered” into the test facility, while in the plant the conditions at the inlet of the heat exchanger depend on the conditions in the RPV, and are not independent variables). However, the venting of the test unit closely matched the performance of the plant unit, and demonstrated that the IC can vent the gases and resume condensation at low pressure.

#### **4.2.3.3 PIRT Phenomena and Coverage**

[

Redacted

]

[

Redacted

]

#### **4.2.3.4 Scaling**

Scaling issues for the PANTHERS IC test are addressed in Section 4.6 of Reference 4.2-4. Applicability of the PANTHERS IC test data to the SBWR is based on the fact that the test facility is a full-scale prototype of one-half of an IC unit and the condenser pool. Considering the dual-module design of the condenser, it is reasonable to conclude that there will be no significant distortion in thermal-hydraulic performance as compared to testing of a full condenser.

#### **4.2.4 TRACG Model and Nodalization**

[

Redacted

]

[

Redacted

]

#### **4.2.4.1 Model Description**

##### **4.2.4.1.1 Inlet Line (TEE21) and Gas Injection Line (VLVE05)**

[

Redacted

]

##### **4.2.4.1.2 Headers (PIPE91 and TEE25)**

[

Redacted

]

##### **4.2.4.1.3 Condenser Tubes (PIPE95)**

[

Redacted

]

[  
Redacted  
]

4.2.4.1.4 Drain Line (VLVE47)

[  
Redacted  
]

4.2.4.1.5 Vent Line (VLVE51)

[  
Redacted  
]

4.2.4.1.6 Steam Pressure Vessel (VSSL01)

[  
Redacted  
]

4.2.4.1.7 IC Pools (VSSL01 and TEE40)

[  
Redacted  
]

[

Redacted

]

**4.2.4.2 TRACG Heat Transfer Correlations**

[

Redacted

]

**4.2.5 Test Simulation**

[

Redacted

]

**4.2.5.1 Steady-State Tests**

[

Redacted

]

#### **4.2.5.2 Transient Tests**

[

Redacted

]

#### **4.2.6 Results and Discussion**

[

Redacted

]

**4.2.6.1 Steady-State Tests**

[

Redacted

]

**4.2.6.2 Transient Tests**

[

Redacted

]

**4.2.6.2.1 Transient Gas Injection Tests**

[

Redacted

]

[

Redacted

]

4.2.6.2.2 Transient Water Level Test

[

Redacted

]



#### 4.2.6.3 Accuracy of TRACG Calculations

[

Redacted

]

#### 4.2.7 Summary and Conclusions

The comparisons between TRACG calculations and PANTHERS IC test results, (Section 4.2.6) support the use of TRACG to model the SBWR Isolation Condenser System (ICS). The post-test evaluation included three steady-state pure-steam tests, two transient tests with noncondensable gas accumulation and venting, and one transient test in which the condenser pool water level was varied. As discussed in Section 4.2.3: (1) the steady-state tests covered the range of condenser pressures at which the IC could operate during SBWR transients and postulated post-LOCA conditions; (2) the transient noncondensable injection tests considered typical operating conditions in the presence of radiolytic gas release; and (3) the transient water level test bounded the pool level reduction which could occur during the 72-hour “hands off” period following a postulated LOCA.

For the steady-state simulations, comparisons between TRACG calculations and test results were made in terms of the condenser pressure required to condense steam at a prescribed rate and, equivalently, in terms of the heat transfer rate at a given pressure. For the transient tests with noncondensable gas injection, comparisons were made in terms of condenser pressure as a function of accumulated gas inventory during the injection period, and in terms of condenser pressure vs. time following the opening of the vent. For transient tests with pool water level variation, comparisons were made in terms of condenser pressure as a function of pool water level.

##### 4.2.7.1 Pure Steam Condensation Performance

[

Redacted

]

[

Redacted

]

**4.2.7.2 Noncondensable Accumulation and Venting**

[

Redacted

]

**4.2.7.3 IC Pool Level Effects**

[

Redacted

]

**4.2.7.4 Evaluation of TRACG Qualification Needs**

[

Redacted

]

**4.2.7.4.1 IC Capacity (Q2)**

[

Redacted

]

[

Redacted

]

4.2.7.4.2 Secondary Side Heat Transfer (Q5)

[

Redacted

]

#### 4.2.8 References

- [4.2-1] *SBWR Test and Analysis Program Description*, NEDC-32391P, Rev. C, August 1995.
- [4.2-2] *Pre-Test Analysis for PANTHERS IC Test*, SBWR MFN 097-95, June 1995.
- [4.2-3] *PANTHERS-IC Test Report*, SIET document 00458RP95, Rev. 0, April 19, 1996.
- [4.2-4] *Scaling of the SBWR Related Tests*, NEDC-32288P, Rev. 1, October 1995.
- [4.2-5] I.E Idelchik, *Handbook of Hydraulic Resistance*, 2nd Ed., Springer Verlag, 1986.
- [4.2-6] *TRACG Model Description*, NEDE-32176P Rev. 2, December 1999.
- [4.2-7] *Assessment of MIT and UCB Wall Condensation Tests and of the Pre-Release RELAP5/Mod 3.2 Code Condensation Models*, INEL 95/0050, January 1995.

**Table 4.2-1  
PANTHERS IC Test Maximum Measurement Uncertainties**

[

Redacted

]

**Table 4.2-2  
PANTHERS IC Steady-State Performance Matrix for TRACG Post-Test Analysis**

[

Redacted

]

**Table 4.2-3  
PANTHERS IC Transient Performance Matrix for TRACG Post-Test Analysis**

[

Redacted

]

**Table 4.2-4**  
**Components for Simulation of PANTHERS IC Test**

[

Redacted

]

**Table 4.2-5  
TRACG Input Flow Rate and Properties For Noncondensable Gas**

[  
Redacted  
]

**Table 4.2-6  
PANTHERS IC Tests Included in Post-Test Evaluation**

Test Number	Test Type	Data Comparison
T02	Steady state - pure steam	inlet pressure
T06	Steady state - pure steam	inlet pressure
T11	Steady state - pure steam	inlet pressure
T12	Transient - ncg <sup>1</sup> buildup	injected ncg <sup>1</sup> vs. inlet pressure
T13	Transient - ncg <sup>1</sup> buildup	injected ncg <sup>1</sup> vs. inlet pressure
T15	Transient - water level	inlet pressure vs. water level

<sup>1</sup> noncondensable gas

**Table 4.2-7  
Test Conditions for Steady-State Post-Test Evaluation**

Test Number	Steam Flow Rate (kg/s)	Inlet Temperature (°C)
T02	15.02	299.4
T06	10.64	263.5
T11	1.02	134.0
T12	2.07	157
T13	5.86	216

**Table 4.2-8  
Comparison of PANTHERS and TRACG for Steady-State Evaluation**

[  
Redacted  
]

**Table 4.2-9**  
**Comparison of PANTHERS and TRACG Noncondensable Gas Inventory at 7.8 MPa for Test T12**

[

Redacted

]

**Table 4.2-10**  
**Comparison of PANTHERS and TRACG Noncondensable Gas Inventory at 5.2 MPa for Test T13**

[

Redacted

]

**Table 4.2-11**  
**TRACG Calculation of NC Gas Distribution at 5.23 MPa Inlet Pressure**

[

Redacted

]

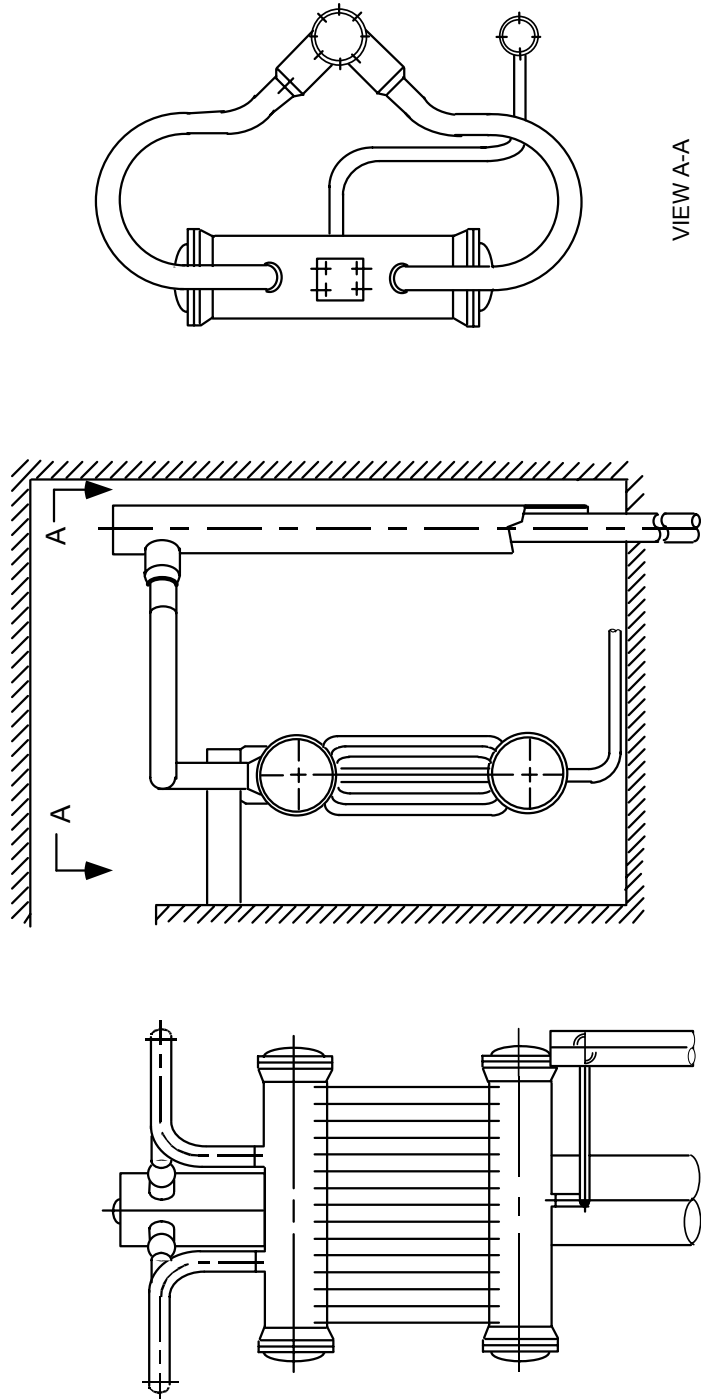


**Table 4.2-12**  
**Assessment of TRACG Accuracy for PANTHERS IC Tests**

[

Redacted

]



VIEW A-A

Figure 4.2-1 Isolation Condenser Heat Exchanger Assembly

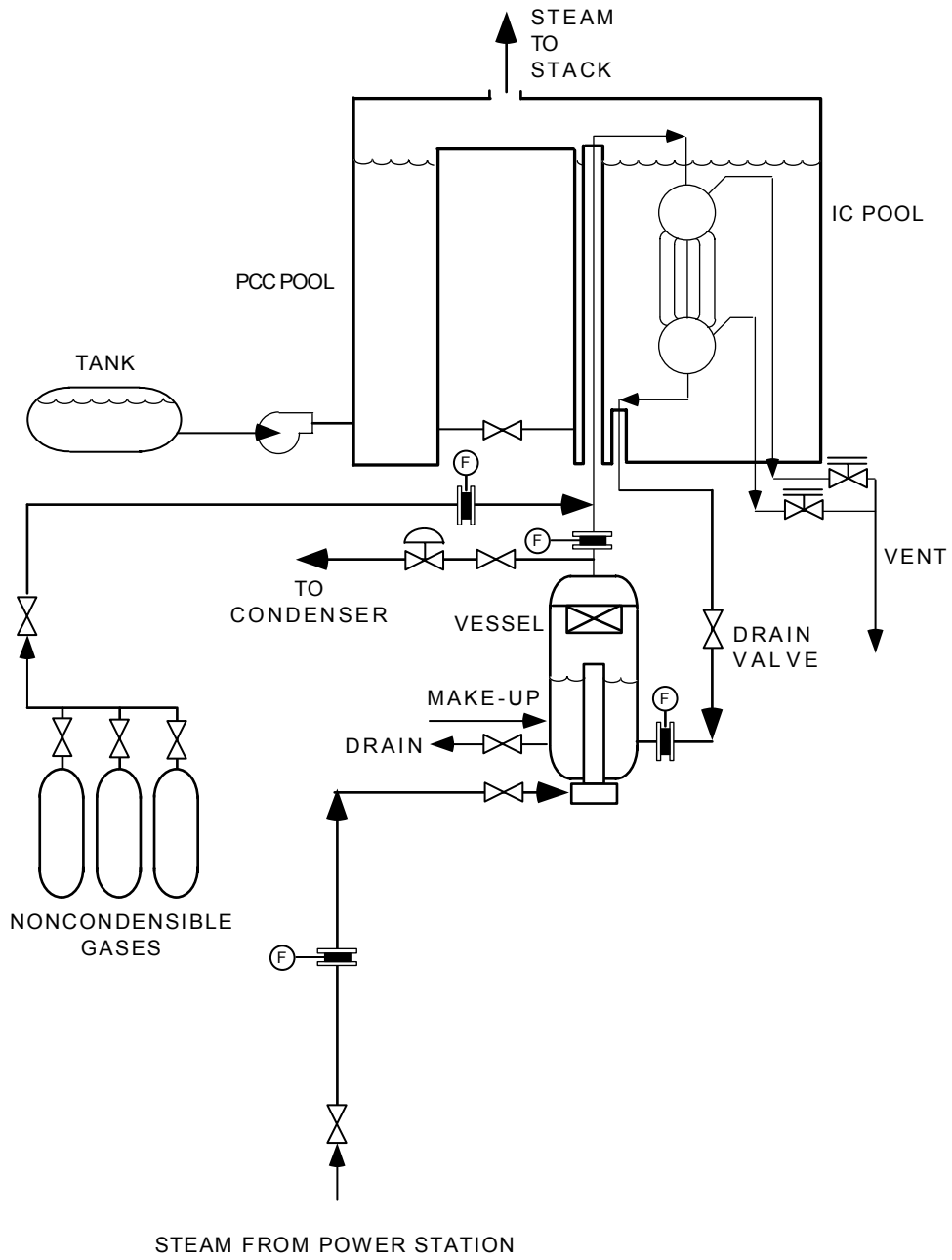


Figure 4.2-2 PANTHERS IC Test Facility Schematic

[

Redacted

]

**Figure 4.2-3 TRACG Nodalization for Simulation of PANTHERS IC Test**

[

Redacted

]

**Figure 4.2-4 Comparison of TRACG and PANTHERS for Steady-State Tests**

[

Redacted

]

**Figure 4.2-5 Comparison of TRACG and PANTHERS Inlet Pressure Transient for Test T12**

[

Redacted

]

**Figure 4.2-6 Comparison of TRACG and PANTHERS Heat Transfer for Test T12**

[

Redacted

]

**Figure 4.2-7 Comparison of TRACG and PANTHERS Inlet Pressure Transient for Test T13**

[

Redacted

]

**Figure 4.2-8 Comparison of TRACG and PANTHERS Heat Transfer for Test T13**

[

Redacted

]

**Figure 4.2-9 Comparison of TRACG and PANTHERS for Pool Level Test**



## 4.3 PANDA PCC Performance

### 4.3.1 Introduction

The purpose of Section 4.3 is to present and discuss the results of TRACG post-test calculations for the PANDA steady-state PCC performance tests. Several tests investigating the steady-state performance of the PCCS were performed at the PANDA facility in 1995. The main objective of the tests was to provide a scaling link which would support the application of the PANDA transient test results for evaluation of the SBWR. The major issue for the post-test evaluation of the PANDA steady-state tests was to qualify the TRACG model for condensation of steam in the presence of a noncondensable gas.

[

Redacted

]

### 4.3.2 Test Facility and Test Matrix

#### 4.3.2.1 Test Facility

The PANDA Test Facility has been described in References 4.3-3 through 4.3-5 and a summary description is included in Section 5.7.2 of this report. The PCC units in the PANDA facility have full-scale tubes, with the number of tubes reduced to achieve a 1/25 power and volume scaling relative to the SBWR. There are three PCC loops in the PANDA facility. PCC3 was selected for the steady-state tests. The DW vessels were isolated and a pipe was installed to deliver steam directly from the RPV to the inlet of PCC3. The inlet pipe was insulated from the RPV to the inlet flange on the upper header. The inlet steam was condensed in the PCC3 unit with heat transfer to the secondary side water pool.

For the steam-air tests, air was injected directly into the inlet line at a point downstream of the steam flow measurement location. The pressures in the GDCS tank and the WW tanks were equalized via an auxiliary steam line. The PCC3 drain line was open to the GDCS tank and the GDCS drain line was open to the RPV. The PCC3 vent line to WW2 was not submerged. This facilitated control of the condenser inlet pressure (an independent variable for the steam-air tests). The pressure was established by controlling the venting rate from the WW air space to the outside environment. For the pure-steam tests, the vent line to the WW was closed and the condenser pressure was allowed to come to the steady-state equilibrium value consistent with the steam flow rate. Data for all tests were collected for 15 minutes after steady-state conditions were established. The time-averaged data were reported in Reference 4.3-6.

For the steam-air tests, the wetwell pressure was controlled to keep the condenser pressure at the specified level (nominally, 3 bar). Condensate flow through the PCC3 drain line was measured to determine the PCCS efficiency. The efficiency of the PCC unit is defined as the fraction of the inlet steam condensed and is calculated as the ratio of the drain line condensate mass flow rate to the inlet steam mass flow rate. For the pure steam tests, the valve on the vent line was closed. The PCCS was fed with the desired steam flow and the condenser pressure was allowed to stabilize at the level required to condense all the steam. In other words, a 100% PCC unit efficiency was forced.

#### 4.3.2.2 Test Matrix

Table 4.3.-1 shows the PANDA steady-state test matrix. The tests in the matrix may be summarized as follows:

- Test S1 was a pure-steam test.
- Tests S2 through S5 were run with the same steam flow as Test S1 and with a range of air flows from 1.5% to 13% of the inlet mixture.
- Test S6 was performed with a pure-steam flow rate which, on a scaled basis, exceeds the SBWR PCC design capacity by about 33%.
- Tests S10, S11 and S12 were at the same conditions as Tests S3, S5 and S6, respectively, and were used to evaluate repeatability of the test results.
- Test S13 was at the same conditions as Tests S6 and S12, except that the PCC pool level was lowered to the bottom of the upper header to evaluate the effect of upper header heat transfer.

### 4.3.3 Applicability of Data to SBWR

#### 4.3.3.1 Overview of Data Applicability and Test Facility Scaling

[

Redacted

]

[

Redacted

]

**4.3.3.2 PIRT Phenomena and Coverage**

[

Redacted

]

[

Redacted

]

#### **4.3.4 TRACG Model**

[

Redacted

]

[

Redacted

]

[

Redacted

]

#### **4.3.5 Test Simulation**

[

Redacted

]

[

Redacted

]

#### **4.3.6 Results of Post-Test Calculations**

[

Redacted

]

##### **4.3.6.1 Comparison of Experimental and Calculated Results**

[

Redacted

]

[

Redacted

]

#### **4.3.6.2 Effect of Reduced Pool Water Level**

[

Redacted

]

#### **4.3.6.3 Accuracy of TRACG Calculations**

[

Redacted

]

### **4.3.7 Summary and Conclusions**

#### **4.3.7.1 Condenser Performance**

The comparisons between TRACG calculations and the PANDA PCC steady-state performance test results, presented in Section 4.3.6, support the use of TRACG to model the SBWR PCCS. The post-test evaluation included four pure-steam tests and six steam-air tests. As discussed in Section 4.3.3, the scaled conditions for these tests represent an upper bound of the SBWR PCCS post-LOCA heat load and cover the expected range of SBWR PCCS inlet



noncondensable gas fractions. In addition to providing data for qualifying TRACG for calculation of PCCS performance, these tests provide an important scaling link between the PANDA test facility and the SBWR (Section 4.1 of Reference 4.3-9).

[

Redacted

]

#### **4.3.7.2 Evaluation of TRACG Qualification Needs**

[

Redacted

]

##### **4.3.7.2.1 PCC Flow/Pressure Drop (PC1)**

[

Redacted

]

##### **4.3.7.2.2 Condensation/Condensation-Degradation on Primary Side (PC2)**

[

Redacted

]

[

Redacted

]

4.3.7.2.3 Secondary-Side Heat Transfer (PC3)

[

Redacted

]

4.3.7.2.4 Parallel PCC Tube Effects (PC4)

[

Redacted

]

[

Redacted

]

#### 4.3.8 References

- [4.3-1] M. Stempniewicz, *Pre Test Calculations of PANDA PCC Steady-State Tests*, KEMA Report 40315-NUC 94-7141, N.V. KEMA, June 1995.
- [4.3-2] M. Stempniewicz and J. R. Fitch, *Post-Test Calculations of PANDA PCC Steady-State Tests*, KEMA Report 40880-NUC-95-2516, N.V. KEMA, October 1995.
- [4.3-3] NEDC-32391P, *SBWR Test and Analysis Program Description*, Rev. C, August 1995.
- [4.3-4] GE Document 25A5587, *PANDA Test Specification*, Rev. 1, January 1995.
- [4.3-5] PSI Document ALPHA-606-0, *PANDA Facility, Test Program and Data Base General Description* (DTR Umbrella Report), May 1996.
- [4.3-6] *Steady-State Data Transmittal Report*, Paul Scherrer Institut, Document No. ALPHA-609-1, November 1996.
- [4.3-7] NEDE-32178P, *Application of TRACG Model to SBWR Licensing Safety Analysis*, Rev. 1, January 1998.
- [4.3-8] J.G.M. Andersen, et al., *TRACG Model Description*, NEDE-32176P, Rev. 2, Class 3, December 1999.
- [4.3-9] NEDC-32606P, *SBWR Testing Summary Report*, Rev. B, Class 3, November 1996.

**Table 4.3-1  
PANDA Steady-State PCC Performance Test Matrix**

<b>Test</b>	<b>Steam Flow (kg/s)</b>	<b>Air Flow (kg/s)</b>	<b>Inlet Pressure (bar)</b>	<b>Pool Level (m)</b>	<b>Remarks</b>
S-1	0.195	0.000	Self adjusting	4.5	Pure steam
S-2	0.195	0.003	3.000	4.5	Air/steam
S-3	0.195	0.006	3.000	4.5	Air/steam
S-4	0.195	0.016	3.000	4.5	Air/steam
S-5	0.195	0.028	3.000	4.5	Air/steam
S-6	0.260	0.000	Self adjusting	4.5	Pure steam
S-10	0.195	0.006	3.000	4.5	Repeat of S3
S-11	0.195	0.028	3.000	4.5	Repeat of S5
S-12	0.260	0.000	Self adjusting	4.5	Repeat of S6
S-13	0.260	0.000	Self adjusting	2.8	Repeat of S12 with reduced pool level

**Table 4.3-2  
Comparison of TRACG PCC Nodalizations for PANDA and SBWR Containment Model**

[

Redacted

]

**Table 4.3-3  
Actual Conditions for PANDA Steady-State Performance Tests  
and TRACG Post-Test Calculations**

<b>Test</b>	<b>Steam Flow (kg/s)</b>	<b>Air Flow (kg/s)</b>	<b>Inlet Pressure (bar)</b>	<b>Pool Level (m)</b>	<b>Remarks</b>
S-1	0.1893	0.00000	2.74	4.65	Pure steam
S-2	0.1933	0.00302	3.02	4.49	Air/steam
S-3	0.1927	0.00599	3.01	4.66	Air/steam
S-4	0.1942	0.01596	3.01	4.77	Air/steam
S-5	0.1960	0.02786	3.02	4.68	Air/steam
S-6	0.2610	0.00000	3.35	4.51	Pure steam
S-10	0.1978	0.00596	3.03	4.43	Repeat of S3
S-11	0.2013	0.02786	2.98	4.63	Repeat of S5
S-12	0.2664	0.00000	3.37	4.63	Repeat of S6
S-13	0.2628	0.00000	3.05	2.80	Repeat of S12 with reduced pool level

**Table 4.3-4  
PCCS Inlet Velocities for TRACG Post-Test Calculations**

<b>Test</b>	<b>Steam</b>		<b>Air</b>	
	<b>Flow (kg/s)</b>	<b>Velocity (m/s)</b>	<b>Flow (kg/s)</b>	<b>Velocity (m/s)</b>
S-1	0.1893	20.01	0.00000	0.00
S-2	0.1933	20.43	0.00302	4.90
S-3	0.1927	20.37	0.00599	9.72
S-4	0.1942	20.53	0.01596	25.94
S-5	0.1960	20.72	0.02786	45.23
S-6	0.2610	27.59	0.00000	0.00
S-10	0.1978	20.91	0.00596	9.66
S-11	0.2013	21.28	0.02786	45.23
S-12	0.2664	28.16	0.00000	0.00
S-13	0.2628	27.78	0.00000	0.00

**Table 4.3-5**  
**Void Fractions in Pool Cells with Liquid Levels**

[

Redacted

]

**Table 4.3-6**  
**Correspondence Between PANDA Measurements and TRACG Model Locations**

[

Redacted

]

**Table 4.3-7**  
**Maximum Measurement Uncertainties for PANDA Steady-State PCC Tests**

[

Redacted

]

**Table 4.3-8**  
**Condenser Efficiencies from PANDA Steady-State Steam-Air Tests Compared**  
**with TRACG Calculations**

[

Redacted

]

**Table 4.3-9**  
**Condenser Inlet Pressures from PANDA Steady-State Pure-Steam Tests Compared with**  
**TRACG Calculations**

[

Redacted

]



**Table 4.3-10**  
**Assessment of TRACG Accuracy for PANDA PCC Tests**

[

Redacted

]

[

Redacted

]

**Figure 4.3-1 TRACG Model of the PANDA PCCS as Modified for the Steady-State Tests**

[

Redacted

]

**Figure 4.3-2 TRACG Model of the PANDA PCCS Inlet Pipe as Modified for the Steady-State Tests**

[

Redacted

]

**Figure 4.3-3 TRACG Model of the PANDA PCCS Secondary Side**

[

Redacted

]

**Figure 4.3-4 Comparison of TRACG Calculations of Condenser Efficiency with PANDA Measurements (Steam-Air Tests)**

[

Redacted

]

**Figure 4.3-5 Comparison of TRACG Calculations of Condenser Inlet Pressure with PANDA Measurements (Pure-Steam Tests)**

## 4.4 Suppression Pool Stratification Tests

### 4.4.1 Introduction

In 1977 and 1978, General Electric conducted a multiphase Mark III Confirmatory Test Program in support of the Mark III pressure suppression containment concept using the horizontal vent system design. This Confirmatory Test Program included a series of tests in the Pressure Suppression Test Facility (PSTF) to investigate how thermal stratification of the suppression pool affected the performance of the Mark III horizontal vent system during loss-of-coolant accident (LOCA) conditions. There were two test series, one set performed with full-scale vents and another performed using one-third area scaled vents ( $1/\sqrt{3}$  diameter scaled). The full-scale tests were designated the 5707 series, and the one-third scale tests were designated the 5807 series.

For TRACG evaluation purpose, one test from the 5707 series and one from the 5807 series were selected to determine TRACG's ability to calculate the suppression pool thermal stratification conditions in both the horizontal and vertical directions. Specifically, Tests 5707-Run 01 and 5807-Run 29 were analyzed using TRACG. For these evaluations, two separate TRACG input models of the PSTF test facility configuration were set up, one for the full-scale 5707 series configuration and another for the one-third area scale 5807 series configuration.

### 4.4.2 Test Facility/Test Matrix

Figure 4.4-1 shows the PSTF test facility configuration for the large-scale 5707 series. An electrically heated pressure vessel simulated the reactor pressure vessel (RPV). The RPV was connected to another pressure vessel, which simulated the drywell (DW), by a blowdown pipe. The blowdown line was connected to a (0.363m I.D.) dip tube inside the simulated RPV, which allowed vapor to be withdrawn above the two-phase level in the RPV vessel and injected at the top of the DW vessel. A rupture disk in the blowdown pipe was used to simulate the breaking of the steam line, and a venturi in the line set the size of the simulated break. The DW volume was augmented with the volume of the 4T tank which was previously used as a suppression pool for Mark II pressure suppression experiments. The DW was connected by a set of three full-scale Mark III horizontal vents to a full-size 8-degree sector of a Mark III suppression pool. As in all pressure suppression containment designs, during a LOCA, the DW was pressurized and, as result, water initially in the vent system was expelled into the pool, ultimately opening a vapor flow path from the DW into the suppression pool.

The 5707 series test matrix included tests with break sizes from 0.054 to 0.076m in diameter, and initial pool temperatures ranging from 21°C to 77°C. In these tests, the wetwell (WW) air space was open to the outside atmosphere. This was done to simulate the large enclosed WW air space of the Mark III containment design. In these tests, the PSTF drywell and 4T vessels were purged of initial air by venting steam prior to the start of the test.

Figure 4.4-2 shows the PSTF test facility configuration for the scaled Test 5807 series. The facility configuration for this series is essentially the same as that for the 5707 series, except that there was no augmentation of the DW volume and the vent diameters and lengths were reduced in accordance with one-third area scaling.

The accuracy of the suppression pool temperature measurements for the 5707 and 5807 test series was approximately  $\pm 1^\circ\text{C}$ . A more detailed description of the 5707 and 5807 tests series is available in References 4.4-1 and 4.4-2, respectively.

#### **4.4.3 Applicability of Data to SBWR**

##### **4.4.3.1 General Data Applicability and Test Facility Scaling**

[

Redacted

]

##### **4.4.3.2 PIRT Phenomena and Coverage**

[

Redacted

]

#### **4.4.3.3 Scaling Parameters Range**

[

Redacted

]

#### **4.4.4 TRACG Model**

[

Redacted

]

[

Redacted

]

#### **4.4.5 Test Simulation**

[

Redacted

]



[

Redacted

]

#### **4.4.6 Results of Post-Test Calculations**

[

Redacted

]

##### **4.4.6.1 Test 5707-01**

[

Redacted

]

[

Redacted

]

**4.4.6.2 Test 5807-29**

[

Redacted

]

**4.4.6.3 Condensation of Blowdown Steam**

[

Redacted

]

#### 4.4.6.4 Accuracy of TRACG Calculations

[

Redacted

]

#### 4.4.7 Summary and Conclusions

[

Redacted

]

#### 4.4.8 References

- [4.4 -1] *Mark III Confirmatory Test Program, Full Scale Condensation and Stratification Phenomena - Test Series 5707*, NEDE-21853-P, August 1978.
- [4.4 -2] *Mark III Confirmatory Test Program,  $1/\sqrt{3}$  Scale Condensation and Stratification Phenomena - Test Series 5807*, NEDE-21596-P, March 1977.
- [4.4-3] *A Comparison of the RELAP Simulation of Mark III Suppression Pool Thermal Stratification with Data from the Pressure Suppression Test Facility*, NEDE-21957P, September 1978.

**Table 4.4-1**  
**Comparison of PSTF and SBWR Parameters**

[

Redacted

]

**Table 4.4-2**  
**Comparison of Pool Total Thermal Energy - TRACG vs Data for Test 5807-29**

[

Redacted

]

**Table 4.4-3**  
**Assessment of TRACG Accuracy for**  
**PSTF Suppression Pool Stratification Tests**

[

Redacted

]

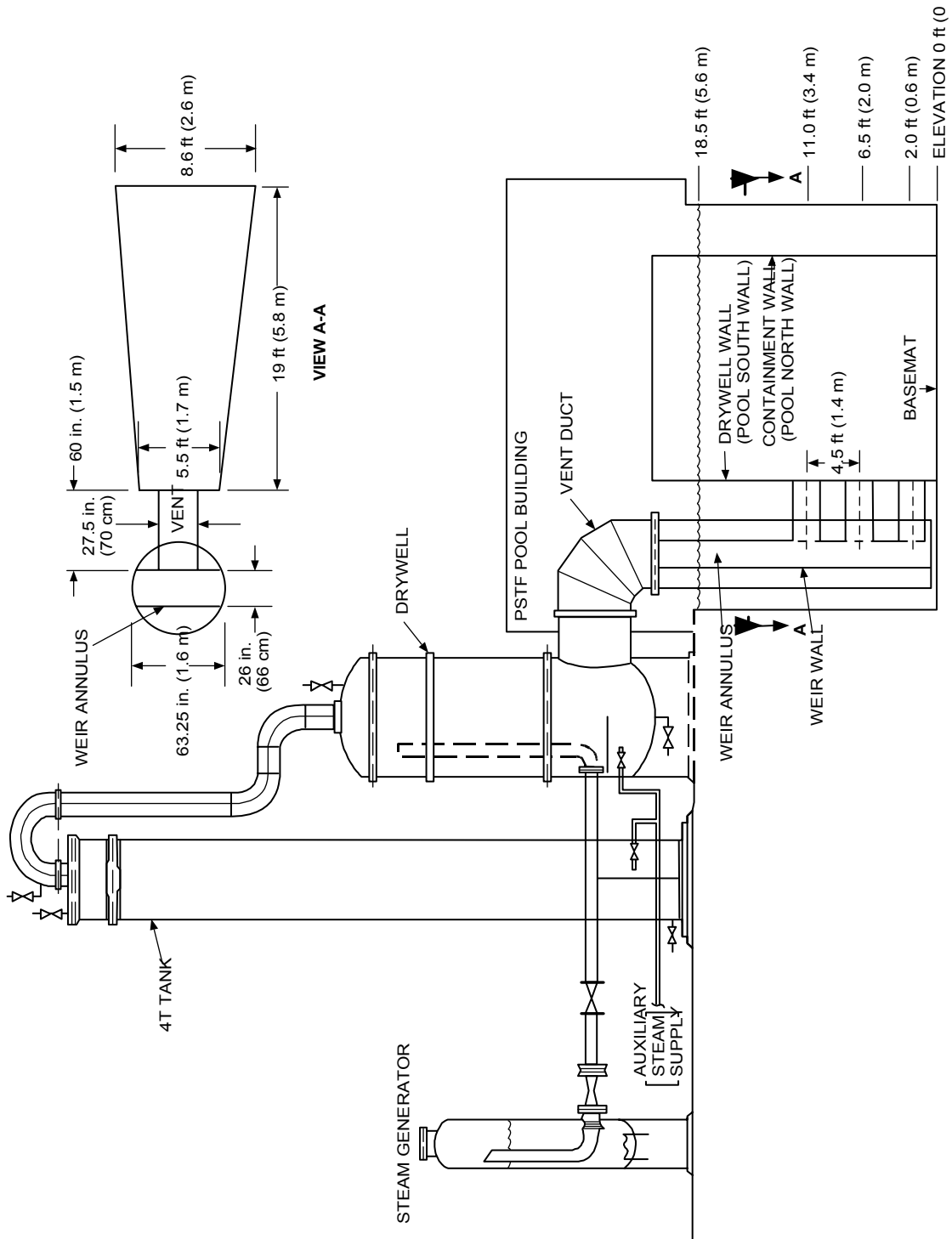


Figure 4.4-1 Pressure Suppression Test Facility - Test 5707 Series

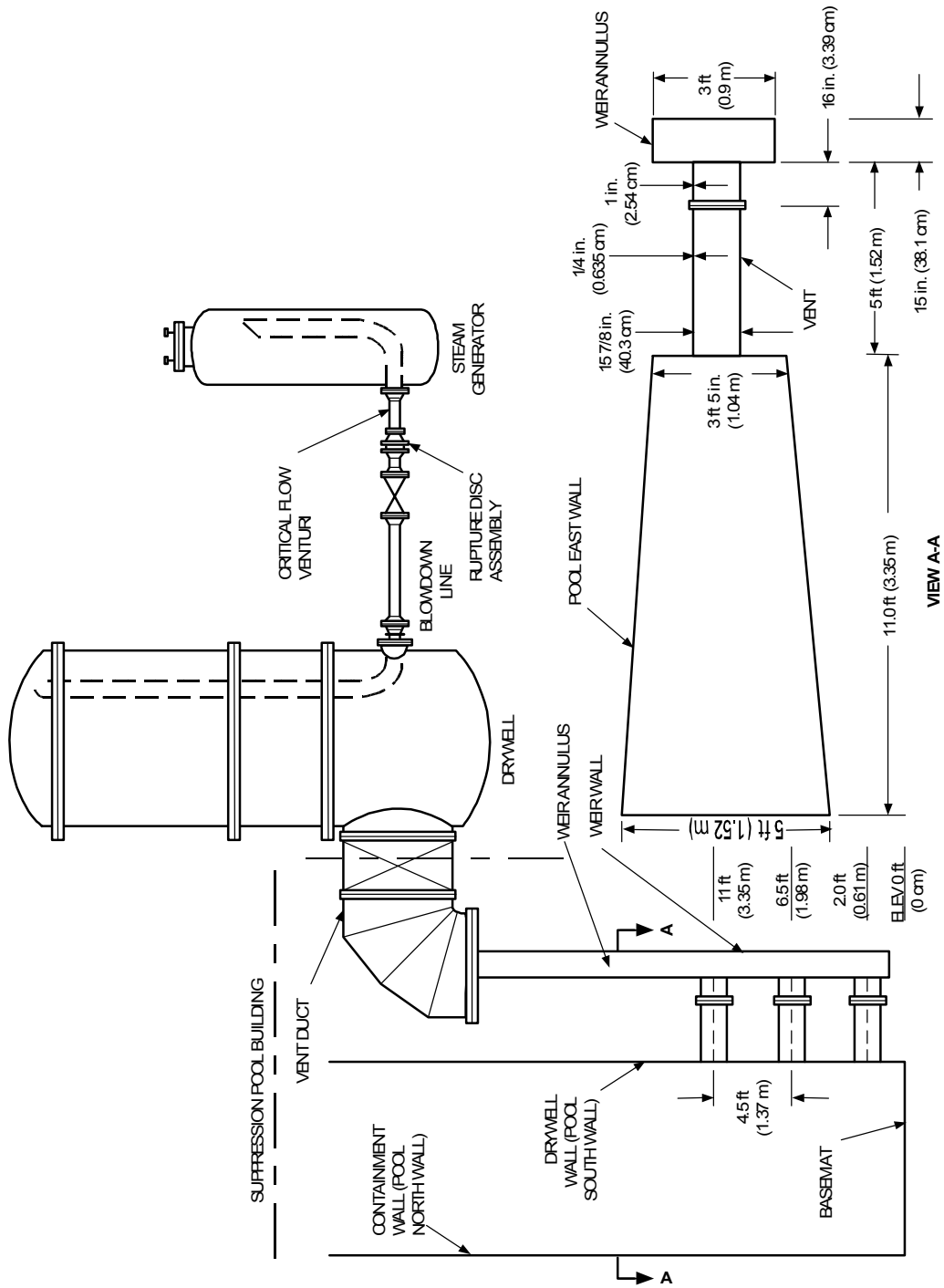


Figure 4.4-2 Pressure Suppression Test Facility - Test 5807 Series



[

Redacted

]

**Figure 4.4-3 TRACG Component Layout**

[

Redacted

]

**Figure 4.4-4 TRACG Modeling of Eight Degree WW Section**

[

Redacted

]

**Figure 4.4-5 TRACG Modeling of Vent System**

[

Redacted

]

**Figure 4.4-6 TRACG Suppression Pool Nodalization**

[

Redacted

]

**Figure 4.4-7 Temperature Profile of Volume 5 - Test 5707-01**

[

Redacted

]

**Figure 4.4-8 Temperature Profile of Volume 1 - Test 5807-29**

[

Redacted

]

**Figure 4.4-9 Temperature Profile of Volume 2 - Test 5807-29**

[

Redacted

]

**Figure 4.4-10 Temperature Profile of Volume 3 - Test 5807-29**



[

Redacted

]

**Figure 4.4-11 Temperature Profile of Volume 4 - Test 5807-29**

[

Redacted

]

**Figure 4.4-12 Temperature Profile of Volume 5 - Test 5807-29**

[

Redacted

]

**Figure 4.4-13 Temperature Profile of Volume 6 - Test 5807-29**